SCHOOL OF
CIVIL ENGINEERING

INDIANA
DEPARTMENT OF TRANSPORTATION

JOINT HIGHWAY RESEARCH PROJECT

FHWA/IN/JHRP-93/5
Final Report

GUIDELINES FOR PERMITTING OVERLOADS - PART I EFFECT OF OVERLOADED VEHICLES ON THE INDIANA HIGHWAY NETWORK

Sameh Zaghloul
Thomas D. White

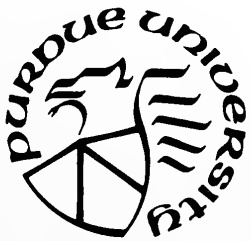

PURDUE UNIVERSITY

JOINT HIGHWAY RESEARCH PROJECT

FHWA/IN/JHRP-93/5
Final Report

GUIDELINES FOR PERMITTING OVERLOADS - PART I EFFECT OF OVERLOADED VEHICLES ON THE INDIANA HIGHWAY NETWORK

Sameh Zaghloul
Thomas D. White

Final Report

GUIDELINES FOR PERMITTING OVERLOADS

PART I

EFFECT OF OVERLOADED VEHICLES ON THE INDIANA HIGHWAY NETWORK

Sameh Zaghloul, Ph.D.h

and

Thomas D. White
Professor of Civil Engineering

Joint Highway Research Project

Project No: C-36-73L
File No: 3-4-12

Conducted in cooperation with the

Indiana Department of Transportation

and

Federal Highway Administration

Purdue University
West Lafayette, IN 47907
June 2, 1994

TECHNICAL REPORT STANDARD TITLE PAGE

1. Report No.	2. Government Accession No.	3. Recipient's Catalog No.
FHWA/IN/JHRP-93-5		

4. Title and Subtitle	5. Report Date
Guidelines for Permitting Overloads	6. Performing Organization Code

7. Author(s)	8. Performing Organization Report No.
Sameh Zaghloul and Thomas D. White	FHWA/IN/JHRP-93-5

9. Performing Organization Name and Address	10. Work Unit No.
Joint Highway Research Project Civil Engineering Building Purdue University West Lafayette, Indiana 47907-1284	11. Contract or Grant No. HPR-2042
	13. Type of Report and Period Covered Final 4-1-91/6-2-94
12. Sponsoring Agency Name and Address Indiana Department of Transportation State Office Building 1000 North Senate Avenue Indianapolis, IN 46204	14. Sponsoring Agency Code

15. Supplementary Notes

16. Abstract

Closed form analysis is commonly used to analyze pavement structures. This type of analysis assumes linear elastic material properties and static loading conditions. In reality, pavement materials are not linear elastic materials. For example, asphalt mixtures are viscoelastic materials and cohesive soils are elastic-plastic materials. Also truck loads are moving loads. The difference between the closed form analysis assumptions and the actual pavement conditions leads to significant difference between measured and predicted pavement response.

A study has been conducted at Purdue University to develop a procedure for permitting overloaded trucks in Indiana. This study was funded by the Indiana Department of Transportation (INDOT) and the Federal Highway Administration (FHWA). As a part of this study a three-dimensional, dynamic finite element program (3D-DFEM) was used to analyze flexible and rigid pavements and develop load equivalency factors. Truck loads moving at different speeds were included in the analysis and a number of material models were used to represent the actual pavement materials behavior under moving loads. The 3D-DFEM was verified for flexible and rigid pavement analysis. Two verification studies was conducted for each pavement type: Static, linear elastic analysis and dynamic, nonlinear analysis. In the static verification studies, linear elastic material properties were assumed and the 3D-DFEM predictions were compared with the results of a multi-layer analysis (for flexible pavement) and Westergaard's equations (for rigid pavement). In the dynamic analysis verification studies, measured pavement deflections were compared with the 3D-DFEM predictions under similar conditions. All verification studies showed excellent agreement between field and predicted pavement response.

Load equivalency factors (LEF) were developed for flexible and rigid pavements. The LEF of any load "j" and cross section "i" was defined as the number of the 18-kip single axle load (SAL) applications required to develop the same pavement response of one pass of load "j" on the same cross section "i". Permanent deformation at the pavement surface which accumulates from different layers is used as the equivalency criteria for flexible pavement LEF's, while total surface deformation, elastic and plastic, is used for rigid pavement LEF's. Both LEF sets are based on nonlinear dynamic analysis and consider the effect of load repetitions. Comparisons between the developed LEF's and the appropriate AASHTO LEF's showed excellent agreement.

17. Key Words	18. Distribution Statement
Pavement analysis, load equivalency factors, overload permitting	No restriction. This document is available to the public through the National Technical Information Service, Virginia 22161

19. Security Classif. (of this report)	20. Security Classif. (of this page)	21. No. of Pages	22. Price
Unclassified	Unclassified		

Form DOT F 1700.7 (8-69)

ACKNOWLEDGMENTS

Thanks are extended to the advisory committee members for their suggestions and helpful comments towards the completion of the pavement evaluation phase of the research study "Guidelines for Permitting Overloads."

Sincere thanks are expressed to Professors Julio Ramirez and Don White, and Mr. Prasad Nbr of the Structures Area of the School of Civil Engineering and Professor Thomas Kuczek of the School of Statistics at Purdue University for their helpful contributions towards this work.

Financial support was provided by the Federal Highway Administration and the Indiana Department of Transportation through the Joint Highway Research Project, School of Civil Engineering, Purdue University, West Lafayette, IN. Their cooperation and encouragement are appreciated.

TABLE OF CONTENTS

Page

LIST OF TABLES.....viii

LIST OF FIGURES.....ix

ABSTRACT.....xiv

CHAPTER 1 INTRODUCTION.....1

CHAPTER 2 LITERATURE REVIEW.....5

2.1. Material Behavior.....5
2.1.1. Material Models.....7
2.2. Load Models.....15
2.3. Analysis Algorithm (Static versus Dynamic Analysis).....16
2.3.1. Effect of Stress Reversal.....16
2.3.2. Rate-Dependent Response.....17
2.3.3. Dynamic Effects.....18
2.4. Pavement Analysis.....18
2.4.1. Flexible Pavement Analysis.....19
2.4.2. Rigid Pavement Analysis.....22
2.5. Load Equivalency Factors (LEF).....29
2.5.1. Load Equivalency Factors for Flexible Pavement.....29
2.5.2. Load Equivalency Factors for Rigid Pavement.....32
2.5.3. Load Equivalency Factors for Composite Pavements.....34
2.6. Current Procedure for Permitting Overloaded Trucks in Indiana.....35

CHAPTER 3 THE THREE-DIMENSIONAL DYNAMIC FINITE ELEMENT PROGRAM.....38

3.1. Element Types.....39
3.1.1. Solid (Continuum) Stress/ Displacement Elements.....39
3.2. Material Models.....40
3.2.1. Extended Drucker-Prager Model.....41
3.2.2. Cam-Clay Model.....42
3.2.3. Concrete Model.....43
3.2.4. Viscoelastic Material Model.....44

3.2.4. Viscoelastic Material Model.....44
3.3. Load Models.....45
3.4. Stress Analysis Procedures.....45
3.4.1. Static Stress Analysis.....46
3.4.2. Dynamic Analysis.....46
3.4.3. Geostatic Stress State.....49
3.5. Response Parameters.....50

CHAPTER 4 ANALYSIS OF FLEXIBLE PAVEMENT.....51

4.1. Features of the Finite Element Model.....52
4.1.1. Model Geometry.....52
4.1.2. Boundary Conditions.....53
4.1.3. Pavement/Shoulder Modeling.....54
4.2. Material Properties.....54
4.3. Loading Cycles.....55
4.4. Finite Element Model Verification.....56
4.4.1. Static Analysis Verification.....56
4.4.2. Dynamic Analysis Verification.....58
4.5. Sensitivity Analysis.....59
4.5.1. Material and Layer Characteristics....59
4.5.2. Cross Section Attributes.....60
4.5.3. Load Attributes.....64
4.6. Rut Depth Predictions.....66

CHAPTER 5 ANALYSIS OF RIGID PAVEMENT.....69

5.1. Features of the Finite Element Model.....70
5.1.1. Model Geometry.....70
5.1.2. Boundary Conditions.....70
5.1.3. Longitudinal and Transverse Joints....71
5.2. Material Properties.....71
5.3. Loading Cycles.....72
5.4. Finite Element Model Verification.....72
5.4.1. Static Analysis Verification.....72
5.4.2. Dynamic Analysis Verification.....73
5.5. Sensitivity Analysis.....74
5.5.1. Effect of Moving Load Speed.....75
5.5.2. Effect of Load Position.....76
5.5.3. Effect of Axle Loads and Slab Thickness.....76
5.5.4. Effect of Subbase Course.....77
5.5.5. Effect of Dowel Bars.....78
5.5.6. Effect of Joint Width.....80

CHAPTER 6 LOAD EQUIVALENCY FACTORS.....81

6.1. Flexible Pavement LEF's.....84
6.1.1. Comparison Between Different LEF Methods.....84
6.1.2. The 3D-DFEM Analysis.....84
6.1.3. Purdue LEF's for Asphalt Pavements....85
6.2. Rigid Pavement Analysis.....90

6.2.1. Comparison Between Different LEF Methods.....90
6.2.2. The 3D-DFEM Analysis.....90
6.2.3. Purdue LEF's for Rigid Pavements.....91
6.3. Composite Pavement LEF's.....95
6.3.1. Comparison Between Different LEF's for Composite Pavements.....95
6.3.2. The 3D-DFEM Analysis.....95
6.3.3. Purdue LEF's for Composite Pavements..96
6.4. Advantage of Purdue LEF's.....100

CHAPTER 7 THE OVERLOAD PERMITTING PROCEDURE.....102

7.1. Indiana Truck Weight Regulations.....102
7.2. Typical Pavement Cross Sections for Indiana....104
7.3. Stress Models.....105
7.4. The Overload Permitting Procedure.....107
7.4.1. Network Level Analysis.....109
7.4.2. Project Level Analysis.....113

CHAPTER 8 SUMMARY AND CONCLUSIONS.....115

REFERENCES.....122

APPENDIX A.....217

APPENDIX B.....219

LIST OF TABLES

Table		Page
2.1	Boussinesq's Equations for a Point Load	127
2.2	Available FEM's for Rigid Pavements	128
3.1	Features of SSD Elements	142
3.2	Material Options Available in ABAQUS	143
3.3	Response Parameters Used in the Analysis	146
4.1	Design of Experiment of the Static Analysis Verification	152
4.2	Comparison Between the Multi-layer Analysis and the 3D-DFEM Predictions	153
4.3	Material Properties Used in the Dynamic Analysis Verification	154
4.4	Comparison Between Measured and Predicted Flexible Pavement Deflections	155
4.5	Subgrade Properties	156
5.1	Factor Levels Included in the Static Analysis Verification	173
5.2	Comparison Between Measured and Predicted Rigid Pavement Deflections	173
6.1	Factor Levels Included in the FDOE1	185
6.2	Regression Coefficient of Different DOE's	186
6.3	Factor Levels Included in the FDOE2	187
6.4	Factor Levels Included in the RDOE1	187
7.1	Typical Material Properties Used in the Analysis	209
7.2	Summary of the Route Independent Model	211

7.3 Summary of the Route Dependent Model.....211

A.1 Minimum Axle Spacing for Different Load Levels.....218

LIST OF FIGURES

Figure Page

2.1 Material Characteristics....129

2.2 Stress Dependent Material Behavior....130

2.3 Linear and Non-Linear Materials....131

2.4 Elliptical Yield Locus for Cam-Clay Model....132

2.5 Drucker-Prager Model....133

2.6 Typical Yield/Flow Surfaces in the Deviatoric Plane for Drucker-Prager Model....134

2.7 Viscoelastic Models....135

2.8 Viscoelastic Response....135

2.9 Viscoplastic Model....136

2.10 Development of Shear Strain During Repeated Load Test....137

2.11 The Effect of Stress Reversals on Stiffness....137

2.12 Rate-Dependent Response of Clays....138

2.13 The Two-Layer Theory....139

2.14 Generalized N-Layer Elastic System....139

2.15 Difference Between a Winkler Subgrade and an Elastic Subgrade....140

2.16 CanRoad LEF's for Tridem Axle Configuration....141

2.17 Comparison Between the AASHTO LEF's and CanRoad LEF's....141

3.1 Linear Elastic Material Model....147

3.2 Yield Stress of an Elastic-Plastic Material....147

3.3 Yield Surface in the p-t Plane for Drucker-Prager Model....148

3.4 Critical State Surface in the Principal

effective Stresses Plane.....149

3.5 Yield and Failure Surfaces for Concrete.....150

3.6 Stress-Strain Curve for Concrete.....150

3.7 Examples of Load Amplitude.....151

4.1 Finite Element Mesh for Flexible Pavement Analysis.....157

4.2 Flexible Pavement Cross Sections.....158

4.3 Effect of Loading Time and Temperature on Asphalt mixtures Stiffness.....158

4.4 Load Cycle Used in the Analysis.....159

4.5 Static Analysis Verification (Flexible Pavement)....160

4.6 Dynamic Analysis Verification (Flexible Pavement)...161

4.7 Effect of Subgrade Type on Pavement Deflection.....162

4.8 Effect of Deep Foundation Type on Pavement Deflection.....163

4.9 Effect of Shoulder Width on Pavement Deflection.....164

4.10 Effect of Pavement/Shoulder Joint on Pavement Deflection.....164

4.11 Effect of G-Ratio on Vertical Compressive Strain....165

4.12 Effect of Temperature on Vertical Compressive Strain.....165

4.13 Components of Horizontal Tensile Strains.....166

4.14 Effect of Load Repetitions on Horizontal Tensile Strain.....166

4.15 History of Horizontal Tensile Strain at the Bottom of the Asphalt Layer.....167

4.16 Effect of Load Repetitions on Vertical Compressive Strain.....167

4.17 Effect of Speed on Pavement Deflection.....168

4.18 Effect of Speed on Pavement Rutting.....169

4.19 Effect of Axle Configuration on Pavement Deflection.....169

4.20 Effect of Axle Load on Pavement Deflection.....170

4.21 Effect of Axle Load on Pavement Rutting.....171

4.22 Predicted Pavement Rutting (58-kip SAL).....171

4.23 Predicted Pavement Rutting (18-kip SAL).....172

5.1 Finite Element Mesh for Rigid Pavement Analysis.....174

5.2 Static Analysis Verification (Rigid Pavement).....175

5.3 Dynamic Analysis Verification (Rigid Pavement).....176

5.4 Effect of Truck Speed on Pavement Response.....177

5.5 Effect of Load Position on Pavement Response.....178

5.6 Effect of Axle Load and Slab Thickness on Pavement Deflection.....179

5.7 Effect of Load Repetitions on Pavement Deflection.....179

5.8 Effect of Load Repetitions on Permanent Deformation.....180

5.9 Effect of Subbase on Pavement Deflection.....181

5.10 Effect of Dowel Bars on Surface Deflection (No Subbase).....181

5.11 Effect of Dowel Bars Diameter on Surface Deflection.....182

5.12 Effect of Dowel Bars Spacing on Surface Deflection.....182

5.13 Effect of Dowel Bars length on Surface Deflection.....183

5.14 Effect of Dowel Bars on Surface Deflection (with 4" Granular Subbase).....183

5.15 Effect of Joint Width on Surface Deflection.....184

5.16 Effect of Joint Width on Load Transfer Efficiency.....184

6.1 Flexible Pavement LEF's for Single Axle Configuration.....188

6.2 Flexible Pavement LEF's for Tandem Axle Configuration.....189

6.3 Purdue LEF's for Flexible Pavements.....190

6.4 Comparison Between Main Effects and Full Interaction Models.....191

6.5 Comparison Between Purdue LEF's and Other Flexible Pavement LEF's (Single Axle Configuration).....192

6.6 Comparison Between Purdue LEF's and Other Flexible Pavement LEF's (Tandem Axle Configuration).....193

6.7 Effect of Asphalt Layer Thickness on LEF's (Single Axle Configuration).....194

6.8 Effect of Total Pavement Thickness on LEF's (Single Axle Configuration).....194

6.9 Effect of Asphalt Mixture Quality on LEF's (Single Axle Configuration).....195

6.10 Effect of Asphalt Layer Thickness on LEF's (Tandem Axle Configuration).....195

6.11 Effect of Asphalt Layer Thickness on LEF's (Tridem Axle Configuration).....196

6.12 Effect of Asphalt Layer Thickness on LEF's (Four Axle Configuration).....196

6.13 Comparison Between the AASHTO LEF's and Fatigue Analysis LEF's (Single Axle Configuration).....197

6.14 Purdue LEF's.....198

6.15 Effect of Speed on LEF's.....199

6.16 Comparison Between the AASHTO LEF's and Purdue LEF's (Single Axle Configuration).....200

6.17 Comparison Between the AASHTO and Purdue LEF's (Tandem Axle Configuration).....201

6.18 Effect of Slab Thickness on LEF's (Single Axle Configuration).....202

6.19 Effect of Slab Thickness on LEF's (Tandem Axle Configuration.....202

6.20 Effect of Number of Axles on LEF's.....203

6.21 Purdue LEF's.....204

6.22 Comparison Between AASHTO LEF's for Concrete Pavements and Purdue LEF's for Composite Pavements..205

6.23 Effect of the Slab Thickness on LEF's.....206

6.24 Effect of the Overlay Thickness on LEF's.....207

6.25 Effect of Number of Axles on LEF's.....208

7.1 Flow Chart of the Overload Permit Procedure.....212

7.2 Effect of LEF's on Maximum Surface Deflection.....216

EXECUTIVE SUMMARY

Truck weight regulations are used to control the rate of damage accumulation for pavements and bridges. Permitting heavier loads can increase the rate at which pavement damage accumulates and the cost of maintaining pavements in good condition. Truck loads, load configuration, and number of trucks also lead to bridge deterioration with associated load limitation and need for early replacement.

Legal truck weight and overloaded truck weight limits have always been controversial. They involve sensitive trade-offs between the costs to build and maintain highways and the costs of transporting goods by truck, and they have implications for highway safety, traffic flow and highway finance. Although improvements in truck performance have resulted in higher truck loads, careful investigation into the impact of such heavy trucks on the highway system is required. Each state has legal truck weight limits,. In many cases trucks carrying weights higher than legal limits, overloaded trucks, need to use the highway system. In this case a special overload permit is required.

A study has been conducted at Purdue University to develop an enhanced procedure for permitting overloaded trucks in Indiana. In this procedure, damage effects of overloaded trucks were evaluated for pavements and bridges. This report is concerned mainly with pavement analysis. Bridge analysis is reported by NBR et al. 1993. A three-dimensional, dynamic finite element program (3D-DFEM) [ABAQUS, 1989a] was used in this study to analyze flexible, rigid and composite pavements. A composite pavement is an asphalt overlaid concrete pavement. The 3D-DFEM was verified for flexible and rigid pavement analysis. Two verification studies were conducted for each pavement type: static, linear elastic analysis and dynamic, nonlinear analysis. The verification studies for both pavement types showed excellent agreement between

field and predicted pavement response.

1. Features of the Finite Element Model

1.1. Model Geometry

In this analysis, pavements were modeled as three-dimensional problems. Mesh dimensions in the horizontal plan were selected to match the pavement geometry, such as pavement and shoulder widths, and load configuration, such as axle and wheel spacings. In the vertical direction the mesh dimension were selected to represent the pavement layer thicknesses (i.e., surface, base and subbase). The number of layers required to model the subgrade depends on the detail desired in predicting the vertical pavement response. Adhesion between layers was consider as a function of friction and normal pressure on the layers (Mohr-Coulomb Theory).

1.2. Boundary Conditions

Boundary conditions for the finite element model have a significant influence on the predicted response. Reasonable boundary conditions were assumed for edges parallel and perpendicular to the traffic direction, bottom of the mesh (deep foundation) and joints (such as lane/shoulder joint for flexible pavements and longitudinal and transverse joints for concrete pavements).

2. Material Properties

Pavement materials were divided into four groups: asphalt concrete, portland cement concrete, unbound granular and cohesive soils. Actual material behavior under repeated loads for each group was considered.

Asphalt concrete was modeled as a visco-elastic material. This type of material is time and temperature dependent [Yoder and Witczak, 1975]. The time dependent properties were represented by instantaneous and long term shear modulus [ABAQUS, 1989b]. Instantaneous shear modulus was selected at a loading time of 0.1 second which is equivalent to a speed of 40 mph. Long term shear modulus was selected at a loading time of 1.0 second which is equivalent to a speed of 1.5 mph. The temperature effect was considered through the shear modulus values.

Granular materials, base, subbase and subgrade in some cases, were modeled using the Drucker-Prager model [Drucker and Prager, 1952 and ABAQUS, 1989b]. This is an elastic-plastic model in which granular materials are assumed to behave elastically for low stress levels. When the stress level reaches a certain yield stress the material will start to behave as an elastic-plastic material.

The Cam-Clay model [Schofield et al., 1968, Parry, 1972 and ABAQUS, 1989b] was used to model cohesive soils. This model uses a strain rate decomposition in which the rate of deformation of the clay is decomposed addictively into an elastic and a plastic part.

Three stages of portland cement concrete (PCC) were modeled: elastic, plastic and after-failure stages. If the PCC slab is subjected to a stress level less than its yield stress, it will behave elastically. When the stress level exceeds the yield stress of PCC, the behavior is elastic-plastic until the failure stress. At that point the after-failure stage will start [ABAQUS, 1989b].

Other material and layer characteristics required in the analysis include modulus of elasticity, Poisson's ratio, damping coefficient and bulk density.

3. Loading Cycles

The 3D-DFEM was used to simulate truck loads moving at highway speeds. At speeds

less than 20 mph a truncated sawtooth load function is used while a step load function is used for speeds greater than 20 mph. The change in loading function was made because for speeds greater then 20 mph the time required to reach the maximum load magnitude is very short.

4. Finite Element Model Verification

Prior to general application, the 3D-DFEM was verified for both asphalt and concrete pavements. The verification included evaluation of the 3D-DFEM capabilities to predict pavement response for both static and dynamic loading.

4.1. Static Analysis Verification

Design of experiments (DOE) were developed for the elastic, static case. Subsequently, analysis of sections with factor combinations satisfying the design of experiment were conducted with a layered elastic analysis for asphalt pavements and Westergaard analysis for concrete pavements, These results were compared with the 3D-DFEM analysis assuming elastic material properties for the various layers and static loading.

Three factors were included in the asphalt pavement DOE, surface layer thickness (T_s), base course thickness (T_b) and subgrade modulus of elasticity (E_{sg}). Two levels for each factor were included, low and high. Three factors were also included in the concrete pavement DOE, slab thickness (3 levels), load position (3 levels) and subgrade type (2 levels). Linear correlation analyses were made between multi-layer analysis predictions for asphalt pavements and Westergaard analysis predictions for concrete pavement and the corresponding 3D-FEM predictions. Results of the analysis showed high linear correlations were found for both asphalt and concrete pavements (R^2 = 96.4% and 97.8%, respectively).

4.4.2. Dynamic Analysis Verification

A study was also conducted to evaluate the time dependent dynamic analysis feature of the 3D-DFEM. Since there is no standard dynamic analysis method for the dynamic case as there is for the static case, a decision was made to compare the predictions with measured response of pavements due to moving loads. High linear correlations between the measured and predicted pavement deflections are found for both asphalt and concrete pavements, (R^2 = 99.9% and 99.6% respectively). These high correlations imply that the 3D-DFEM can be used to predict the dynamic response of pavements subjected to moving loads.

5. Load Equivalency Factors (LEF's)

A sample of overload permit applications was reviewed to determine truck configurations being permitted. The sample revealed that permits were requested for trucks with up to nine axles in one group as well as trucks with axle loads up to 72 kips per axle. Load equivalency factors (LEF) were required to account for the variation in truck configurations. There are two types of LEF's: analytical based LEF's and empirical based LEF's. Current pavement analysis methods used to develop the analytical based LEF's incorporate unrealistic assumptions, such as static loads and linear elastic material properties, while, the empirical LEF's, such as the AASHTO LEF's, are based on data that is limited to single and tandem axle configurations with maximum axle loads of 40 and 48 kips, respectively. Because of these limitations, the 3D-DFEM was used to develop LEF's for the overload permitting study. Load equivalency factor sets were developed: for flexible pavements, rigid pavements and composite pavements. Permanent deformation at the pavement surface which accumulates from different layers is used as the equivalency criteria for flexible pavement LEF's, while total surface deformation, elastic

and plastic, is used for rigid and composite pavement LEF's. The LEF's developed also consider the effect of load repetitions. Comparisons between the LEF's developed for asphalt and concrete pavements and the appropriate AASHTO LEF's showed excellent agreement.

6. Typical Pavement Cross Sections for Indiana

Based on the Highway Inventory Annual Report [IDOH 1989], there are approximately 91,500 miles of roads within the state of Indiana. INDOT is respobsible fore approximately 11,300 miles and the rest are under the respobsibility of different local government units. The 11,300 miles of roads that are the responsibility of INDOT have about 28,203 lane miles. The Road Life data base [Lindly and White 1989 and Pumphrey and White 1989] has detailed information about the cross section and the subgrade for 14,766 lane miles (more than 50% of the total lane miles). These data were used to obtain pavement structure distribution for different highway classes; Interstate (I), United States (US) and State Roads (SR). Based on this distribution typical cross sections were selected are used for evaluating the damage effect of overloaded trucks at the network level.

7. THE OVERLOAD PERMITTING PROCEDURE

A user friendly computer software was developed to implement the overload permitting procedure. The procedure has the following steps:

1. Data entry, which includes:
    - Permit type (overweight, oversize or mobile home)
    - Vehicle information (overall length, width and height, number of axles, gross load, axle loads and spacing, company name, license,..., etc.)

- Trip information (origin, destination and route, if any).

The user is permitted to enter, review, and make changes in the data.

2. Load parameters for bridge and pavement analyses are extracted from the vehicle information. Bridge analysis load parameters include: wheel base, gross load, number of equivalent axles. An equivalent axle is any group of axles that are within a distance of 9 feet. Pavement analysis load parameters include: grouping the truck axles into sets (tandem, tridem,...) based on the distance between axles (if less than 5.5 feet) and calculating the axle group load, spacing, number of wheels and number of axles for each axle group.

3. Selection of the level of analysis:

   - Network level (default). In this analysis typical pavement cross sections are used representing the different highway classes. A route independent formula is used for bridge analysis.
   - Project level. In this analysis the user has to enter the pavement cross section parameters and material properties. Default values are provided as a guide to the user. A route dependent formula is used for bridge analysis.

4. Selection of type of analysis:

   - Bridge analysis only.
   - Pavement analysis only.
   - Bridge and pavement analysis (default).

If the user selects bridge and pavement analyses (the default) the bridge analysis is made first. The pavement analysis will be run regardless of the results of the bridge analysis. If the truck is not permitted, the reason why the truck is not permitted, bridge, pavement or both, will be

shown in the permit.

Based on the user selections, the truck damage effects on bridges and pavements are evaluated as shown below.

7.1. Network Level Analysis

7.1.1. Bridge Analysis

The truck must satisfy the following:

- A minimum of 6 equivalent axles if the wheel base is more than 70 feet or a minimum of 3 equivalent axles if the wheel base is more than 25 feet. The number of equivalent axles for any given truck is obtained by counting closely spaced axles, within 9 feet, as a single equivalent axle.
- The wheel base has to be in the range of 10-120 feet.

If the truck satisfies the above conditions, a route independent model, depending only on truck parameters, is used to evaluate the bridge damage. The variance in the allowable load (W) is not found to be homogeneous for the entire range of wheel base. The variance actually increases with the level of allowable load.

$$\sqrt{W}=C_1L+C_2$$

Where C_1 and C_2 are regression coefficients [NBR and et al. 1993].

7.1.2. Pavement Analysis

The typical pavement cross sections are used in this analysis to represent different

highway classes (Interstate, United States and State Roads). Truck are represented as a set of axle groups. A sample of overload permit applications was reviewed and it was found that the 5 feet axle spacing is a break point. Therefore, the spacing between any two successive axles with axle spacing equal to or less than 5.5 feet are considered to be in one group. The pavement analysis has the following steps:

1. Evaluate Stress Levels

The purpose of this step is to estimate stress levels developed by the overloaded truck axle groups in the unbound layers and concrete slabs of the typical pavement sections. These stresses are compared with the corresponding yield stress of the unbound layers and the modulus of rupture of the concrete, respectively. Statistical models were developed to estimate stress levels in the unbound layers and the concrete slabs of the typical sections as a function of truck parameters. Analysis showed that the effect of static loads are more severe for pavements than moving loads, therefore, static loads were used in the development of the statistical models. For each of the typical cross sections, if the yield stress in any of the unbound layers, including the subgrade, is exceeded or the concrete stress ratio (stress/modulus of rupture of the concrete) exceeds 0.5, the overloaded truck will not be permitted to use this highway class. Further analysis will be made only for the typical cross sections which passed this check (satisfactory cross sections).

2. Load Equivalency Factors

For each satisfactory cross section, the LEF of each axle group will be determined using Purdue LEF sets. If the axle group LEF exceeds 32 the truck will not be allowed to use this

highway class. Also, accumulated LEF for the truck is also calculated by summing the LEF's of all axle groups. If the accumulated LEF exceeds a certain limit, depending on the highway class, the truck will not be permitted to use this highway class.

The truck is permitted to use highway classes which pass the previous checks. These highway classes will be shown on the permit.

7.2. Project Level Analysis

7.2.1. Bridge Analysis

In this analysis the allowable load at the operating stress level depends on both bridge and truck parameters. The bridge parameters referred to as HS truck capacity is introduced to develop a route depended model.

$$\sqrt{W}=C_1(HS_{truckcapacity})L+C_2$$

Where, W is the allowable load, and C_1 and C_2 are regression coefficients. The $HS_{truck\ capacity}$ of a bridge is defined as the maximum gross vehicle load that the bridge can carry within the operating stress level for a vehicle having the same configuration in terms of axles and axle load distribution as the standard HS20 truck with variable axle spacing. Also, the truck has to satisfy both the minimum number of axles/wheel base and length of the wheel base [NBR et al. 1993].

7.2.2 Pavement Analysis

In this option, the user has to provide information about the pavement cross section and material properties. This information includes:

1. Pavement type (asphalt, concrete or composite pavement)
2. Layer thicknesses.
3. Material properties of each layer:
    - Asphalt surface layer: modulus of elasticity, Possion's ratio, G-ratio $(1-\frac{LongTermShearModulus}{InstantaneousShearModulus})$, damping coefficient and bulk density.
    - Granular layers: modulus of elasticity, Possion's ratio, initial yield stress, yield function, cohesion, angle of internal friction, damping coefficient and bulk density.
    - Cohesive layers: modulus of elasticity, Possion's ratio, initial yield surface, yield function, water content, cohesion, angle of internal friction, damping coefficient and bulk density.

Typical default values for these properties are provided to the user.

Similar to the network level analysis, the overloaded truck has to pass the stress level and LEF checks in order to be permitted.

CHAPTER 1 INTRODUCTION

Truck weight regulations are used to control the rate of damage accumulation for pavements and bridges. Permitting heavier loads can increase the rate at which pavement damage accumulates and the cost of maintaining pavements in good condition. Legal truck weight and overloaded truck weight limits have always been controversial. They involve sensitive trade-offs between the costs to build and maintain highways and the costs of transporting goods by truck, and they have implications for highway safety, traffic flow and highway finance. Although improvements in truck performance have resulted in higher truck loads, careful investigation into the impact of such heavy trucks on the highway system is required. Each state has legal truck weight limits. In many cases trucks carrying weights higher than legal limits, overloaded trucks, need to use the highway system. In this case a special overload permit is required.

A study was conducted at Purdue University to develop a procedure for permitting overloaded trucks in Indiana. The study addresses permitting special vehicles, super loads, as well as providing recommendations of vehicle configuration for various load levels. A realistic pavement analysis procedure was required to evaluate the damage effect of overloaded trucks on Indiana highway network.

In the various pavement analysis theories assumptions have been made to simplify pavement structures and loading conditions. These simplifications are reflected in the accuracy of the predicted pavement response. Million of dollars are invested every day in pavement construction and maintenance activities. A significant portion of this money can be saved if

better analysis methods are used to design and evaluate pavements. None of the existing pavement analysis procedures was found suitable for the overload permitting study.

A three-dimensional, dynamic finite element program (3D-DFEM) [ABAQUS, 1989a] was used in the overload permitting study to analyze flexible, rigid and composite pavements. The 3D-DFEM is capable of simulating truck loads moving at different speeds. Also, the 3D-DFEM includes a number of material models which can represent pavement material behavior under moving loads. The 3D-DFEM was verified for flexible and rigid pavement analysis. Two verification studies was conducted for each pavement type: Static, linear elastic analysis and dynamic, nonlinear analysis. The verification studies for both pavement types showed excellent agreement between field and predicted pavement response.

A sample of overload permit applications was reviewed to determine truck configurations being permitted. The sample revealed that permits were requested for trucks with up to nine axles in one group as well as trucks with axle loads up to 72 kips per axle. Load equivalency Factors (LEF) were required to account for the variation in truck configurations. There are two types of LEF's: analytical based LEF's and empirical based LEF's. Current pavement analysis methods used to develop the analytical based LEF's incorporate unrealistic assumptions, such as static loads and linear elastic material properties, while, the empirical LEF's, such as the AASHTO LEF's, are limited to single and tandem axle configurations with maximum axle loads of 40 and 48 kips, respectively. Also, there are no LEF's available for composite pavements. Because of these limitations, the 3D-DFEM was used to develop LEF's for the overload permitting study. Three LEF sets were developed: flexible pavement LEF's, rigid pavement LEF's and composite pavement LEF's. Permanent deformation at the pavement surface which

accumulates from different layers is used as the equivalency criteria for flexible pavement LEF's, while total surface deformation, elastic and plastic, is used for rigid and composite pavement LEF's. All LEF sets consider the effect of load repetitions. Comparisons between the developed LEF's for flexible and rigid pavements, and the appropriate AASHTO LEF's showed excellent agreement.

A user friendly computer software was developed to implement this permitting procedure. The software allows the user to run damage analysis for overloaded trucks at the network level (e.g. route independent analysis) as well as at the project level for specific pavement and/or bridge structures. At both levels, three options are available: check for pavements only, check for bridges only, or check for both, the default option. At the project level, the user is permitted to enter all cross section and load parameters. Typical default values for material properties are provided. At the network level, typical pavement cross sections were included in the study to represent different highway classes in Indiana, Interstate (I), United States (US) and State Roads (SR). Selection of these representative cross sections was made based on the information available in the Road Life data base and was reviewed by the Materials and Test Division of the Indiana Department of Transportation. The truck damage effect is evaluated for both project and network levels in two steps:

1. Check if any of the unbound layers is subjected to a stress level higher than its yield stress. Also, check if the ratio of stress/modulus of rupture of the concrete exceeds 0.5.
2. Calculate the LEF of each of the overloaded truck axle groups as well as the total LEF of the truck, which is the sum of the truck axle groups LEF's

Based on these checks overloaded trucks may be permitted to use one or more of the highway classes.

CHAPTER 2 LITERATURE REVIEW

Pavement structural analysis is a procedure which can be used to study and predict pavement structural response to different loads. Pavement structural analysis has three components:

1. Material models.
2. Loads models.
3. Analysis Algorithm (procedure).

These three components must go hand in hand. The structural analysis of pavements is different from that of bridges and buildings. Pavement structures lie exposed on the ground and, hence, are greatly influenced by environmental factors, such as frost action. Also, pavements are subjected to vehicle traffic loads. Load magnitude, spacing and number; tire pressure; speed, ..., etc. have a significant effect on pavement response.

All of the above factors should be considered in pavement structural analysis, which results in a complex problem. Therefore, simplifications are always made. Several analysis procedures ignore some load parameters, such as speed and load repetitions, while others simplify the behavior of the pavement materials and foundation soils. These simplifications have a significant effect on the accuracy of predicted pavement response.

2.1. Material Behavior

Three relationships are usually used to describe pavement material response to loads

[Yoder and Witczak, 1975]:

1. The relationship between stress and strain, linear or nonlinear.
2. The time dependency of strain under a constant stress level, viscous or nonviscous.
3. The degree to which the material can rebound or recover strain after stress removal, plastic or elastic.

In Figure 2.1a [Yoder and Witczak, 1975] the fundamental difference between a linear and nonlinear material response is shown. Nonlinear material behavior has two stages, pure elastic and elastic-plastic. These two stages are delineated by at a yield stress. If the applied stress level is less than the yield stress, the material will act as a linear elastic material, e.g. all the strain is recoverable. When the stress level exceed the yield stress both elastic and plastic strain occur, only the elastic strain is recoverable.

Viscous and nonviscous material response is shown in Figure 2.1b [Yoder and Witczak, 1975]. Maxwell and Kelvin mechanical models can be used to describe viscous material response. The Maxwell model consists of a spring connected in series to a dashpot, while the Kelvin model consists of a spring connected in parallel to a dashpot. In the Maxwell model, the strain has two parts, an instantaneous and fully recoverable part, represented by the spring and a time dependent part, represented by the dashpot. In the Kelvin model, the strain approaches the elastic value as the loading time approaches infinity. When the load is released all the strain is recovered fully.

In Figure 2.1c [Yoder and Witczak, 1975], the basic distinction between an elastic and plastic material is shown. Ideally, this difference refers to whether all of the strain is recovered

(elastic) when the load is released or whether residual deformation remains (plastic).

2.1.1. Material Models

The goal of material modeling is to reproduce the vital aspects of material response. Material models can be used to predict response to any general changes in effective stresses and strains and can be divided according to their complexity, and the extent to which they are able to reproduce important features of material response [Wood, 1990]:

"1. *Children's models, such as linear elastic and perfect plastic, which are rather simple to use (and which underpin many classical soil mechanics calculations) but which do not reproduce key features of material response, particularly volume change characteristics and non-linearity under working loads.*

2. *Students models, such as elastic work-hardening plastic models, which are helpful in explaining and bringing together apparently disparate aspects of material response at a pedagogic level but do not successfully match any given set of data.*

3. *Engineer's models, which go beyond the student's models, introducing those extra features which the engineer, using his judgement, reckons to be necessary for particular application, for example, non-linear elasticity, anisotropic elasticity and viscous properties.*

4. *Philosopher's models, which aims to describe all aspects of material response but which will usually be too elaborate and sophisticated for their application to be contemplated in any but the most sensitive projects, such as nuclear power*

stations and radio active disposal facilities, where unforeseen material response may have extremely serious consequences."

2.1.1.1. Linear Elastic Material Models

The simplest material models are the linear elastic models in which the material follows Hooke's Law. The relationship between stress and strain is assumed to be a unique straight line with constant slope, one-to-one relationship. This slope, which is the modulus of elasticity does not vary with stress or strain levels.

$$E=\frac{\sigma}{\epsilon}$$

Where, E = modulus of elasticity.

σ = stress.

ϵ = strain.

Two material properties are required for this type of model, modulus of elasticity and Poisson's ratio or shear modulus and bulk modulus.

2.1.1.2. Stress Dependent (Piece-Wise Linear Elastic) Material Models

In these models the material modulus of elasticity depends on the stress level. The relationship between stresses and strains is a one-to-one linear relationship represented by a number of linked straight lines, as can be seen in Figure 2.2. For each stress level, there is a

unique modulus of elasticity value and within any stress range the material follows Hooke's Law [Elliott and David, 1989].

$$E_{ij}=\frac{\sigma}{\epsilon}$$

Where, E = modulus of elasticity for stress level $<$ i and $>$ j.

2.1.1.3. Non-Linear Material Models

There is not a straight line relationship between stresses and strains in non-linear material models. The material response could be pure elastic (non-linear elastic) or elastic-plastic (non-linear elastic plastic) depending on the material response to release of the applied load. In general, for most pavement materials nonlinearity is associated with elastic-plastic behavior. Figure 2.3 shows the stress-strain relationship for a linear and non-linear materials.

2.1.1.4. Elastic-Plastic Material Models

For many materials the overall stress-strain relationship cannot be considered a unique relationship as in the case of elastic materials, e.g. many states of strain can correspond to one state of stress and vice versa. When this type of material is loaded with a load level higher than a previous load level, some additional permanent deformation will be developed. If the second load level is less than the previous load level, an elastic response will be observed. The irrecoverable, permanent, deformation that remains under zero load can be regarded as defining new reference states from which subsequent elastic response can be measured, provided the past

maximum load is not exceeded. The departure from elastic response that occurs as reloading proceeds beyond the past maximum load is called "yielding" and the past maximum load becomes a current yield point [Wood, 1990].

Elastic-plastic models incorporate the following assumptions:

1. For some changes in effective stress the response is fully recoverable.
2. The yield surface is a limit to the region of effective stress space that can be reached with purely elastic response. The history of changes in effective stress which the material has experienced controls the shape, size and location of the yield surface.
3. Whether a change in effective stress takes the material outside or inside its current yield surface will control whether or not irrecoverable (plastic) deformations will occur.

The elastic-plastic model has four components [O'Reilly and Brown, 1991]:

1. Elastic component, which represents the pure elastic response of the material inside its current yield surface.
2. Yield surface, which is a boundary between pure elastic response and elastic-plastic response of the material.
3. Plastic potential function and flow rule, which describe the mechanism of plastic deformation and indicates the direction in which the plastic strain increment vector happens.
4. Hardening rule, which is the link between change in size and/or position of the yield surface and the magnitude of the plastic strains.

Roscoe and Burland, 1968, modeled cohesive soils as elastic-plastic materials (Cam-Clay Model). The Cam-Clay Model assumes that yield loci and plastic potentials are identical and elliptical in the p':q effective stress plane. subsequent studies [Wood, 1990] showed a good agreement between Cam-Clay Model predictions and the laboratory measured results. Figure 2.4 [Wood, 1990] shows the yield surface of the Cam-Clay Model. The elliptical yield loci can be determined from the following equation:

$$\frac{P'}{P'_o} = \frac{M^2}{M^2+\eta^2}$$

Where, $\eta = q/P'$.

M = shape factor.

P' = effective stress.

P'_o = reference size of yield locus.

q = deviator stress.

This equation describes a set of ellipses, all having the same shape (controlled by M), all passing through the origin, and having sizes controlled by P'_o. When the soil is yielding, the changes in size P'_o of the yield locus is linked with the changes in effective stresses through the following differential equation [Wood, 1990]:

$$\frac{\delta P'}{P'}+\frac{2\eta\delta\eta}{M^2+\eta^2}-\frac{\delta P_o'}{P_o'}=0$$

Where, $\delta P'$ = the change in the effective stress

$\delta P_o'$ = the charge in the size of yield locus

The Drucker-Prager Model [Drucker and Prager, 1952 and ABAQUS, 1989b] is an elastic-plastic model commonly used to analyze cohessionless materials. Cohessionless materials are assumed to behave as elastic materials for low stress levels. When the stress level reaches a certain yield stress the material will start to behave as an elastic-plastic material. A linear strain rate decomposition is assumed so that

$$\delta\epsilon=\delta\epsilon^e+\delta\epsilon^p$$

Where, $\delta\epsilon$ = total strain.

$\delta\epsilon^e$ = elastic strain.

$\delta\epsilon^p$ = plastic strain.

The elastic strain follows Hooke's Law, while the plastic strain can be determined as follow:

$$\delta\epsilon^p=\frac{\upsilon\epsilon\cdot}{(1-\frac{1}{3}\tan\varphi)}\frac{\upsilon g}{\delta\sigma}$$

Where, $g = t - p \tan(\varphi)$.

φ = dilation angle.

Figure 2.5 shows the assumed stress-strain curve for a granular material, while Figure 2.6 shows different yield surfaces for the Drucker-Prager model [Drucker and Prager, 1952 and ABAQUS, 1989b].

2.1.1.5. Visco-Elastic Material Models

Viscoelasiticty introduces a time-dependent contribution into the elastic response of the material. The loading time, rate of loading and duration between repeated loads have a significant effect on the response of these types of materials. The response of viscoelastic materials can be described with reference to the one-dimensional systems of linear springs and dashpots shown in Figure 2.7 [O'Reilly and Brown, 1991], Voigt parallel model (a), Maxwell series model (b) and the combined standard linear solid model (c). The linear spring produces a deformation proportional to the applied load, while the dashpot produces a rate of deformation proportional to the applied load. All of these models will represent effects of creep (deformation under constant applied load) and relaxation (change of load under constant deformation), see Figure 2.8 [O'Reilly and Brown, 1991]. The basic equation linking variation of force F and displacement u with time t for the standard linear solid model is:

$$F+\frac{\lambda}{S_1}\frac{dF}{dt}=S_2[u+\frac{\lambda(S_1+S_2)}{S_1S_2}\frac{du}{dt}]$$

Where, S_1 and S_2 are spring constants and represents the velocity-dependent resistance of the dashpot. The Voigt model can be obtained from this equation by setting S_1 to infinity, while the Maxwell model can be obtained by setting S_2 to zero [O'Reilly and Brown, 1991].

These one-dimensional models can be extended without introducing any new concepts. Separate, superimposed viscoelastic models might be used for the distortional and volumetric response of the material.

2.1.1.6. Elastic-Viscoplastic Material Models

Some elastic-plastic materials such as clays may have viscous properties. Such material behavior can be represented as a combination of a visco-elastic and an elastic-plastic response. Elastic-viscoplastic materials are time dependent materials. Also, for low stress levels, the material response is elastic. When the stress exceeds the yield stress, such material starts to behave as an elastic-plastic material. Figure 2.9 [O'Reilly and Brown, 1991] shows a one-dimensional elastic, viscoplastic model. In this model, the elastic response is governed by the spring. The parallel spring, slider, and dashpot introduce plastic and viscous response.The constitutive equations for this model are:

[O'Reilly and Brown, 1991]:

$$F = S_1 u \qquad \text{for F} > \text{Y}.$$

$$\frac{F(S_1+S_2)}{S_1} + \frac{\lambda}{S_1}\frac{dF}{dt} = Y + S_2 u + \lambda \frac{dF}{dt} \qquad \text{for F} > \text{Y}.$$

2.2 Load Models

Pavement structures are subjected to traffic loads and environmental effects. Vehicle type, axle load, axle configuration, tire pressure, speed and number of load applications are factors that have to be included in pavement structural analysis. Truck traffic is typically modeled in two ways:

1. Static load distributed uniformly over an area, e.g., circular area. The effect of speed, rate of load application and number of load applications is ignored in this case. Static loading is common by assumedfor pavement analysis [Yoder and Witczak, 1975].
2. Dynamic moving load, point or distributed uniformly over an area. In this case the effect of speed, rate of load application and number of load applications is consider in the analysis.

Environmental factors have a great influence on pavement behavior. Environmental factors include [Yoder and Witczak, 1975]:

1. Frost action, when a pavement is subjected to freezing, water will be stored as ice lens or crystals. When the temperature increases, the ice melts creating a high moisture content and causing a reduction in the soil strength.
2. Temperature, temperature changes have a significant effect especially on rigid pavements. The change in temperature causes a change in the volume of concrete slabs, which develop high internal stress levels, warping and friction stresses. Also, temperature has a significant effect on asphalt mixtures. Asphalt mixtures' stiffness is lowered with increase in temperature.

3. Moisture, moisture content affect cohesive soil strength. Dry clays show high strength. However, near saturation their strength is reduced significantly. Rainfall and other water sources may cause subdrainage related problems for rigid pavements, such as pumping and erosion. Similar to temperature changes, moisture changes cause high internal stress in rigid pavements.

2.3. Analysis Algorithm (Static versus Dynamic Analysis)

A materials' behavior under repeated (cyclic) loads can be significantly different from its behavior under static loads. When the magnitude of the non-constant component of loading is large, such as truck traffic loads, the cyclic nature of loading can be of very considerable importance and , hence, cannot reasonably be ignored. This difference can be categorized into three distinct classes [O'Reilly and Brown, 1991]:

1. Effect of stress reversal.
2. Rate-dependent response.
3. Dynamic effects.

2.3.1. Effect of Stress Reversal

Stress reversal refers not to a change in the sign of a stress but to a change in the sign of the rate of stress increase. For example, an increase in the stress magnitude followed by reduction would, in this sense, be a stress reversal despite the fact that all stresses continue to act in the same direction. Figure 2.10 indicates the behavior of dry granular soil subjected to cyclic stress-controlled loading. Each load cycle is accompanied by a change in shear strain,

some of which is recoverable and some of which is not. The magnitude of the recoverable strain remains fairly constant during each cycle. On the other hand, the irrecoverable or plastic strain developed during each successive cycle tends to reduce with the increase of the number of load cycles. Eventually, the soil attains a form of equilibrium for this loading pattern, at which stage the magnitude of the recoverable strain experienced during any cycle greatly exceeds the plastic strain increment for that cycle [O'Reilly and Brown, 1991].

The stress reversals' importance appears in two closely interrelated phenomena exhibited during the application of load cycles: changes in material stiffness and the dissipation of energy within the material. In Figure 2.11 the stiffness exhibited during a sequence of cyclic loading is illustrated. It can clearly be seen that immediately after each stress reversal the stiffness increases dramatically and subsequently decreases. Further, during the stress cycle the stress sustained at any strain level of the unloading phase is lower than that at the corresponding strain during the loading. This phenomenon, which is clearly observed in Figure 2.10, means in crude terms that the soil is not pushing back as hard as it was pushed. This is known as "hysteresis" and indicates that the soil has failed to return all the energy put into it during loading. In dynamic analysis, hysteresis is known as "material damping" and indicates the capacity of the material to suppress its own vibration by absorbing energy.

2.3.2. Rate-Dependent Response

Rate dependency is the influence of the rate of loading, or alternatively the rate of strain, on the strength and stiffness of a material. This phenomenon can be attributed to two sources: the viscous interpartical action and the time dependent dissipation of excess pore pressure

generated during loading in situations which include the possibility of drainage. Figure 2.12 shows the rate dependency of both strength and stress-strain response for clay soils. From this figure it is clear that the shear strength of clays increases when higher strain rates are imposed.

2.3.3. Dynamic Effects

Dynamic loading cycles include significant dynamic effects, especially when the loading frequency is high. Normal truck traffic loading frequency tends to be in the range of 1 to 20 Hz. In dynamic analyses, factors such as damping, realistic modeling of boundary conditions and stiffness of materials at small strain levels take on enhanced importance.

2.4. Pavement Analysis

Pavement structural analysis procedures have to address three main issues: material models, load model and analysis algorithm. It is complicated to consider actual pavement material and load characteristics at the same time. For example, pavement materials are either elastic-plastic or visco-elastic materials. Truck loads are dynamic moving loads, and therefore, dynamic analysis should be used to analyze pavements subjected to truck loads. Also, environmental effects, such as temperature and moisture changes, have to be considered in the analysis. Most of the existing pavement analysis procedures simplify the problem by ignoring one or more of these conditions. In the following section some of the existing pavement structural analysis procedures will be discussed and the important assumptions highlighted.

2.4.1. Flexible Pavement Analysis

2.4.1.1. Boussinesq's Equations

In 1885 Boussinesq formulated a set of equations to calculate the stresses, strains and deflections of a soil mass subjected to a point load [Boussinesq, 1885]. These equations are based on the following assumptions:

1. The soil mass is homogeneous and isotropic.
2. The soil mass is linear elastic and extended to infinity in the horizontal plane and semi-infinite in the vertical direction.
3. The applied load is a static point load.

Two material properties are required to calculate the response to any load: modulus of elasticity (E) and Poisson's ratio (μ). Table 2.1 [Ullidtz, 1987] shows Boussinesq's equations for a point load. Boussinesq extended these equations to be used to calculate the stresses, strains and deflections under distributed loads .

2.4.1.2 Odmark's Method

The principle of Odmark's method [Odmark, 1949] is to transform a system consisting of layers with different moduli into an equivalent system where all layers have the same modulus, and on which Boussinesq's equations can be applied. Odmark's transformation is based on equal stiffness criteria as follows:

$$h_e = h_i \sqrt[3]{\frac{E_i(1-\mu_e^2)}{E_e(1-\mu_i^2)}}$$

Where, h_e and h_i are the thickness of the i^{th} and the equivalent layer, respectively.

2.4.1.3 Burmister's Method (Two Layer Analysis)

Burmister solved the two-layer system by applying the methods of the "mathematical theory of elasticity" to the problem [Burmister, 1943]. He used the stress and displacement equations of elasticity for the three-dimensional problem in his solution. The following assumptions were required for the two-layer analysis:

1. The two-layer system consists of a surface layer or pavement of a certain thickness h_1, which rests continuously upon and reinforces a weaker subgrade layer.
2. A surface load is applied, uniformly distributed over a flexible bearing area of radius r.
3. The soils of each of the two layers are homogeneous, isotropic, elastic materials, for which Hooke's law is valid.
4. The surface reinforcing layer is assumed to be weightless and to be infinite in extent in the horizontal direction, but of finite thickness h_1. The subgrade layer is assumed to be infinite in extent both horizontally and vertically downward.
5. The solution of the problem must satisfy certain necessary boundary conditions, namely, that the surface of layer 1 must be free of normal and shearing stresses outside the limits of the loaded area, and that at infinite depth the stresses and displacements on the subgrade layer must be equal to zero.
6. The solution for the two-layer system must satisfy certain essential continuity

conditions of stress and displacement across the interface between layer 1 and 2. It is assumed that the two layers are continuously in contact and act together as an elastic medium.

7. Poisson's ratio (μ) has to either 0 or 0.5 in both layers.

The two-layer system assumed by Burmester [Burmister, 1943] is shown in Figure 2.13.

2.4.1.4 N-Layer Analysis

Based on Burmister's method Acum and Fox [Acum and Fox, 1951] presented exact solutions for the boundary stresses in the center line of a circular, uniformly distributed load acting on the surface of a three-layer half-space. They produced the first extensive tabular summary of normal and radial stresses in three-layer systems at the interaction of the plate axis with the layer interface [Yoder and Witczak, 1975]. Jones [Jones, 1962] and Peattie [Peattie, 1962] subsequently expanded these solutions to a much wider range of solution parameters.

With the advent of computers, a number of computer programs were developed to calculate stresses, strains and deflections of layered elastic systems subjected to one or more static loads. Most of these programs are based on a modified form of Burmister's method. Figure 2.14 shows the general concept of a multilayered elastic system [Yoder and Witczak, 1975]. Bitumen Structures Analysis in Roads (BISAR) [BISAR, 1972] is one of the most commonly used programs to analyze flexible pavements as a multi layer elastic system subjected to circular loads. BISAR has the capability to analyze layered systems without interface friction mobilized and the presence of surface shearing forces [Yoder and Witczak, 1975]. Chevron [Santucci, 1977] developed another multi-layer pavement analysis program.

2.4.2. Rigid Pavement Analysis

Rigid pavements respond differently to loads than flexible pavements. Flexible pavement layers have limited bending strength. However, a rigid pavement slab has a significant bending strength and stresses from applied loads are distributed over underlying layers by bending action. Rigid pavement boundaries, such as joints and edges, create critical loading points that result in high stresses in the rigid pavement.

2.4.2.1 Westergaard Solution

Westergaard's work [Westergaard, 1925] was the first serious attempt to find a theoretical solution for rigid pavement analysis. He made one important simplification compared to elastic theory. He assumed that the subgrade cannot transfer shear stress, e.g., Winkler subgrade. This means that the vertical pressure or reaction of the subgrade on the slab is a proportionat to the lab deflection, e.g., modulus of subgrade reaction (k) times the deflection. In Figure 2.15 a Winkler and an elastic subgrade are shown. In Westergaard's original work [Westergaard, 1925] the following assumptions were made:

1. The concrete slab acts as a homogenous elastic solid in equilibrium.
2. The reaction of the subgrade is solely vertical, and proportional to the deflection of the slab.
3. The slab is resting on a set of springs with spring constant k (modulus of subgrade reaction), Winkler foundation.
4. The thickness of the slab is uniform.
5. The load at the interior and the corner of the slab is distributed uniformly over

a circular contact area.

6. The Load at the interior edge of the slab is distributed over a semicircular area.

7. The load is carried by the loaded slab only.

2.4.2.2. Pickett Solution

In 1951, Pickett and Ray [Pickett and Ray, 1951] developed a formula for predicting rigid pavement response to corner loads considering two conditions:

1. Protected corner. Provision is made to transfer 20% or more of the load from one slab to the other by mechanical means.

2. Unprotected corners. No provision for load transfer.

2.4.2.3. Linear Elastic Layered Method

As mentioned earlier, the discontinuity of rigid pavements at joints and edges violates the assumption of infinite lateral and longitudinal extent for n-layer analysis. Therefore, n-layer analysis cannot be used directly to predict rigid pavement response to corner or edge loading. The stress due to interior loading in two- and three-layered elastic systems such as a slab or slab-and-subbase resting on uniform subgrade can be determined using Burmister [Burmister, 1943] or Acum and Fox [Acum and Fox, 1951] methods.

2.4.2.4. Finite Element Method

The finite element method is a numerical method for solving problems with complicated geometries, loading and material properties. In general, it is not possible to obtain analytical

solutions for these type of problems [Logan, 1986]. There are two general approaches associated with the finite element method: force, or flexible method, and displacement, or stiffness method. The latter method is most commonly used and is the basis of the implicit ABAQUS [ABAQUS, 1989c] theoretical formulation. In the stiffness method nodal displacements are unknown. Equations are developed that represent the nodal displacements based on the equations of equilibrium and a relation between forces and displacements. Virtual work, direct equilibrium and weighted residuals are commonly used to relate nodal forces to nodal displacements [Logan, 1986]. A finite element method generates a number of algebraic equations. The number of these equations depends on the number of nodes. Computer system speed determines how fast finite element method solutions can be obtained.

Several rigid pavement structural analysis finite element method (FEM) computer programs are available. In the following section some of these FEM computer programs will be reviewed.

2.4.2.4.1. ILLI-SLAB Finite Element Model

ILLI-SLAB is a two-dimensional finite element program originally developed in 1977 for the Federal Highway Administration (FHWA) and Federal Aviation Administration (FAA) for structural analysis of one- or two-layer concrete pavements, with or without mechanical load transfer systems at joints and cracks [Tabatabaie, 1977]. The original ILLI-SLAB model is based on the classical theory of a medium-thick plate on Winkler foundation. ILLI-SLAB has been continually revised and expanded to improve the program's accuracy and ease of application; and to incorporate new foundation models and thermal gradient modeling techniques. The 1986

version of this program is applicable to the structural evaluation of jointed plain concrete pavements. Continuously reinforced and jointed reinforced concrete pavements, however, may also be modeled indirectly [FHWA, 1989]. The 1986 version of ILLI-SLAB has the following assumptions [FHWA, 1989]:

1. Small deformation theory of an elastic, homogeneous medium-thick plate is employed for the concrete slab, stabilized base and overlay.
2. In case of a bounded stabilized base or overlay, full strain compatibility is assumed at the interface. For the unbounded case, shear stress at the interface is neglected.
3. Dowel bars at joints are linear elastic and located at the neutral axis of the slab.
4. When aggregate interlock is specified for load transfer, load is transferred from one slab to an adjacent slab by shear.
5. Linear elastic properties are assumed for the concrete slab, base and overlay.
6. Loads are assumed to be static loads and the program uses a linear elastic analysis.

The following limitations were found in the 1986 version of ILLI-SLAB [FHWA, 1989]:

1. Jointed reinforced and continuously reinforced concrete pavements can be analyzed in an indirect way only.
2. The maximum number of layers that can be considered is three including the subgrade.
3. If temperature gradients are considered, only a single slab and Winkler subgrade can be used.

4. Does not consider that the effect of drainability of the pavement section may exist.
5. Does not consider traffic volume or moving load effects.
6. Considers only transverse joints and/or cracks with identical connection and load transfer mechanisms.
7. Considers only longitudinal joints and/or cracks with identical connection and load transfer mechanisms.
8. All joints and cracks must run parallel to, and along the entire length of the X and Y directions.
9. Fatigue properties and durability of the concrete slab or the subbase are not considered in the program.
10. Models the slab and subbase interface as either fully bounded or unbounded, partial bounding cannot be considered.
11. ILLI-SLAB does not consider any climatic effects except thermal gradients through the slab.

2.4.2.4.2 JSLAB Finite Element Model

JSLAB is a two-dimensional finite element program developed to model and analyze jointed reinforced concrete pavements [Tayabji and Colley, 1984]. Assumptions in the development of JSLAB are identical to ILLI-SLAB with the following exception:

The stiffness matrix in both JSLAB and ILLI-SLAB for the subgrade considered is based on the work done by Tabatabaie [Tabatabaie, 1977]. The concept of strain energy is currently

used in developing the subgrade stiffness matrix instead of the principle of virtual work which is used in JSLAB. Both approaches yield identical results, however, an error was found in the stiffness matrix that can lead to 3 to 5 percent error in ILLI-SLAB results [Zienkiewicz, 1977 and Ioannides and et al., 1984]. In the 1986 version of ILLI-SLAB, this error has been fixed and the stiffness matrix corrected [FHWA, 1989].

JSLAB has identical capabilities as ILLI-SLAB with the exception of partial contact between slabs and the subgrade. In addition, JSLAB is able to consider nonuniformly spaced dowels. JSLAB has limitations similar to those of ILLI-SLAB with the exception of the limitation regarding moisture gradient through the slab. Other limitations include:

1. The principle bending stresses and the vertical stress on the subgrade are not calculated.
2. Only a one-layer pavement system with uniform thickness can be analyzed when a moisture gradient through the slab is considered.
3. When vertical slab displacements are specified, applied loads cannot be located at that particular node or over any element adjacent to that node.

2.4.2.4.3. WESLIQID Finite Element Model

WESLIQID is a two-dimensional finite element computer program developed to analyze concrete pavements subjected to multiple wheel-loads. The following assumptions are involved with the development of WESLIQID [FHWA, 1989]:

1. The subgrade is modeled as a Winkler foundation and the concrete slab is modeled as medium-thick plate.

2. Assumptions regarding bonding of layers and dowels are identical to ILLI-SLAB.
3. The external loads are converted to a system of statically equivalent nodal loads, which often are not work equivalent to the applied load [Tabatabaie, 1977].

WESLIQID has the following limitations:

1. Jointed reinforced concrete pavements and continuously reinforced concrete pavements can be analyzed only in an indirect way.
2. Maximum number of layers is three including the subgrade.
3. Temperature gradients may only be considered for slab configurations of uniform thickness.

2.4.2.4.4. WESLAYER Finite Element Model

WESLAYER is a two-dimensional finite element computer program developed to compute the stresses in concrete pavements supported on an elastic solid or layered elastic foundation [Chou, 1981]. WESLAYER's method of solution is very similar to WESLIQID and their assumptions are identical with the exception of the subgrade modeling. WESLAYER uses Boussinesq's and multi-layered elastic analysis to model single and layered subgrades, respectively.

WESLAYER can analyze jointed and continuously reinforced concrete only in an indirect way and it can model not more than two slabs with one joint. The subgrade is limited to five layers maximum and the temperature gradient may only be considered for uniformly thick slab configurations.

Other rigid pavement structural analysis models include: H51 [Pickett, et al., 1951],

CRCP-2 [McCullough, et al., 1975], JCS-1 [Sawan, et al., 1982] and RISC [Majidzadeh, et al., 1984]. These models assume assumptions more or less similar to those assumed by ILLI-SLAB and WESLAYER. A summary of the important assumptions for different rigid pavement structural analysis models is presented in Table 2.2.

2.5. Load Equivalency Factors (LEF)

Truck traffic is a significant factor in highway pavement design, maintenance and evaluation. A broad measure of truck traffic is number of trucks per day or number of total trucks. However, trucks vary in load, number of axles and axle spacing. Such variation has an effect on pavement performance and should be addressed. To account for the variation in loading effects, a mixed traffic stream is converted to an equivalent amount of traffic of a standard axle load. An 18-kip single axle load with dual tires is commonly used as the standard axle load [Yoder and Witczak, 1975].

2.5.1. Load Equivalency Factors for Flexible Pavements

There are several approaches to evaluate the effect of loads on pavements, and therefore to determine LEF's. The LEF's can be based on equal loss of pavement serviceability, equal pavement response (e.g, surface deflection), or equal pavement distress (e.g., fatigue cracking or rutting).

2.5.1.1. Loss of Serviceability Approach (AASHTO LEF's)

In 1959 and 1960, the AASHO Road Test was conducted in Ottawa, IL [AASHO, 1962].

Two types of truck loading were used, single and tandem axles. The AASHTO Interim Design guide [AASHTO, 1972] used the results of the AASHO Road Test and the concept of Present Serviceability Index (PSI) as a measure of pavement performance. PSI is in general a function of pavement slope variance (roughness), cracking, and patching and for flexible pavements rutting. Pavement failure at the AASHO Road Test was defined in terms of a terminal serviceability instead of strict structural failure. Empirical relationships were developed to correlate PSI, as a measure of pavement performance, to the number of load repetitions. Based on these two factors, PSI and load repetitions, the AASHTO LEF's were developed. In the AASHO Road Test the maximum axle loads were 40 and 48 kips for single and tandem axles, respectively. In the 1986 AASHTO design guide [AASHTO 1986] LEF's for higher loads and for triple axle configuration are presented by extrapolating the statistical models developed based on the AASHO Road Test results.

2.5.1.2. Equal Pavement Response Approach (CanRoad LEF's)

In the summer of 1985, pavement surface deflection and interfacial tensile strain were recorded for trucks with single, tandem and triple axle configurations at fourteen sites located across Canada [CanRoad 1986]. Testing was conducted with different axle spacing, loads and speeds. Two sets of LEF's were developed using equal pavement response. These LEF sets are based on equal surface deflection and equal interfacial tensile strain [Rilett and Hutchinson, 1988], respectively.

These LEF's are determined for a given load as the sum of the ratios of peak response under the axles of this load to the peak deflection under the standard load. Figure 2.16 shows

the surface deflection profile of a triple axle load configuration and the formula used to calculate the deflection based LEF's for this axle configuration. LEF's based on the interfacial tensile strain were determined in the same way.

Both the AASHTO and CanRoad LEF's are presented in Figure 2.17. The load range of the CanRoad LEF's is smaller than that of AASHTO LEF's, especially for single axles.

2.5.1.3. Analytical Based LEF's

As another approach to determine LEF's, multi layer elastic analysis [Yoder and Witczak, 1975] has been used to predict pavement response. Assuming linear elastic properties for paving materials and static loading condition, the multilayer analysis can predict the elastic pavement response for different load parameters, such as axle load and spacing. The pavement damage due to different load parameters can be estimated using the predicted elastic pavement response and empirical correlations.

Fatigue cracking has been related to horizontal, elastic tensile strain at the bottom of the asphalt layer. A relation frequently used to estimate fatigue cracking due to different loading conditions was developed by Finn et al [Finn, et al., 1977]. This model can be used to predict the number of load repetitions required to develop a percent of fatigue cracking (i.e., 10 percent) of the wheel path area for the standard load and any other load (i). Consequently, the LEF for load (i) will be:

$$(LEF)_i = \frac{[N_f]_{18}}{[N_f]_i}$$

Where, $[N_f]_{18}$ and $[N_f]_i$ are the number of repetitions of the standard load and load (i) required to develop 10% fatigue cracking, respectively.

Flexible pavement structure rutting occurs because of permanent deformation of the asphalt layer(s), base, subbase or subgrade. An analysis procedure such as multi layer elastic analysis does not provide permanent pavement deformation directly. In using such procedures, the failure criterion for rutting is expressed as a function of vertical elastic compression strain at the top of the subgrade. Consequently, only rutting in the subgrade is considered [Mahoney, 1988]. Based on this concept, Chevron [Santucci, 1977] developed a model to estimate the number of load repetitions which causes 0.75 inch rut depth. As in the case of equal fatigue cracking, an LEF set based on rutting could be developed as the ratio of number of repetitions to failure of the standard load to that of any other load.

VESYS 5, a pavement analysis computer program developed by the Massachusetts Institute of Technology [Kenis, 1987], was used to develop two sets of LEF's based on pavement cracking and rutting, respectively. The program is based on static loading and linear elastic layer theory [Cobb and Kenis, 1990].

2.5.2. Load Equivalency Factors for Rigid Pavements

Several literature searches were conducted for LEF's for highway rigid pavement.

As mentioned earlier, AASHTO LEF's are based on the AASHO Road Test data [AASHTO 1962] and the concept of Present Serviceability Index (PSI) as a measure of pavement performance. For concrete pavements, PSI is a function of pavement slope variance (roughness), cracking and patching. Empirical relationships were developed to correlate PSI, as a measure

of pavement performance, to the number of load repetitions for a range of slab thickness. Based on these two factors, PSI and load repetitions, the AASHTO LEF's were developed. Similar to flexible pavements, in the 1986 AASHTO design guide [AASHTO, 1986] LEF's for load levels higher than those included in the AASHO Road Test and for triple axle configuration are developed by extrapolation. These LEF's are developed using the statistical models based on the AASHO Road Test results.

Fatigue analysis was used to develop a concept of LEF's for rigid pavements [Hallin and et al., 1983]. The number of load application to failure for different loads was predicted using the following formula:

$$N_i = 225{,}000(M_r/\sigma)^4$$

Where, N_i = number of repetitions to failure.

M_r = Modulus of rupture of the concrete, psi.

σ = Tensile stress, psi.

Then LEF's were assumed to be:

$$LEF_i = \frac{N_{18}}{N_i}$$

The stress analysis was made with assumptions similar to those for the multi-layer elastic analysis, linear elastic materials and static loads.

2.5.3. Load Equivalency Factors for Composite Pavements

As mentioned earlier the most commonly used LEF's are those developed by the American Association of State Highway Officials (AASHO) [AASHTO 1972]. These LEF's are based on the AASHO Road Test [AASHO 1962] results and the concept of pavement serviceability. In the AASHO Road Test, asphalt and concrete pavement sections were constructed and tested with single and tandem axle loads. The present serviceability index (PSI), which is a function of slope variance (roughness), cracking and patching for concrete pavement plus rutting for asphalt pavement, was used as a measure of pavement performance. Empirical relationships were developed to correlate PSI to the number of load repetitions for asphalt and concrete pavements. No composite pavement sections of asphalt overlaying concrete were constructed for the AASHO Road Test and therefore, no LEF's were developed for composite pavements. The 1993 AASHTO design guide [AASHTO 1993] recommends the use of concrete pavement LEF's for composite pavements. In this case, the effect of traffic on composite pavements is assumed to be similar to that of concrete pavements.

Other empirical LEF's, such as CanRoad LEF's [CanRoad 1986], do not address composite pavements. Analytically based LEF's, such as those reported by Finn et al. 1977, are based on multi-layer elastic analysis which assumes that pavements are extended to infinity in the lateral and longitudinal directions and the subgrade has infinite depth or a rigid. Assumptions are also made in multi-layer analysis that pavement materials are linear elastic and truck loads are static. Previous analysis. A lack of agreement between these type of LEF's and the AASHTO LEF's was found and presented in this report.

2.6. Current Procedure for Permitting Overloaded Trucks in Indiana

Indiana legal truck weights limits of [Oversize-Overweight Vehicular Permit Handbook IDOH 1988] are stated as follows:

" *The total gross weight, in pounds, of any vehicle or combination of vehicles with load shall not exceed an overall gross weight on a group of two or more consecutive axles as computed by the following formula:*

$$W=500[(\frac{LN}{N-1})+12N+36]$$

Where,

W = *Overall gross weight on any group of two or more consecutive axles to the nearest 500 pounds.*

L = *Distance in feet between the extreme of any group of two or more consecutive axles.*

N = *Number of axles in the group under consideration.*

However, the weight may not exceed:

- *Maximum gross weight - 80,000#*
- *Maximum Single Axle Weight - 20,000#*
- *Maximum Tandem Axle Weight - 17,000#*
- *Maximum Wheel Weight - 800# per linear inch of tire measured between the flanges of the rim.*

Exception to the formula is for two consecutive sets of tandem axles which may carry a gross

load of 34,000 pounds each, providing the overall distance from center to center between the first and last axles is 36 feet or more. Also, the following weights take precedent when they are grater than the weights allowed by the formula:

- *Maximum gross weight - 73,280#*
- *Maximum Single Axle Weight - 18,000#*
- *Maximum Tandem Axle Weight - 16,000#*
- *Maximum Wheel Weight - 800# per linear inch of tire measured between the flanges of the rim."*

Trucks exceeding these limits, overloaded trucks, are required to have an overload permit before using the Indiana highway network. The permit is guaranteed for a fee if the overloaded truck does not exceed the following limits [IDOH 1988]:

- Maximum gross weight - 108,000#
- Maximum Single Axle Weight - 28,000#
- Maximum Tandem Axle Weight - 24,000#
- Maximum Axle Group Weight - 51,000#
- Maximum Wheel Weight - 800# per linear inch of tire measured between the flanges of the rim.

Current INDOT regulations allow a truck exceeding the above limits to apply for an overload permit. In this case, the overload permit is evaluated for bridges and processed in two phases. In Phase 1, a simply supported beam and a two equal-span continuous beam are analyzed for the given permit vehicle for spans from 20 to 120 feet in increments of 10 feet. The equivalent HS loading of the given overloaded truck is calculated by comparing the bending moments

induced by the overloaded truck with those induced by the HS20 design truck [AASHTO 1983]. The overloaded truck will be permitted if its equivalent HS loading is less than HS30, i.e., 1.5 times the HS20 design truck. When a truck matches a prior permitted truck, the prior results from Phase 1 are used for a quick evaluation. If the overloaded truck does not satisfy Phase 1 criteria, Phase 2 is implemented which involves a detailed load rating. The detailed load rating of Phase 2 requires specific information about the truck and bridges on the route for which the permit is requested. No evaluation for the damage effect of overloaded trucks on pavements is currently made.

CHAPTER 3 THE THREE-DIMENSIONAL DYNAMIC FINITE ELEMENT PROGRAM

ABAQUS [ABAQUS, 1989a] is a general finite element program. It designed as a flexible tool for numerical modeling of structural response. ABAQUS has been used to analyze buildings, mass concrete structures, soil masses and small engine parts, subjected to static and dynamic load. In the analysis presented in this report, ABAQUS was configured to analyze flexible, rigid and composite pavements. A finite element model (FEM) consists of a geometric description (finite element mesh of nodes and elements), set of properties associated with the elements describing their attributes (material models) and representations of special features such as interface elements, gap elements, ..., etc. FEM must contain a set of constraints, such as boundary conditions, which are imposed at the start of the analysis. Initial conditions, such as initial stresses, temperatures or moisture contents, may be required. Depending on the FEM capability, applied load parameters, such as load type, magnitude and frequencyare specified. In some cases, environmental properties, such as fluid surrounding the model, should be included. The general FEM features of ABAQUS may be grouped as:

1. Element types.
2. Material models.
3. Load models.
4. Analysis procedures.
5. Response parameters.

In this chapter ABAQUS' features which are used in this study to analyze pavements will be presented.

3.1. Element Types

ABAQUS has an element library intended to provide a complete geometric modeling capability. Any combination of elements may be used to make up the model. All elements use numerical integration to allow complete generality in material behavior. ABAQUS element library has two- and three-dimensional elements. The following element types are available:

1. Stress-displacement elements.
2. Heat transfer elements.
3. Effective stress/pore pressure elements (for soils).
4. Interface elements.
5. Coupled temperature/displacement elements.
6. Coupled temperature/displacement interface elements.
7. Rigid surface interface elements.
8. Slide line interface elements.
9. User defined elements.
10. Acoustic and acoustic interface elements.

In the following analysis, pavement structures were modeled using three-dimensional stress-displacement elements. Interface elements and effective stress/pore pressure elements were also applied in the analysis [ABAQUS, 1989b and ABAQUS, 1989c].

3.1.1. Solid (Continuum) Stress/Displacement Elements

Solid stress/displacement (SSD) elements have no special bending terms. The SSD element library includes first order (linear) interpolation elements, and second order (quadratic)

interpolation elements, in one, two, or three dimensions. All of these elements are fully isotropic, that is, coordinate interpolation is the same as displacement interpolation, so that curved (parabolic) edges can be used on the second order elements. Table 3.1 summarizes different features of SSD elements used in the analysis.

A reduced integration option is available for this type of element. It uses a lower order of integration to form the element stiffness. The mass matrix and distributed loadings are still integrated exactly. Reduced integration usually provides more accurate results and significantly reduces running time, especially for three-dimensional elements.

3.2. Material Models

The material library in ABAQUS is intended to provide comprehensive coverage of linear, nonlinear, isotropic and anisotropic material models. The use of numerical integration in the elements means that this flexibility in material modeling can be used to full advantage to analyze the most complex composite structures.

Material behavior is often specified as a function of independent variables. Very commonly temperature is one of the independent variables. Figure 3.1 shows the relationship for a simple, isotropic linear elastic material in terms of modulus of elasticity and Poisson's ratio as a function of temperature. In this case six values are used to specify the material. In some cases, several independent variables are needed. As an example, Figure 3.2 shows the yield stress of an elastic-plastic material as a function of two independent variables, plastic strain and temperature.

ABAQUS provides a broad range of possible material behaviors. A material is defined

by choosing options which, together describe its behavior for the purpose of the analysis. The use of some material options is completely unrestricted. These options may appear alone or together with other options. Some options require the presence or exclude others. In Table 3.2 different material options available in ABAQUS that can be used in pavement analysis are presented. Combined options are presented in the same table [ABAQUS, 1989b].

In additional to these material options, ABAQUS provides some widely accepted material models, such as Cam-Clay model and Drucker-Prager model. In the following section, material models used in the subsequent analysis are presented.

3.2.1. Extended Drucker-Prager Model

The extended Drucker-Prager [Drucker and Prager, 1952] plasticity model is often used to model the plastic component of granular materials. Drucker-Prager uses a smoothed Mohr-Coulomb yield surface, associated inelastic flow in the deviatoric plane and separate dilation and friction angles. The use of a smooth surface in the deviatoric plane, instead of a true Mohr-Coulomb surface that exhibits vertices, has restrictive implications with respect to flow localization studies for granular materials. This is not expected to be of major significance for design applications where the Drucker-Prager model is intended to be used. Input data parameters define the shape of the failure and flow surface in the deviatoric plane as well as the friction and dilation angles [ABAQUS, 1989c].

The Drucker-Prager model has the following components:

1. Yield surface, shown in Figure 3.3.
2. Degree of plasticity, which describes the relationship between plastic strains and

the corresponding change in yield stresses. Perfect plasticity means that the yield stress does not change with plastic strain.

3. Hardening model, which describe changes in the yield surface size corresponding to the change in the yield stress. Isotropic hardening means that the yield surface changes size uniformly in all directions, so that as plastic straining occurs the yield stress increases (or decreases) in all stress directions.

3.2.2. Cam-Clay Model

Inelastic constitutive theories provided in ABAQUS for modeling clay materials are based on the critical state plasticity theory developed at Cambridge [Schofield et al., 1968 and Parry, 1972]. The specific model provided in ABAQUS is an extension of the modified Cam-Clay theory. Analysis is entirely in terms of effective stress: the soil may be saturated with a permeating fluid which carries a pressure stress and is assumed to flow according to D'Arcy's law.

Modified Cam-Clay theory is a classical plasticity model, which uses a strain rate decomposition in which the rate of mechanical deformation of the soil is decomposed additively into an elastic and a plastic part. Cam-Clay model has the following components: an elasticity theory, a yield surface, a flow rule and a hardening rule. Main features of the model are an increasing bulk elastic stiffness as the material undergoes compression, and, for the inelastic part of the deformation, a particular form of yield surface with associated flow, and a hardening rule that allows the yield surface to grow or shrink. Elasticity is modeled by assuming that the volumetric elastic response of the material is defined as a linear dependence of the change in the

logarithm of the equivalent pressure stress on the elastic part of the ratio of current to original volume. The elastic response may be linear or may also depend on the equivalent pressure stress.

A key feature of the model is the hardening/softening concept, which is developed around the introduction of a critical state surface (the locus of effective stress state where unrestricted, purely deviatoric, plastic flow of the soil skeleton occurs under constant effective stress). This critical state surface is assumed to be a cone in the space of the principal effective stress, as can be seen in Figure 3.4. The cross section of the surface in the Π-plane (the plane in principal stress space orthogonal to the equivalent pressure stress axis) is circular in the original form of the critical state model (in ABAQUS this has been extended to more general shape as shown in Figure 3.4) [ABAQUS, 1989c].

3.2.3. Concrete Model

The concrete model in ABAQUS is designed to provide a general capability for modeling plain and reinforced concrete. The model is designed for applications in which the concrete is subjected to essentially monotonic straining at low confining pressure.

The plain concrete model is intended primarily for the analysis of reinforced concrete structures. ABAQUS provides an option to model different types of steel reinforcement. Reinforcement is modeled as one-dimensional strain elements (rods). Standard plasticity models are used to describe the behavior of reinforcing materials. Effects associated with the reinforcement/concrete interface, such as bond slip and dowel action, may be modeled by introducing some tension stiffening to simulate load transfer across cracks.

Cracking is assumed to occur when the stress reaches a failure surface, which is called the "crack detection surface". This failure surface is taken to be a simple Coulomb line written in terms of the equivalent pressure stress, p, and the Mises equivalent deviatoric stress, q. Figure 3.5 shows yield and failure surfaces in the (p-q) plane.

Concrete in compression is modeled as an elastic-plastic material. Figure 3.6 shows the stress-strain curve assumed for concrete. A simple form of yield surface written in p and q stress is used, as well as, associated flow and isotropic hardening rules [ABAQUS, 1989b].

3.2.4. Viscoelastic Material Model

The viscoelastic material model used in this analysis models the dissipative losses caused by viscous (internal friction) effects in the material. There are elastic and viscous components of the model. A linear, small strain elastic or hyperelastic material model is used to describe the elastic part of the viscoelastic material behavior. The viscoelastic material model is a time dependent model, in which the material properties for instantaneous and long term loading are included to describe the effect of loading time.

Viscoelastic material models can be used in static analysis (inertia effects ignored) or in dynamic analysis. A linearized viscoelastic response is used in the dynamic analysis. This linearized viscoelastic response is a perturbation about a nonlinear pre-loaded state, which is computed on the basis of purely elastic behavior and assuming that the vibration amplitude is sufficiently small so that both the kinematic and material response in the dynamic analysis can be treated as linear perturbations about the pre-deformed state [ABAQUS, 1989b].

3.3. Load Models

ABAQUS allows for two types of loads; static and dynamic loads (function of time). In the subsequent analysis dynamic loads were used. Figure 3.7 shows some examples of load functions. Point loads can be applied at nodes. Distributed loads are prorated based on the element area to the nearest node.

3.4 Stress Analysis Procedures

A large class of stress analysis problems can be solved with ABAQUS. Stress problems are devided into static and dynamic response, the distinction is based on whether or not inertia effects are significant. ABAQUS allows a combination of static and dynamic analysis. Static preload might be applied, such as dead weight of pavement layers, then a linear or nonlinear dynamic analysis might be used to predict response to dynamic load, such as a moving truck load.

Stress analysis problems are also devided into linear or nonlinear response cases. In linear, static analysis, model response to loads can be obtained directly, while in the case of nonlinear dynamic analysis the harmonic response of the model must be predicted. Generally the natural modes of the model are extracted and used for this purpose. There are three general sources of nonlinearity [ABAQUS, 1989b]:

1. Material nonlinearity. ABAQUS offers models for a wide range of nonlinear material behavior as described above in the material models section. Most of these materials are history dependent, i.e., the material's response at any time depends on what happened to it at previous times. Material nonlinearity is the

main source of nonlinearity in pavement response [Yoder and Witczek, 1975].

2. Geometric nonlinearity. For large displacement analysis when the kinematic relationships are nonlinear, such as in case of buckling or collapse.

3. Boundary nonlinearity, such as in friction and contact problems. The contact problem is relatively straightforward in static modeling, although iteration is needed to determine if a particular point is in contact or not. In dynamic analysis, there must be a loss of energy associated with two nodes coming into contact, to represent the local solution (stress wave) which cannot be modeled on the scale of the discrete finite element mesh. ABAQUS solves impact equations at contact providing new initial conditions for the continuation of the dynamic response after contact. In pavement analysis, this type of nonlinearity exists around joints and wide cracks.

3.4.1. Static Stress Analysis

Static stress analysis is used when inertia effects can be neglected. Linear static analysis involves the specification of load cases and appropriate boundary conditions. If nonlinearity exists, nonlinear static analysis should be used. Nonlinear static analysis requires the solution of nonlinear equilibrium equations. ABAQUS uses Netwon's method for this purpose [ABAQUS, 1989b and 1989c].

3.4.2. Dynamic analysis

ABAQUS offers several methods for dynamic analysis. Linear dynamic problems are

generally performed by using eigenmodes of the model as a basis for calculating the response. In such cases, model frequencies have to be extracted first. Several response options are available in ABAQUS [ABAQUS, 1989b and ABAQUS, 1989c]:

1. Time history analysis; the response of the model is defined as a function of time, based on a given time dependent loading.

   This option was used in the subsequent analysis.

2. Response Spectrum analysis; the magnitude of the generalized displacement associated with each natural mode is defined as a function of the frequency of oscillation of that mode.

3. Steady-state analysis; this option is used when a model is subjected to a harmonic loading at a given frequency.

4. Random response analysis; this option is used when a model is subjected to a nondeterministic continuous excitation that is expressed in a statistical sense using a power spectral density function.

Nonlinear dynamic analysis requires that all of the equations of motion of the system must be integrated through time. Therefore, direct integration of the system must be used. Three approaches for direct integration are available in ABAQUS:

1. Standard method, which uses an implicit time integration operator. The integration method is a slight modification of the "Trapezoidal Rule" and is called "Hilber-Hughes-Tayler Operator" [Hilber et al., 1978]. The Hilber-Hughes-Tayler operator is implicit, which means that the nonlinear dynamic equilibrium equations must be solved at each time increment. This is done iteratively using Newton's method or quasi-Newton method. The standard method was used in the subsequent analysis.

2. Central difference method. This method is fully explicit but only conditionally stable. The stability limit (the longest time increment that can be taken without the method generating large, rapidly growing errors) is closely related to the time required for any stress wave to cross the smallest element dimension in the model, so that the time increment has to be very short if the mesh contains small elements, or if the bulk modulus of the material is very high. The method is therefore only computationally attractive for problems where the total dynamic response time that must be modeled is only a few orders of magnitude longer than this stability limit, such as wave propagation studies.

3. Subspace projection method. In this method the eigenmodes of the linear system, extracted prior to the dynamic analysis, are used as a small set of global basis vectors to solve the problem, as a classical Ritz method. For some cases this method can be very effective. As with other direct integration methods it is more

expensive in terms of computer time than the modal methods of purely linear dynamic analysis, but it is often significantly less expensive than the methods of direct integration of all of the equations of motion of the model, standard method. This method is implemented in ABAQUS using the explicit operator to integrate the equations of motion projected onto the eigenmodes of the linear system.

3.4.3. Geostatic Stress State

The geostatic stress state is an equilibrium configuration of the undisturbed soil or rock body under geostatic loading (such as dead load of pavement layers) and usually includes both horizontal and vertical stress components. The initial stresses are first defined according to boundary conditions and geostatic loading. ABAQUS checks the equilibrium against user specified tolerances and iterates, if needed, to obtain a stress state which equilibrates the prescribed boundary conditions and loads [ABAQUS, 1989b].

3.5. Response Parameters

Output parameters depend on the previous parameters (element types, material models, load models and analysis procedures). For example, inelastic strains cannot be output of linear elastic analysis. Table 3.3 shows the general response parameters that can be predicted using ABAQUS.

CHAPTER 4 ANALYSIS OF FLEXIBLE PAVEMENT

Predominately, flexible pavement structural response to loads is predicted using elastic multi-layer analysis. This type of analysis assumes that pavements are only loaded statically [Yoder and Witczak, 1975], while in reality pavements are subjected to both static and moving loads. Also, it assumes that paving and subgrade materials are linear or piece-wise linear elastic materials. However, asphalt mixtures are visco-elastic materials and clays exhibit plasticity. The inability of multi-layer analysis to represent actual loading conditions and pavement materials is significant. This significance is reflected in differences between predicted and measured pavement response. The simplicity and speed of multi-layer analysis has been used as justification for the relative results obtained. However, the three-dimensional, dynamic finite element program (3D-DFEM) [ABAQUS, 1989a], explained in Chapter 3, is available and provides a more realistic analysis for predicting pavement response.

The 3D-DFEM was used to analyze flexible pavements. The validity and then the application of the 3D-DFEM to flexible pavement analysis were examined. Validation was accomplished by analysis of both static and dynamic cases. These static and dynamic verification studies showed that the 3D-DFEM can be used, with confidence, to predict actual pavement response to moving loads. A sensitivity analysis was conducted using the 3D-DFEM non-linear, dynamic analysis capabilities. Factors ignored by elastic layer analysis were addressed, such as moving loads, system damping and visco-elastic and plastic behavior of pavement and foundation materials. The results of the verification studies and the sensitivity analysis are presented in this chapter.

4.1. Features of the Finite Element Model

4.1.1. Model Geometry

Conventional flexible pavements consist of layers, i.e. surface, base, and subbase on a subgrade. At some depth the subgrade can be considered as a deep foundation. The deep foundation may be an extension of the subgrade soil or another soil type. In some cases the subgrade or deep foundation is bedrock.

The first step in finite element analysis is to create the finite element mesh. Three factors control the finite element mesh (FEM) geometry:

1. Pavement geometry, which control the general size of the FEM.
2. Load configuration, such as distance between wheels and axles.
3. Degree of detail, i.e., locations where pavement response parameters will be predicted.

In general, FEM mesh dimensions have to be small enough to allow detailed analysis of the pavement section. However, small mesh dimensions increase the number of elements. As a result, memory and computational time increase. On the other hand, a coarse FEM mesh will not allow detailed analysis. A compromise is to use a fine FEM where a detailed analysis is desired and a coarse mesh elsewhere. An example of the mesh used in the subsequent analysis is shown in Figure 4.1. This FEM mesh consists of two equally spaced meshes in the horizontal (xy) plane. A coarse mesh with a 22.2" spacing was used in both the transverse (x) direction and longitudinal (y) direction. In the region of the load path finer mesh with a 4.44" spacing was used in the x direction. Mesh dimensions in the vertical direction were selected to match the pavement layer thicknesses (i.e., surface, base and subbase). The number of layers required to

model the subgrade depends on the detail desired in predicting the vertical pavement response. In this study, the surface and base course were each modeled as a single layer, while the subgrade was modeled as a set of five layers. The FEM mesh presented in Figure 4.1 has 5,670 nodes and 5,278 3-dimensional elements. This large number of nodes was used to ensure reasonable representation of the problem. Adhesion between layers was consider as a function of friction and normal pressure on the layers (Mohr-Coulomb Theory).

4.1.2. Boundary Conditions

Boundary conditions for the finite element model have a significant influence on the predicted response. Therefore, potential boundary conditions for pavements need to be considered.

- Edges Parallel to the Traffic Direction (Y Axis). Flexible pavements could have one of the three cross section geometries shown in Figure 4.2. At the pavement edge, two forces exist between the pavement edge and adjacent soil; vertical friction (F) and lateral, passive pressure (P). The friction force, F, depends on relative movement, coefficient of friction, gap between the pavement and the adjacent soil and the lateral passive earth pressure from the adjacent soil. Lateral earth pressure, P, depends on soil type and the weight of the soil wedge expected to affect the pavement. For the configuration number "a" in Figure 4.2, the soil wedge is small and both forces, F and P, can be neglected. In this case, the pavement edge can be assumed to be free to move laterally and vertically. Lateral and vertical forces for configurations "b" and "c" may be significant. Both the friction force and the passive pressure were included in the 3D-DFEM analysis.

- Edges Perpendicular to the Traffic Direction (Parallel to X Direction). The analysis model should represent adequate length to reduce any edge effect error. However, analysis of an extended length increases the size of the problem and the analysis time. An evaluation of section length was conducted with lengths ranging from 200" to 1400". For sections with length greater than 400", no significant effect on the pavement response was found. The length of various sections included in this study was 600" and the load was applied to the middle 200" only.

4.1.3. Pavement/Shoulder Modeling

Three conditions for the degree of continuity at the pavement/shoulder joint were considered:

1. No crack.
2. Narrow crack, pavement and shoulder are in contact with friction.
3. Wide initial crack (1") with possible interaction because of deformation.

4.2. Material Properties

Flexible pavement materials were divided into three groups: asphalt mixtures, granular materials and cohesive soils. The actual material behavior for each group was considered. Asphalt mixtures were modeled as a visco-elastic material. This type of material is time and temperature dependent [Yoder and Witczak, 1975]. The time dependent properties were represented by instantaneous and long term shear modulus [ABAQUS, 1989b]. Instantaneous shear modulus was selected at a loading time of 0.1 second which is equivalent to a speed of 40 mph. Long term shear modulus was selected at a loading time of 1.0 second which is equivalent

to a speed of 1.5 mph. The temperature effect was considered through the shear modulus values. Figure 4.3 shows the effect of loading time and temperature on asphalt mixtures stiffness.

Granular materials, base coarse, subbase and subgrade in some cases, were modeled using the Drucker-Prager model [Drucker and Prager, 1952 and ABAQUS, 1989b], while cohesive materials were modeled using the Cam-Clay model [Schofield et al., 1968, Parry, 1972 and ABAQUS, 1989b]. Details of these models can be found in Chapters 2 and 3.

Other material and layer characteristics required in the analysis include modulus of elasticity, Poisson's ratio, damping coefficient and bulk density.

4.3. Loading Cycles

The 3D-DFEM analysis can be used to simulate truck loads moving at highway speeds. At speeds less than 20 mph a truncated sawtooth load function is used while a step load function is used for speeds greater than 20 mph. Figure 4.4 shows the truncated sawtooth load cycle used in the analysis. The load cycle begins with a load magnitude equal to zero at time T_0. After time T_0, the load is increased linearly to a maximum value at time T_1. The load magnitude remains constant between time T_1 and time T_2. After time T_2 the load is decreased linearly to zero at time T_3. The length of time from T_0 to T_1, T_1 to T_2 and T_2 to T_3 are functions of speed and the length of the contact area between the truck tire and pavement surface. The length of the contact area or tire print was calculated by assuming the area to be a combination of a central rectangle with semicircles at the ends, as shown in Figure 4.4 [Yoder and Witczak, 1975].

$$L = \sqrt{\frac{A}{0.5226}}$$

Where, A = contact area, square inches.

In the step function load cycle $T_0 = T_1$ and $T_2 = T_3$. Load cycle application in the 3D-DFEM analysis considers that no load is applied at a point, n, on a pavement prior to time T_0. After T_0 the load cycle is applied at point n and to subsequent points at increments of time equal to the distance between the axles.

Times $T_0, \ldots, T_3$ were calculated as follows:

$$T_i = j\frac{L}{V}$$

Where, L = Length of the tire print, inches

V = Speed , inch/second

i = 0, 1, 2 and 3, respectively

j = 0.0, 0.3, 0.7 and 1.0, respectively for V < 20 mph

= 0.0, 0.0, 1.0 and 1.0, respectively for V > 20 mph

In initial studies an 18-kip single axle with dual wheels was assumed.

4.4. Finite Element Model Verification

Prior to general application, the 3D-DFEM was verified in a two step process. These two steps included evaluation of its capabilities to predict pavement response for both static and dynamic cases.

4.4.1. Static Analysis Verification

For, the elastic, static case a design of experiment (DOE) was developed. Subsequently,

analyses of sections with factor combinations satisfying the design of experiment were conducted with both a layered elastic analysis and the 3D-DFEM analysis. In the later case elastic material properties were used for the various layers as well as static loading.

Three factors were included in the design of experiment, surface layer thickness (T_s), base coarse thickness (T_b) and subgrade modulus of elasticity (E_{sg}). Two levels for each factor were included, low and high, as shown in Table 4.1. Eight different pavement cross sections were analyzed using the multi-layer procedure and the 3D-DFEM. Pavement deflection at different lateral distances(x) as well as at different depths (z) were predicated using Bitumen Structures Analysis in Roads Program (BISAR)[BISAR 1972] and the 3D-DFEM for the eight pavement cross sections. Table 4.2 shows the deflections predicted using BISAR and the 3D-DFEM. A regression analysis of the results included three variables, deflection predicted using BISAR (DB), deflection predicted using ABAQUS (DF) and the cross section number (PTYPE). Because the sections analyzed represent significantly different pavement, the section number was included in the analysis as a dummy variable. The deflection predicted using BISAR (DB) was considered as the dependent variable while the other two variables, DF and PTYPE, and their interaction, DF*PTYPE, were considered as the independent variables. The interaction term, DF*PTYPE, was used to check whether the linear correlation between DB and DF depends on the range of pavement cross sections. Figure 4.5 shows the results of this regression analysis. From the regression analysis, a high linear correlation between DB and DF was found (R^2 = 0.96). Also, as can be seen in Figure 4.5, both variables, DF and PTYPE, show significant effect on DB. The interaction term, DF*PTYPE, shows insignificant effect on DB, which means that this linear correlation is independent of pavement cross section, i.e. this relationship can be

generalized for the flexible pavement cross sections included in the analysis.

4.4.2. Dynamic Analysis Verification

A study was also conducted to evaluate the time dependent dynamic analysis feature of the 3D-DFEM. Since there is no standard dynamic analysis method for the dynamic case as there is for the static case, a decision was made to compare the predictions with measured dynamic response of pavements due to moving loads.

A study in Canada [CanRoad, 1986], involved measuring horizontal tensile strain and surface deflection for asphalt pavements at fourteen sites across Canada. Field measurements were made at three nominal speeds of 6 mph, 12 mph and 50 mph for a number of load levels and load configurations. The structural numbers (SN) were estimated for the fourteen sections. Three of the fourteen sections with low, medium and high values of SN were selected for analysis. These three sections are located in Quebec (section numbers 3a and 4) and Alberta (section number 10) Provinces. A finite element mesh was created for each site to match the pavement cross section given by the CanRoad report [CanRoad,1986]. Reasonable material properties were assumed for each layer based on the material description given in the CanRoad report [CanRoad, 1986]. Table 4.3 shows the assumed material properties for the three sites. For the three selected sites, the surface deflections were predicted for two load levels of 9,182 kilograms and 11,127 kilograms and for the low (6 mph), and high (50 mph) speeds. Table 4.4 shows the measured and predicted deflection values for the three sites. An analysis was made to check if there was a linear correlation between the predicted and measured deflections. The deflections as can be seen from Figure 4.6 were found to be highly correlated (R^2 = 99.9%).

This high correlation implies that the 3D-DFEM can be used to predict the dynamic response of pavements subjected to moving loads.

4.5 Sensitivity Analysis

After verifying the 3D-DFEM analysis, a sensitivity analysis was conducted to investigate the effect of different factors on pavement response. These factors were divided into two groups:

- Cross section attributes:
    - Subgrade type.
    - Deep foundation type and location.
    - Shoulder width.
    - Pavement/Shoulder joint.
    - asphalt mixture properties.
- Load attributes:
    - Load repetitions.
    - Speed.
    - Axle configuration.
    - Axle load.

4.5.1. Material and Layer Characteristics

The basic cross section considered in the subsequent sensitivity study has the following characteristics [George, 1992, Kim and Stokoe, 1992, Roque and Ruth, 1987 , Derucher and Korfiatis, 1984, and ABAQUS 1989b]:

- asphalt concrete surface layer:
  - Thickness : 4"
  - Modulus of Elasticity : 600,000 psi
  - Poisson's Ratio : 0.3
  - G-ratio : 0.8
  - Damping Coefficient : 0.05
  - Bulk Density : 150 pcf
- granular base coarse:
  - Thickness : 10"
  - Modulus of Elasticity : 60,000 psi
  - Possion Ratio : 0.3
  - Damping Coefficient : 0.05
  - Bulk Density : 140 pcf
  - Angle of Internal Friction : 38
  - Cohesion : 0
- sandy subgrade:
  - Modulus of Elasticity : 30,000 psi
  - Poission Ratio : 0.3
  - Damping Coefficient : 0.05
  - Bulk Density : 125 pcf
  - Angle of Internal Friction : 30
  - Cohesion : 0

where G-ratio = $$1 - \frac{LongTermShearModulus}{InstantaneousShearModulus}$$

The base course and subgrade moduli of elasticity were determined as 1500 times their CBR [Yoder and Witczak 1975]. The asphalt layer properties used in this example are based on the annual average temperature in Indiana (57 °F, approximately)[Coree and White 1988]. These properties are used in the balance of the sensitivity analysis unless noted.

4.5.2. Cross Section Attributes

4.5.2.1. Effect of Subgrade Type

The basic pavement cross section described above was analyzed with three types of

subgrade soil: clay, silt and sand. Properties assumed for these soils are shown in Table 4.5. The Drucker-Prager model [Drucker and Prager, 1952 and ABAQUS, 1989b] was used to analyze both the sandy and the silty subgrades. The Cam-Clay model [Schofield et al., 1986, Parry, 1972 and ABAQUS, 1989b] was used to analyze the clayey subgrade. Loading was assumed to be an 18-kip single axle load moving at a speed of 1.75 mph. The variation in pavement deflection for the three cross sections is shown in Figure 4.7. As expected, the pavement with sandy subgrade showed the lowest deflection, while the pavement with clayey subgrade showed the highest deflection. Although there is a difference in the deflection magnitude among the three cross sections, the deflection basins of the three cross sections have the same shape. Essentially, for the applied load, the subgrade stress did not exceed the yield stress. Therefore, all three subgrades behave as elastic soils.

4.5.2.2. Effect of Deep Foundation Type

Pavement response is affected by the deep foundation type and condition. An analysis was conducted to investigate the effect of deep foundation type on pavement response predicted by the 3D-DFEM analysis. The above pavement section was analyzed with each of the following deep foundations:

1. Shallow bed rock, starts at 64" below the pavement surface.
2. Shallow, soft to medium clay layer (cohesion = 500 psf), starts at 64" below the pavement surface.
3. Shallow, stiff clay layer (cohesion = 1000 psf), starts at 64" below the pavement surface.

4. Deep bed rock, starts at 164" below the pavement surface.

The subgrade above these deep foundations was assumed to be sandy silt subgrade. Load was applied as an 18-kip single axle load moving at a speed of 1.75 mph. Figure 4.8 shows the variation in surface deformation with lateral distance (x), as well as vertical distance (z) for the four cross sections. The cross section with soft to medium clay foundation showed a higher deflection than that of the other cross sections. Therefore, it is important to consider the deep foundation type in pavement design and evaluation.

4.5.2.3. Effect of Shoulder Width

Shoulders provide lateral support to pavement structures [AASHTO, 1990]. Multi-layer elastic analysis cannot be used to examine the questions of shoulder versus no shoulder and degree of discontinuity at the pavement/shoulder joint. The 3D-DFEM readily accounts for these conditions. An evaluation was conducted for two shoulder conditions. One analysis included a cross section with an 8 foot shoulder. The other analysis was for the condition of no shoulder. The shoulder structure for the 8 foot width was assumed to be the same as the traffic lane of the basic section. Load was applied as an 18-kip single axle load, one ESAL, moving at a speed of 1.75 mph. The outer wheel centerline of this load was positioned approximately 3 feet from the outer edge of the traffic lane. As shown in Figure 4.9, the surface deflection of the no shoulder cross section is 33% higher than that of the section with the 8 foot shoulder. The variation of vertical deflection with depth (z) for both cross sections is also presented in the same figure. As expected, the cross section with no shoulder shows higher deflection than the cross section with the 8 foot shoulder. This analysis shows the effect of lateral support provided by shoulders on

pavement response. Rational analysis and design procedures should include actual shoulder conditions.

4.5.2.4. Effect of Pavement/Shoulder Joint

To study the effect of pavement/shoulder joint conditions on pavement response, three pavement cross sections were analyzed. The three cross sections assumed 8 foot shoulders with the same structure as the traffic lanes. The first condition analyzed was a wide longitudinal crack extending to the base course. Even with a wide crack there is the possibility of interaction between the pavement and shoulder with significant deflection. Friction will develop with interaction. The second condition analyzed was a narrow crack with friction assumed. The friction force at the pavement and shoulder interface is a function of normal pressure and the coefficient of friction. Complete continuity at the interface was assumed for the third condition. As before, load was applied as an 18-kip single axle load moving at a speed of 1.75 mph. The centerline of the outer wheel path was positioned approximately 3 feet from the pavement/shoulder joint. Deflection basins for the three cross sections are presented in Figure 4.10. A greater deflection occurs as a result of the wide crack. The deflection basin also has a different slope at the crack. In general, the deflection basin shape for the narrow crack is similar to that for the wide crack but with lower maximum deflection. Deflection for the case of no crack is lower than the conditions with cracks. However, because of the continuity or moment transfer, the deflection at the points of loading are lower and at the joint higher than those of the cross sections with cracks. The difference in maximum surface deflection for the three conditions was found to be small because in all three the shoulder provides lateral support to the

pavement. This shows the importance of shoulders, even earthen shoulders.

4.5.2.5. Effect of the Asphalt Mixtures Properties

The asphalt layer was modeled in this analysis as a visco-elastic material. Elastic as well as visco-elastic properties are required to define asphalt mixtures. Loading time and temperature are two significant parameters for this type of material. Shear modulus ratio (G-Ratio) was used to define the effect of loading time on the asphalt layer and therefore the pavement. In Figure 4.11 the effect of G-ratio on the predicted vertical compression strain is presented. To study the temperature effect on asphalt mixture stiffness and pavement response, two analysis were made of the basic pavement structure. One analysis was made with asphalt layer properties measured at 59°F (approximate annual average temperature in Indiana), while the other analysis was made with the asphalt layer properties at 120°F [Roque and Ruth, 1989 and Battelle, 1991]. The vertical plastic compression strain (VPCS) at the pavement surface for the two analysis is presented in Figure 4.12. From this figure, as the temperature increases the asphalt mixture becomes less viscous and hence the plastic strain increases.

4.5.3. Load Attributes

4.5.3.1. Effect of Load Repetitions

The 3D-DFEM predicts the effects of load repetitions on the pavement plastic and elastic response. This information is important in understanding and predicting pavement performance. When a pavement is subjected to a moving load, a horizontal tensile strain develops at the bottom of the asphalt layer. This strain is associated with fatigue cracking. The horizontal tensile

strain has two components, elastic and plastic. The elastic component of this strain is fully recovered after the load is released, while the plastic component remains, as can be seen from Figure 4.13. The basic cross section was analyzed for effect of repetition of an 18-kip single axle load. Figure 4.14 shows the effect of these load repetitions on the horizontal tensile strain at the bottom of the asphalt layer. From this figure, it can be seen that after the first loading cycle, the elastic strain is almost constant. However, the plastic strain accumulates with each loading cycle. The history of total horizontal tensile strain at the bottom of the asphalt layer under repeated loads is represented in Figure 4.15 by the path ABCDEF. Figure 4.16 shows the effect of load repetitions on the total vertical compressive deformation at the pavement surface. The plastic vertical deformation component can be used to represent the expected pavement rutting.

4.5.3.2. Effect of Moving Load Speed

Previous studies [Papagiannakis and et al., 1990], have shown that static loads are more damaging to pavements than moving loads. A comparison was made of on the pavement response due to trucks moving at a creep speed, 1.75 mph, a slow speed, 10 mph, and a relatively high speed, 30 mph. These results are presented in Figure 4.17. As can be seen from this figure, the pavement deflection at 10 mph is significantly less than at 1.75 mph. However, the difference between the pavement deflection at speeds of 10 mph and 30 mph is relatively small. In Figure 4.18, the effect of truck speed on the rut depth is shown to be significant. The rut depth was assumed to be equal to the total plastic deformation accumulated at the surface of the pavement. It should be noted that multi-layer analysis cannot account for the effect of speed

on pavement response.

4.5.3.3. Effect of Axle Configuration

Three axle configuration were analyzed: 18-kip single axle load with single wheels, 18-kip single axle load with dual wheels, and 18-kip tandem axle load with dual wheels. These loads were applied to the basic pavement section at a speed of 1.75 mph. Deflections resulting from these three loading cases are shown in Figure 4.19. Underneath a wheel, the lowest pavement deflection occurred for the dual tandem configuration, while the highest deflection occurred for single axle with single wheels. From these results it can be concluded that replacing the dual wheels of a tandem axle with a single wheel will cause higher pavement deflection and associated increase in pavement damage.

4.5.3.4. Effect of Axle Load

To investigate the effect of axle loads on pavement response, three single axle loads with dual wheels were considered, 18-kip, 24-kip and 32-kip. The surface deflection as well as the vertical deflection at different depths was predicted for these loads. The results are plotted in Figure 4.20 and show that as the axle load increases, the pavement deflection increases. It should be noted that none of these loads generated a stress in excess of the yield stress of any layer.

4.6. Rut Depth Prediction

The 3D-DFEM has the capability to predict pavement rutting. In this analysis rut depth

is defined as the total permanent deformation which accumulates at the pavement surface. This total deformation is the sum of the permanent deformation of different pavement layers, including the subgrade.

Granular subgrades and untreated granular layers can be considered as elastic-plastic materials. The behavior of this type of material depends on the imposed stress level. If this stress level is below the yield stress, the material will act as a linear elastic material, which means all the deformation will be fully recovered after the load is released. If the stress level exceeds the yield stress of the material, it will act as an elastic-plastic material. In other words, when these materials are subjected to stress higher than their yield stress, elastic deformation as well as permanent plastic deformation will occur. The permanent plastic deformation accumulates as pavement rutting.

Asphalt mixtures are visco-elastic materials. Visco-elastic material response is more complex than elastic-plastic materials. The behavior depends not only on the stress level, but also on factors such as temperature, rate of loading, and loading time.

Flexible pavement rutting was predicted for two single axle loads with dual wheels, 18-kip and 58-kip. These loads were applied to the basic pavement section at a speed of 1.75 mph. Results are shown in Figure 4.21. The predicted rut depth of the 58-kip load was found to be approximately 100 times higher than that of the 18-kip. To show why the 58-kip load caused this severe rutting, the permanent deformation of each layer was plotted for both loads and are presented in Figures 4.22 and 4.23. Permanent deformation for the 18-kip load developed primarily in the asphalt layer. While 85% of the permanent deformation developed in the subgrade layer for the 58-kip axle load. This occurred because the 58-kip axle load subjected

the subgrade to a stress level higher than its yield stress. Permanent deformation in the base course and asphalt surface as a result of the 58-kip axle load were about 10% and 5% of the total permanent deformation, respectively. High axle loads should be prevented from using pavements for which they were not designed. A few passes of such heavy loads can cause considerably pavement rutting.

CHAPTER 5 ANALYSIS OF RIGID PAVEMENT

The conventional analysis method for rigid pavement is usually based on a closed-form solution for an infinitely long pavement subjected to static loads [Zaman, et al., 1990]. The fact that rigid pavements have finite slab dimensions and are subjected to moving loads make the predicted pavement response under the closed-form assumptions inappropriate. Finite element methods (FEM) can be used to better model concrete pavements. In the literature, a number of studies were found to use FEM in the analysis of rigid pavement. However, most of these studies assume that the concrete slab is a thin or thick plate resting on a Winkler, dense liquid, or elastic solid foundation. Also, static loading conditions are assumed. Table 2.1 in Chapter 2, summarizes assumptions associated with the FEM's.

A three-dimensional dynamic finite element method (3D-DFEM) [ABAQUS, 1989] discussed in Chapter 3 was used to analyze rigid pavement. Concrete pavements were modeled as three-dimensional slabs resting on a layered foundation. The linear and non-linear material properties of the different layers; concrete slab, subbase and subgrade; were represented. Moving truck loads at different speeds were applied and the elastic and plastic response predicted. Prior to application, the 3D-DFEM was verified for static and dynamic analysis of loadings. Both static and dynamic loading verification studies showed that the 3D-DFEM can be used, with confidence, to predict actual pavement response from moving loads. Also, the 3D-DFEM was used to conduct a sensitivity analysis to test the effect of different load and cross section parameters on pavement response. In this chapter results of the verification study and the sensitivity analysis are presented.

5.1. Features of the Finite Element Model

5.1.1. Model Geometry

A jointed reinforced concrete pavement (JRCP) cross section consists of a concrete slab with limited dimensions. It is commonly supported by a subbase course and a subgrade resting on top of a deep foundation. The typical highway concrete slab length ranges from 18 to 36 feet, with a width of 12 feet. A subbase provides improved support, erosion control and a facility for draining the pavement. It may be unstabilized or stabilized. The deep foundation type is site specific and can range from bed rock to a soft clay. The deep foundation may start a few feet under the pavement surface or may start much deeper.

Analysis using the 3D-DFEM involves as stated in the previous chapter selecting an effective finite element mesh (FEM) size. Figure 5.1 shows one of the mesh configuration used in the rigid pavement analysis study. The spacing in the traffic direction, y, is constant, 18", while the spacing in the transverse direction, x, is varied. For areas which are close to the loading points, a high level of detail was desired, therefore a mesh with 6" spacing was used. For the area located between the loads, the need for detail is not as great; therefore, a mesh with 24" spacing was used. A mesh with 24" spacing was also used to model the shoulder. The subgrade is modeled as a set of layers. The number of layers depends on the degree of detail required in predicting the pavement response in the vertical direction.

5.1.2. Boundary Conditions

The boundary conditions for the finite element model are important and have a significant influence on the predicted response. Therefore, boundary conditions similar to those of actual

pavements need to be considered. Similar to flexible pavement, rigid pavement cross section could have one of the three geometries shown in Figure 4.2, presented in Chapter 4. At the slab edge, two forces exist: vertical friction between the concrete slab edge and the adjacent soil (F) and lateral passive pressure of the adjacent soil (P). These two forces were considered in the subsequent rigid pavement analysis.

5.1.3. Longitudinal and Transverse Joints

Two types of joints are considered: longitudinal joints, which are parallel to the traffic direction; and transverse joints, which are perpendicular to the traffic direction. Joint openings in the range of 3/8" to 3/4" was considered for both types of joints [Yoder and Witczak, 1975]. Tie bars are used across the longitudinal joints in some cases to tie two slabs together or to tie concrete shoulders to the traffic lane slabs. For transverse joints, a load transfer device (dowel bar) is commonly used to insure positive load transfer between slabs.

5.2. Material Properties

Westergaard analysis, as well as most FEM's, assumes that the paving materials are linear elastic. In this analysis, rigid pavement materials were divided into four groups: concrete, granular materials, clays and asphalt aggregate mixtures. The actual material behavior for each group was considered.

The concrete behavior was divided into three stages: elastic, plastic and after-failure stages. Figure 3.6, shows the stress-strain curve used to model concrete. If the concrete slab is subjected to a stress level less than its yield stress, it will behave as an elastic material. When

the stress level exceeds the yield stress of concrete, the concrete behavior is elastic-plastic until the stress reaches the failure limit. At that point the after-failure stage will start [ABAQUS, 1989b].

The Drucker-Prager model [Drucker and Prager and 1952, ABAQUS, 1989c] was used to model granular material, while the extended Cam-Clay model [Schofield et al., 1968, Parry, 1972 and ABAQUS, 1989c] was used to model clays. Asphalt mixtures, for subbase and shoulders, were modeled as visco-elastic materials. Details of material models used in the rigid pavement analysis can be found in Chapter 3.

5.3. Loading Cycles

A loading cycle similar to that assumed for flexible pavement analysis was used for rigid pavement analysis.

5.4. Finite Element Model Verification

The 3D-DFEM was verified for static analysis as well as for dynamic analysis.

5.4.1. Static Analysis Verifications

A design of experiment (DOE) was developed to determine whether or not the 3D-DFEM predictions agree with those calculated using Westergaard equations [Westergaard, 1926](static solution). Three factors were included in the DOE: slab thickness, subgrade type and load position. Three levels for the slab thickness, 6, 10 and 14 inches and two subgrade types, sand and clay, were included in the analysis. Assuming a static loading condition and linear elastic

material properties, surface deflections at three loading positions, center, edge and corner, were predicted using the 3D-DFEM and Westergaard equations. Table 5.1 shows factor levels included in the DOE. An analysis of variance (ANOVA) was made of the results to test if there was a linear correlation between the deflections predicted using the 3D-DFEM and those calculated from Westergaard equations. Also, the ANOVA was examined to find out if the correlation was limited to certain cross sections and load positions or if it could be generalized for a range of cross sections and load positions. Three factors were included in the ANOVA: deflections predicted using the 3D-DFEM (SF), deflections calculated using Westergaard equations (STH) and a factor representing the pavement cross section and load position (PTYPE). STH was considered as the dependent variable, while SF and PTYPE were the independent variables. The interaction term, SF*PTYPE, was included in the analysis to determine if the correlation between STH and SF depends on the cross section and load position or not. It was found that there is a very high linear correlation between SF and STH (R^2 = 97.7%). The interaction term, SF*PTYPE, was found to be insignificant, which means that the correlation between STH and SF does not depend on cross section or load position. The results of the ANOVA are shown in Figure 5.2.

5.4.2. Dynamic Analysis Verification

To evaluate the dynamic analysis capabilities of the 3D-DFEM for rigid pavements, it was decided to compare its predictions with actual pavement deflections from a study by the Portland Cement Association (PCA) [Okamoto and Packard, 1989]. In this study a field testing program was conducted at six sites, three of these sites were located in Wisconsin and the other

three in Pennsylvania. The surface deflection was measured under single and tandem axles moving at creep speed, 2 mph. The three pavement sections located in Wisconsin were incorporated in the verification study. Finite element meshes were created to match these cross sections and reasonable material properties were assumed. Moving axle loads similar to those used in the field test were considered in the analysis and the total surface deflection was predicted using the 3D-DFEM. Table 5.2 shows the measured and predicted pavement deflections. A linear correlation analysis between the measured and predicted deflection was conducted to test whether or not the 3D-DFEM predictions agree with field measurements. As can be seen from Figure 5.3, a high linear correlation was found between the measured and predicted deflections (R^2 = 99.64%).

5.5. Sensitivity Analysis

The verification studies, static and dynamic, were extremely successful in demonstrating the capabilities of the 3D-DFEM. With this background, a sensitivity analysis was conducted to investigate the effect on pavement responses of load parameters such as speed and axle load magnitude and cross section parameters such as slab thickness and dowel bars. One advantage of the 3D-DFEM is the capability of simulating actual truck loads and paving material properties. Therefore, the predicted pavement response is expected to be very close to that occurring in the field. Another advantage of the 3D-DFEM is the capability to predict certain parameters, which no other analysis procedure can do. For example, most of the available analysis procedures can predict the elastic deflection at the subgrade surface. The 3D-DFEM not only predicts the elastic pavement response, but also the plastic (permanent) response. Permanent

(plastic) deflection is strongly related to pavement performance. The effect of the following parameters were studied in the sensitivity analysis:

1. Speed.
2. Load position.
3. Axle load magnitude.
4. Slab thickness.
5. Subbase course.
6. Load transfer device (dowel bars).
7. Joint width.

5.5.1 Effect of Moving Load Speed

Previous studies [Idelin et al., 1991] showed that the effect of static loads is more severe than that of moving loads. To investigate the effect of speed on concrete pavement response, an single 18-kip single axle load (SAL) moving at a creep speed (1.75 mph), slow speed (10 mph) and relatively high speed (30 mph), respectively, was considered. The pavement section in the analysis consisted of a 10" concrete slab, 4" granular subbase and sandy subgrade. A 6 foot tied concrete shoulder having the same cross section was assumed. The predicted horizontal tensile strain and total surface deflection from these loads are shown in Figure 5.4. Pavement response decreased significantly with an increase in speed from 1.75 mph to 10 mph as compared to that with an increase in speed from 10 mph to 30 mph. This reduction in the pavement response demonstrates the significance of the speed effect. The speed effect on concrete pavement response is ignored by most of the available analysis procedures.

5.5.2 Effect of Load Position

Concrete slabs have limited dimensions. When a load is applied at the center of the slab, the slab distributes the load. When a load is applied at the edge of the slab (close to a transverse joint and with partial load transer) only a part of the slab carries the load. Therefore, response (such as deflection) to edge loads is expected to be higher than that to interior loads. To evaluate the effect of load positions on rigid pavement response an 18-kip single axle load (SAL) moving at a speed of 1.75 mph was applied on a 10" undoweled concrete pavement resting directly on a sandy subgrade. The pavement section was assumed to have a 6 feet wide asphalt shoulder, 4" asphalt surface and 10" granular base course. The load was applied at two positions, center and transverse joint edge of the slab. The horizontal tensile stress as well as the vertical deflection of the slab is presented in Figure 5.5 for the center and edge loads. The edge loading increases the vertical deflection and corresponding tensile stress by 45% and 40%, respectively. The same pavement section was analyzed using Westergaard equations for interior and edge static loads. The edge load was found to increase the pavement response by similar ratios.

5.5.3. Effect of Axle Loads and Slab Thickness

A non-linear dynamic analysis was conducted to investigate the effect of axle load magnitude and slab thickness on pavement deflection. Results of this analysis is shown in figure 5.6. A range of slab thicknesses resting on a 4" granular subbase course was analyzed with a number of single axle loads moving at a speed of 1.75 mph. For low load levels, the surface deflection was found to increase as the axle load increases and to decrease as the slab thickness increases. As can be seen from this figure, the slab thickness effect is linear, i.e., all curves are

parallel to each other. This occurs because the yield stresses of the pavement materials is not exceeded and therefore they behave as linear elastic materials.

To show the elastic-plastic behavior of rigid pavements, an 18-kip SAL and a 60-kip SAL were repetitively applied on two pavement sections, 8" and 14" concrete slabs on a 4" granular subbase and clay subgrade. Both loads were applied at a speed of 1.75 mph. The pavement response to these loads are shown in Figure 5.7. As can be seen from this figure the pavement deflection from the 18-kip SAL is constant with load repetitions. Obviously, the 18-kip SAL did not develop stress levels higher than the yield stresses of the pavement materials. For the 60-kip SAL, the surface deflection increased with load repetitions. This indicates that some permanent deformation is developed in one or more of the pavement layers because the stress levels developed by the 60-kip SAL were higher than the yield stress of one or more of the pavement layers. Permanent deformation of each layer was predicted and is shown in Figure 5.8. This figure shows accumulation of permanent deformation occurred in the subgrade. There is no permanent deformation developed in the base course or the concrete slab. This effect is used to develop Purdue LEF's for rigid pavement, which are presented in Chapter 6.

5.5.4. Effect of Subbase Course

One of the purposes of using a subbase course underneath rigid pavements is to provide improved support to the concrete slabs. An 8" undoweled concrete pavement resting on a 4" granular subbase course on the top of a sandy silt subgrade was loaded at the edge with an 18-kip SAL moving at a speed of 1.75 mph. The pavement section was assumed to have a 6 feet untied concrete shoulder with the same thickness and layers of the traffic lanes. Pavement

vertical deflection was predicted using the 3D-DFEM and compared with the deflection of an 8" undoweled concrete pavement rested directly on the sandy silt subgrade. As can be seen from Figure 5.9, the effect of this subbase course is to reduce the maximum vertical deflection by 45%. The joint efficiency was calculated for both pavement sections as follows:

$$\xi = \frac{2\Delta_1}{\Delta_1 + \Delta_2} * 100$$

Where,

ξ = joint efficiency

Δ_1 = deflection of the second slab edge

Δ_2 = deflection of the first slab edge (where the load is applied)

Reflective joint efficiency was increased from 55% to 66% as a result of the subbase course.

5.5.5. Effect of Dowel Bars

When a load is applied at one side of an undoweled transverse joint, a part of this load is transferred to the next slab by aggregate interlock. A load transfer device (dowel bar) is commonly used to insure positive load transfer. In Figure 5.10, the effect of dowel bars on pavement deflection is shown. Two similar concrete pavements consist of an 8" concrete slab rested directly on sandy subgrade were loaded with an 18-kip SAL moving at speed of 1.75 mph, a 6 feet untied concrete shoulder was assumed for both cross sections. One pavement cross section was assumed to have 1.25" diameter dowel bars with 12" dowel spacing. The other slab

had no dowel bars. The joint efficiency of the transverse joint increased from 54% for the no dowel case to 66% with dowels. Also, the maximum vertical deflection was reduced by 20% with dowels. The minimal increase in joint efficiency may be attributed to the sandy subgrade.

The effect of dowel bar diameter on surface deflection is shown in Figure 5.11. Two similar pavements, 8" slabs resting on a 4" granular subbase course on a sandy subgrade, were loaded with an 18-kip SAL moving at speed of 1.75 mph. Also a 6 feet untied concrete shoulder was assumed for both cross sections.One pavement was assumed to have dowels with 1" diameter and 12" spacing, while the other pavement was assumed to have dowels with 1.4" diameter and 12" spacing. Although the capacity of the 1.4" dowel is higher than that of the 1" diameter dowels, no significant reduction of surface deflection or improvement of joint efficiency is shown. The reason of this is that the 1" diameter dowels have adequate load transfer capacity.

In Figure 5.12 the effect of dowel bar spacing is shown. Two similar pavement sections, 8" slab resting on a silt subgrade, was loaded with an 18-kip SAL moving at a speed of 1.75 mph. Both pavement sections were assumed to have 1" diameter dowels. The dowels were spaced 6" apart in one cross section and 20" apart in the other. The joint efficiency was found to increase from 58%, in case of 20" spacing, to 68%, in case of 6" spacing.

The effect of dowel bar length on the surface deflection is presented in Figure 5.13. Two similar pavements, 8" slab resting on a 4" granular subbase course on the top of a sandy subgrade, was loaded with an 18-kip SAL moving at a speed of 1.75 mph. Both pavement sections were assumed to have 1" diameter dowels. The dowel bar length was 44" for the first cross section and 88" for the second. As can be seen from Figure 5.13, no change in the surface deflection was found when the dowel bar length increased. This result agrees with previous work

done by Friberg, 1938, in which it was found that dowel embedment length should be about 8 times the dowel diameter, i.e. 8" embedment length for a 1" diameter dowel.

A stiff subbase course reduces rigid pavement deflections. At the joint, the additional support reduces the differences in deflection from one side of the joint to the other. The effect is an apparent increase in joint efficiency. An 18-kip SAL moving at a speed of 1.75 mph was applied on an 8" undoweled concrete pavement rested directly on a sandy subgrade. The joint efficiency was found to be 54%. Using a 4" granular subbase course increases the joint efficiency to 63%. Using 1" diameter dowels spaced at 12" without the subbase increases the joint efficiency to 66%. Using both dowels and subbase increases the joint efficiency to 73% (see Figures 5.10 and 5.14). Therefore, using a subbase course and dowels can significantly increase joint load transfer efficiency.

5.5.6. Effect of Joint Width

To study the effect of joint width on surface deflection a joint efficiency analysis was made of an 8" undoweled concrete pavement resting on a 4" granular subbase course on a sandy subgrade. The pavement was loaded with an 18-kip SAL moving at a speed of 1.75 mph. Three joint widths were considered in the analysis, 0.25", 0.375" and 1.0". As can be seen from Figure 5.15, the pavement deflection decreases when the joint width decreases. The relationship between the joint opening and the joint efficiency is presented in Figure 5.16. As can be seen from this figure, at zero inch joint width, the joint efficiency is assumed to be 100%.

CHAPTER 6 LOAD EQUIVALENCY FACTORS

Truck traffic is a significant factor in highway pavement design, maintenance and evaluation. A broad measure of truck traffic is number of trucks per day or number of total trucks. However, trucks vary in load, number of axles and axle spacing. Such variation has an effect on pavement performance and should be addressed. To account for the variation in loading effects a mixed traffic stream is converted to an equivalent amount of traffic of a standard axle load. An 18-kip single axle load (SAL) with dual tires is commonly used as the standard axle load.

In the overload permit study, two levels of analysis are considered: project level and network level. On the project level, the user is permitted to select any pavement type (flexible, rigid or composite pavements), while on the network level, the Indiana highway network is categorized into three classes; Interstate highways (I), United States highways (US) and State Roads (SR). A typical pavement cross section was selected to represent each category in the analysis. Selection of these representative cross sections was made based on the information available in the Road Life data base [Lindly and White 1987 and Pumphrey and White 1989]. The Road Life data base contains information about pavement structures and subgrade materials for more than 50% of the total lane miles of highways managed by INDOT. It was found that more than 60% of Indiana highways are jointed reinforced concrete pavements (JRCP) overlaid at least once with asphalt concrete. Four typical pavement cross sections were selected for the overload permit study to represent the different highway categories. For Interstate and United States highways, composite cross section representing 70% and 77% of the total lane miles of

each class, respectively, were selected. For State Roads two cross sections were selected; a composite pavement section representing 55% of the SR total lane miles and an asphalt cross section representing 40% of the SR total lane miles [IDOH 1989]. Figure 6.1 shows the typical cross sections included in the overload permit study. Lean Clay (CL) was found to be the predominate soil in Indiana, therefore, a CL subgrade was assumed for the typical sections.

Rational LEF's for different pavement types (flexible, rigid and composite pavements) are required for this study to evaluate damage effects of an overloaded truck on different pavement types. The most commonly used LEF's are those developed by the American Association of State Highway Officials (AASHO) [AASHO 1972]. These LEF's are based on the results of the AASHO Road Test [AASHO 1962] and the concept of pavement serviceability. In the AASHO Road Test, asphalt and concrete pavement sections were constructed and tested with single and tandem axle loads. The present serviceability index (PSI), which is a function of slope variance (roughness), cracking and patching for concrete pavement plus rutting for asphalt pavement, was used as a measure of pavement performance. Empirical relationships were developed to correlate PSI to the number of load repetitions for asphalt and concrete pavements. No composite pavement sections of asphalt overlaying concrete were constructed in the AASHO Road Test and therefore, no LEF's were developed for composite pavements. The 1993 AASHTO design guide [AASHTO 1993] recommends the use of concrete pavement LEF's for composite pavements. In this case, the effect of traffic on composite pavements is assumed to be similar to that of concrete pavements.

Other empirical LEF's, such as CanRoad LEF's [CanRoad 1986], do not address composite pavements. Analytically based LEF's, such as those reported by Finn et al. 1977, are

based on multi-layer elastic analysis which assumes that pavements are extended to infinity in the lateral and longitudinal directions and the subgrade has infinite depth. Assumptions are also made in multi-layer analysis that pavement materials are linear elastic and truck loads are static. Comparisons between these LEF's and the corresponding AASHTO LEF's showed lack of agreement.

A sample of overload permit applications was reviewed to determine truck configurations being permitted. The sample revealed that permits were requested for trucks with up to nine axles in one group as well as trucks with axle loads up to 72 kips per axle. In the AASHO Road Test pavement sections were tested with only single and tandem axle loads up to 40 kips and 48 kips, respectively. LEF's based on AASHO Road Test results are only valid for these number of axles and load ranges. Simple extrapolation of regression relations beyond the range of factors for which data has been collected is risky without realistic material and structural models. This appears to be a short coming of the AASHTO Guide for Design of Pavement Structures [AASHTO 1986] where LEF's are presented for single and tandem axle loads higher than those at the AASHO Road Test as well as for tridem axles which were not used at all. These extrapolations were made using the original serviceability based regression equations for performance.

None of the existing LEF sets were found to be suitable for the overload permitting study, therefore, three LEF sets were developed for this study: flexible, rigid and composite pavement LEF sets. Flexible pavement LEF's are based on equal total permanent (plastic) deformation at the pavement surface (TPD), while rigid and composite pavement LEF's are based on maximum surface deformation (MSD). The three-dimensional dynamic finite element

model (3D-DFEM) [ABAQUS, 1989a] described in Chapter 3 was used in the analysis. The 3D-DFEM was verified for flexible and rigid pavements in two steps; first for static, linear elastic analysis and then for dynamic nonlinear analysis, as explained in Chapters 4 and 5, respectively.

6.1 Flexible Pavement LEF's

6.1.1. Comparison Between Different LEF Methods

In the literature several LEF sets were found available for flexible pavement. The available LEF's were compared with the AASHTO LEF's for single and tandem axle configurations and the results are shown in Figures 6.2. As can be seen from these figure, none of these LEF sets agree with the serviceability based AASHTO LEF's. The analytical models used to develop rational LEF sets were based on assuming static loading conditions and linear elastic analysis. Pavement damage, fatigue cracking and rutting, were predicted based on correlations with pavement elastic responses. Field based LEF's, such as the CanRoad [CanRoad, 1987] LEF's, are based on the pavement response measured under moving trucks. This response is the total pavement response, elastic and plastic. The elastic pavement response is always fully recovered after the load is released, while the plastic response is permanent. In comparison only permanent pavement response (rutting) was recorded at the AASHO Road Test. Such rutting of flexible pavements is incorporated in the PSI value (a measure of serviceability).

6.1.2. The 3D-DFEM Analysis

Flexible pavement sections at the AASHO Road Test were modeled in this analysis as

two 12 foot lanes plus 8 feet shoulders on either side. The pavement structure consists of three layers, asphalt surface, granular base and subbase, and subgrade. Boundary conditions, deep foundation types, loading conditions, section lengths, finite element mesh sizes and element types were checked, evaluated and verified. The details of these evaluation and verification can be found in Chapter 4. Vehicle speed was found to have significant effect on pavement response, as shown in Section 4.5.3.2 of Chapter 4. Therefore, a speed similar to the average speed of the AASHO Road Test [Coree and White 1988] was used in developing the following LEF's.

6.1.3. Purdue LEF's for Asphalt Pavements

A new set of LEF's was developed based on a concept that is similar to that of the AASHO Road Test. The total permanent deformation (TPD) at the pavement surface for representative AASHO Road Test pavement sections was predicted using the 3D-DFEM. A range of single and tandem axle loads was considered. For each cross section, the 18-kip single axle load was applied up to 30 times, and the TPD was determined at the end of each pass. The LEF of any load "j" is the number of 18-kip axle load repetitions required to develop the same amount of TPD developed by one pass of the load "j" on the same cross section. Two statistical models were developed for these LEF's. The first model predicts the TPD developed by one pass of any axle load configuration, including the 18-kip single axle load, on any cross section. The second model is for the 18-kip single axle load only. This model predicts the TPD due to repetitions of the 18-kip SAL on different cross sections. The TPD predicted using the first model is an input for the second model from which the required number of applications of the 18-kip load is obtained. Figure 6.3 shows a graphical representation of Purdue LEFs concept.

6.1.3.1.Design of Experiments

Two design of experiments (DOE's) were implemented to develop the flexible pavement LEF's. The following factors were included in the first DOE (FDOE1):

1. Axle Load (D)
2. Number of Axles
3. Modulus of Elasticity of the asphalt layer (E_{ac}).
4. G-ratio of the asphalt layer.

$$(G-ratio=1-\frac{LongTermShearModulus}{InstantenousShearModulus})$$

5. Asphalt Layer Thickness (T_{ac}).
6. Total Pavement Thickness (T_1).
7. Subgrade Type (SG).

Table 6.1 shows factor levels included in the FDOE1. A partial factorial design was used to develop the model and 104 different load-cross section combinations were analyzed using the 3D-DFEM. An analysis of variance (ANOVA) was made of the results to test the significance of different factors included in the FDOE1. The significant main effects and 2-way interactions were used to develop a regression model which can be used to predict TPD caused by different axle loads. The regression model showed a high correlation, R^2 = 99.3%.

$$TPD_{ij}=a*D_j^4+b*N_j+c*T_t+d*G+e*E_{ac}+f*T_t*(D_j)^4+g*N_j^2+h*N_j*T_{ac}+i*G*E_{ac}$$

Where, TPD_{ij} = Total permanent deformation of cross section "i",caused by load "j".

a, b, lll, i are regression coefficients their values are given in Table 6.2.

To extend the validity of this model, more cases were analyzed to cover wider ranges of factor levels and the results were compared with the extrapolated predictions of this model. It was found that there is no significant difference between the extrapolated results and the ones determined from the extended analysis.

In the second DOE (FDOE2), the same cross section parameters were included, E_{ac9}, G-ratio, T_{p} T_{ac} and SG, plus the number of 18-kip single axle load repetitions (C). Table 6.3 shows factor levels included in the FDOE2. A full factorial design was used to develop this model and all cases were analyzed using the 3D-DFEM. Similar to the FDOE1, an ANOVA was made of the results to test the significance of different factors included in FDOE2. The significant main effects and 2-way interactions were included in regression models which can be used to predict a cross section TPD as a function of the 18-kip SAL repetitions. Two models were found to have high correlations:

- Full Interaction Model (FIM)

$$C = \frac{TPD_i}{a - b * T_{ac} + c * G + d * E_{ac} + e * T_t + f * E_{SG}}$$

Where, TPD_i = Total permanent deformation of cross section "i".

C = The 18-kip SAL repetitions.

a, b, ..., i are regression coefficients their values can are given in Table 6.2.

The FIM model includes the interaction terms of the number of load applications and the cross section parameters, while the MEM model includes the main effect of the cross section parameters only. In the FIM both the initial TPD and the accumulation of TPD depend on the cross section parameters, while for the MEM only the initial TPD depends on the cross section parameters. In other words, the accumulation of TPD is the same for any cross section. From a conceptual point of view, the FIM is project specific. The MEM could be considered as applying to a network, i.e. when the cross section parameters are not well defined. The FIM is used in the subsequent analysis to determine LEF's. A comparison between the LEF's for single axle configuration based on these models is presented in Figure 6.4.

At an approximate AASHO Road Test speed of 35 mph [Coree and White 1988], the subgrade type was found to be insignificant in FDOE1. However, subgrade type was found to be significant in FDOE2. This was an unexpected result dictating additional analysis of the effect of speed. In FDOE1, at slow vehicle speed (< 20 mph), the subgrade response was of a magnitude that the subgrade was found to be significant. At higher vehicle speed (> 20 mph) the short loading time was not sufficient to develop the significant subgrade response. However, for the FDOE2 even for the high speed the subgrade type was found to be significant. This occurs because the load is repeated and the accumulated subgrade response is significant.

6.1.3.2. Comparison Between Purdue LEF's and Other LEF's

Purdue LEF's were compared with other reported LEF's, including the AASHTO LEF's. In Figures 6.5 and 6.6, Purdue LEF's, as well as, other LEF's for single and tandem axle

configurations are shown. As can be seen from these figures, Purdue LEF's are very close to the AASHTO LEF's for both single and tandem axle configurations.

6.1.3.3. Sensitivity Analysis

In Figure 6.7 Purdue LEF's for a single axle configuration is presented. A set of cross sections were analyzed. All cross sections have the same total thickness, 16 inches, and material properties. The asphalt layer thickness ranged from 4 inches to 12 inches. The effect of the asphalt layer thickness is clear from this figure. As the asphalt layer thickness increases, the overall pavement stiffness increases and the LEF's decrease. The AASHTO LEF's are also plotted on Figure 6.7. The AASHTO LEF's were found to lie somewhere between the LEF curves of 4 and 5 inches of asphalt layer thickness. This was expected because the asphalt layer thickness of the AASHO Road Test sections was in this range. The effect of asphalt layer thickness is not included in the AASHTO LEF's. As a result, the AASHTO LEF's are not valid for full depth asphalt cross sections.

The effect of total pavement thickness on LEF's for single axle configurations is presented in Figure 6.8 also the LEF's for cross sections having the same asphalt layer thicknesses, 5", and different total thicknesses are shown along with the AASHTO LEF's. As expected, the thicker the pavement, the lower the LEF's. The LEF's of the cross sections with total thickness of 10 to 20 inches were the closest LEF's to the range of the AASHO Road Test sections.

The effect of asphalt mix quality on LEF's is shown in Figure 6.9. Three levels of mix quality were used based on mix stiffness; low, medium and high. As the asphalt mix quality

stiffness increases, the LEF's decreases. The AASHTO LEF's were found to lie some where between the medium and high quality curves.

For two, three and four axle configurations, the effect of asphalt layer thickness on LEF's are presented in Figures 6.10, 6.11 and 6.12, respectively. As in the case of single axle configuration, the thicker the asphalt layer, the lower the LEF's.

6.2. Rigid Pavement Analysis

6.2.1. Comparison Between Different LEF Methods

A comparison between the AASHTO LEF's [AASHTO, 1977] and LEF's based on fatigue analysis [Hallin et al. 1989] for single axle configuration is presented in Figure 6.13. LEF's based on fatigue analysis are significantly different from the AASHTO LEF's. The fatigue analysis LEF's were found to underestimate the pavement damage caused by any axle load for both single and tandem axle configurations. This was expected because the fatigue analysis LEF's are based on the elastic response of pavements, while the AASHTO LEF's are based on slope variance (roughness) which is a function of pavement permanent deformation.

6.2.2. The 3D-DFEM Analysis

A jointed reinforced concrete pavement (JRCP) cross section similar to that of the AASHO Road Test was modeled in this analysis as two 12 foot lanes plus 8 foot shoulders on either side. The pavement structure consists of three layers, concrete slab, granular subbase and subgrade. Granular shoulders were used in the analysis to be consistent with the AASHO Road Test. Prior to analysis; boundary conditions, deep foundation types, loading conditions, section

lengths, finite element mesh size, element types and material models were evaluated and presented in Chapter 5 of this report. Vehicle speed was found to have significant effect on pavement response. Therefore, a speed similar to the average speed of the AASHO Road Test, 35 mph [Coree and White 1988], was used in developing these LEF's.

6.2.3. Purdue LEF's for Rigid Pavements

A LEF set was developed for concrete pavements (Purdue LEF's) based on equal maximum surface deflection (MSD). Maximum surface deflection consists of the combined elastic and plastic deformation. For a given load and speed the plastic deformation in the unbound layers increases with number of load applications until an asymptotic value is reached. This asymptotic value and the rate of deflection increase with number of load applications are a function of load magnitude, speed and slab thickness. The elastic deformation of the slab increases because of reduced support from the accumulating permanent deformation. Figure 5.8 (in Chapter 5) shows the effect of load repetitions on the unbound layers permanent deformation and on the total surface deflection for two slab thicknesses, 8 and 14 inches.

There is a logic as to why concrete pavement MSD would correlate for concrete pavements so effectively with the AASHO Road Test serviceability concept. Fatigue of concrete pavements is related to elastic defection while roughness is related to permanent deformation. Therefore it takes the combined MSD to provide a scale for rigid pavement serviceability. In application, the LEF of any load "j" is the number of 18-kip single axle load (SAL) required to develop the same MSD developed by one pass of the load "j" on the same pavement cross section.

Two statistical models were developed for Purdue LEF's. The first model predicts the MSD developed by one pass of any axle load configuration, including the 18-kip SAL, on a range of rigid pavement cross sections while the second model predicts the MSD due to repetitions of the 18-kip SAL. The two models are used together to predict the LEF's. The first model predicts the MSD due to load "j" on cross section "i", then the predicted MSD is used as an input to the second model to estimate the number of the 18-kip SAL repetitions required to develop the same MSD in cross section "i", which is LEF_{ij}. Figure 6.14 shows a graphical representation of the concept of Purdue LEF's for rigid pavements.

6.2.3.1. Design of Experiments

Two design of experiments (DOE) were implemented to develop the rigid pavement LEF's. The following factors were included in the first DOE (RDOE1):

1. Axle load (D).
2. Number of axles (N).
3. Slab thickness (T).
4. Speed (S).

Table 6.4 shows factor levels included in RDOE1. As mentioned earlier, the subgrade type was found to be insignificant for flexible pavement LEF's at a speed of 35 mph. Based on this experience and because of the concrete pavement surface rigidity, a decision was made not to include subgrade type in RDOE1. A 4" granular subbase was assumed for all cross sections included in this analysis. The sample of overload permit applications showed that the average axle spacing is 4 foot, therefore, a 4 feet axle spacing was assumed for n-axle configurations.

A partial factorial design was used to develop the first model. Different load-cross section combinations were analyzed using the 3D-DFEM. An analysis of variance (ANOVA) was used to test the significance of different factors included in RDOE1. The significant main effects and 2-way interactions were used to develop a regression model to predict a MSD for various axle load configurations. From this analysis, it was found that speed is a significant factor. The MSD's for high speeds ($>$ 20 mph) are small compared with those for low speeds ($<$ 20 mph), therefore, two regression models were developed to predict MSD, one model for low speeds and the other for high speeds. Both models showed high correlations, R^2 = 98.4% and 99.5%, respectively.

- Low Speeds Model (LSM)

$$MSD = a*D^4 + b*N + c*T + d*N^2 ....(R^2 = 98.4\%)$$

- High Speeds Model (HSM)

$$MSD = a*D^4 + b*N + c*T + d*S*N + e*S*D^4 + f*S^2 .....(R^2 = 99.5\%)$$

Where, D = Axle load (kip per single axle).

T = Slab thickness (inch).

N = Number per axles.

S = Speed (mph).

a, ..., f = Regression coefficients their values are given in Table 6.2.

Two LEF sets were developed, for low and high speeds. A comparison between these two sets and the AASHTO LEF's is presented in Figure 6.15. As can be seen from this figure, LEF's based on the HSM agrees with the AASHTO LEF's. This is because the mean speed at the AASHO Road Test was approximately 35 mph [Coree and White, 1988]. Subsequent analysis is made using the HSM . To extend the validity of the HSM, more cases were analyzed to cover a wider range of factor levels and the results were compared with the extrapolated predictions of this model.

A second design of experiment (RDOE2) was implemented to consider the effect of 18-kip SAL repetitions. Two factors were included in RDOE2, slab thickness (T) and number of 18-kip SAL repetitions (C). Three levels for slab thickness were included in the analysis, 6", 12" and 18", and the 18-kip SAL was repeated up to 30 times. A regression analysis on the results obtained using the 3D-DFEM and the following regression model was developed:

$$MSD=(a+b*T)*C.....(R^2=97.8\%)$$

Where, a and b are regression coefficients their values are given in Table 6.2.

6.2.3.2. Comparison Between Purdue LEF's and Other LEF's

Purdue LEF's for different slab thickness were compared with the corresponding AASHTO LEF's for single and tandem axle configurations. Figures 6.16 and 6.17 show the results of this comparison. Purdue LEF's were found to agree with the AASHTO LEF's for both single and tandem axle configurations.

6.2.3.3. Sensitivity Analysis

The effect of slab thickness on LEF's is shown in Figures 6.18 and 6.19 for single and tandem axle configurations, respectively. When slab thickness increases, pavement damage due to loads decreases and therefore LEF's decrease. As can be seen from Figures 6.18 and 6.19, the LEF's decrease as slab thicknesses increase, as expected. The same is true for the AASHTO LEF's for thin slabs (6 to 8 inches). For thicker slabs (> 8 inches) the AASHTO LEF's increase with increase of slab thickness. This could be associated with surface factors such as spalling and joint faulting. LEF's for two, three and four-axle configurations are shown in Figure 6.20.

6.3 Composite Pavement LEF's

6.3.1 Comparison Between Different LEF's for Composite Pavements

No references in the literature were found for LEFs.

6.3.2. The 3D-DFEM Analysis

The typical composite pavement cross sections for Interstate, United States and State Roads showed in Figure 6.1, were modeled in this analysis as two 12 foot lanes plus 8 feet shoulders on either side. The pavement structure consists of three layers, asphalt surface, concrete slab and granular subbase on top of lean clay (CL) subgrade. Shoulders were modeled to be asphalt shoulders. Boundary conditions, longitudinal and transverse joints, deep foundation types, loading conditions, section lengths, finite element mesh sizes and element types were checked and evaluated. Details of these evaluations can be found in Chapter 5. Vehicle speed

similar to the average speed of the AASHO Road Test, 35 mph [Coree and White 1988], was used in developing the LEF's.

It should be noted that concrete slabs are assumed to be repaired before construction of the overlay, which is a common technique in Indiana. Longitudinal and transverse joints were modeled in the concrete slab and corresponding reflected cracks extending into the shoulder were modeled for the asphalt overlay.

6.3.3. Purdue LEF's for Composite Pavements

Asphalt overlays have a significant effect on concrete pavement response, performance and failure mechanism. The failure mechanism of composite pavements is different from that of flexible and rigid pavements. When a heavy load is applied and repeated on a flexible pavement, some permanent deformation develops in the different layers, including the surface layer. These permanent deformations accumulate at the pavement surface as "pavement rutting". When the rut depth reaches a certain limit the pavement is considered to be failed.

When a similar heavy load is applied and repeated on a concrete pavement no permanent deformation is expected in the concrete slab. Some permanent deformation may be developed in asphalt bound or unbound layers underneath the concrete slabs resulting in a void. The total surface permanent deformation in this case is almost zero because the concrete slab returns to its original position when the load is removed. The void under the slab will lead to a larger slab deflection when the load is repeated. When the slab deflection reaches a certain limit, a crack is initiated and the pavement fails.

The failure mechanism of composite pavements is a combination of those of flexible and

rigid pavements. Permanent deformation occurs in the asphalt overlay as well as in asphalt bound or unbound layers underneath the slab. However rut depth at the surface only reflects permanent deformation of the asphalt layer because the rigid slab rebounds. The total loaded deflection (elastic and plastic) reflects the elastic and plastic deformation of the asphalt overlay, elastic deformation of the rigid slab as well as, the elastic and plastic deformation of the material under the slab. The total deflection increases with number of load applications and is proposed as the basis of a rational equivalency criteria for composite pavements. Simply stated the LEF of load "j" on cross section "i" (LEF_{ij}) is equal to the number of the 18-kip single axle load (SAL) repetitions on cross section "i" required to develop the same total surface deformation (TSD) as one pass of the load "j" on the same cross section "i".

Two statistical models were developed for composite pavement LEF's. The first model predicts the TSD from one pass of load "j" on cross section "i", then the predicted TSD is used as input for the second model to estimate the number of 18-kip SAL repetitions required to develop the same TSD in cross section "i", which is the LEF_{ij}. Figure 6.21 shows a graphical representation of the concept of the Purdue LEF's for composite pavements.

6.3.3.1. Design of Experiments

Two design of experiments were implemented to develop the composite pavement LEF's. The following factors were included in the first DOE (CDOE1):

1. Axle load (D).
2. Number of axles (N).
3. Slab thickness (T_{con}).

4. Overlay thickness (T_{asp})

Table 6.5 shows factor levels included in CDOE1. The selected factor levels for slab and overlay thicknesses represent the range of thicknesses used in Indiana. Subgrade type was not included in the CDOE1 because it was found insignificant in development of flexible pavement LEF's and because of concrete slab rigidity, the subgrade type is not expected to be significant for composite pavement LEF's. A lean clay (CL) subgrade was assumed for all cross sections. The 3D-DFEM analysis was conducted for a speed similar to that of the AASHO Road Test speed, 35 mph, to be consistent with previously developed flexible and rigid pavement LEF's.

A partial factorial design was used to develop the first model. Different load-cross section combinations were analyzed using the 3D-DFEM analysis. An analysis of variance (ANOVA) was conducted of the results to test the significance of different factors included in CDOE1. The significant main effects and 2-way interactions were used to develop a regression model for predicting TSD for different axle load configurations. Results of the regression analysis are shown in Figure 6.21. The regression model is :

$$TSD = a*D^4 + b*N + c*D^4*(T_{asp} + T_{con}) \ldots\ldots\ldots R^2 = 98.72\%$$

Where, a, b and c are regression coefficients their values are given in Table 6.2.

D = Axle load (kip/axle).

N = Number of Axles.

T_{asp} and T_{con} are the asphalt overlay and slab thickness, respectively.

A second design of experiment (CDOE2) was implemented to consider the effect of the 18-kip SAL repetitions. Three factors were included in CDOE2, slab thickness (T_{con}), asphalt

overlay thickness (T_{asp}) and number of the 18-kip SAL repetitions (C). Two levels for slab thickness , 6"and 12", and two levels for overlay thickness, 4" and 8", were included in the analysis. The 18-kip SAL was repeated up to 30 times. A full factorial design was used to develop this model. Different overlay/slab thickness combinations were analyzed using the 3D-DFEM. An analysis of variance (ANOVA) was conducted on the results to test the significance of different factors included in CDOE2. The significant main effects and 2-way interactions were used to develop a regression model to predict TSD as a function of the 18-kip SAL repetitions. The form of the progression model is:

$$TSD=a+c[b+c\ T_{con}\ +\ d\ T_{asp}].....(R^2=97.78)$$

Where, a, b and c are regression coefficients. Their values are given in Table 6.2.

To extend the validity of theses models, more cases were analyzed to cover wider ranges of factor levels and the results were compared with the extrapolated predictions of this model.

6.3.3.2. Sensitivity Analysis

A comparison between the AASHTO LEF's for concrete pavement and Purdue LEF's for composite pavement are shown in Figure 6.22. The highest and lowest AASHTO LEF's for different slab thickness are presented. Four cases were considered for the composite pavement LEF's in the analysis:

- Thin overlay (4") on thin slab (6"),
- Thin overlay (4") on thick slab (12"),
- Thick overlay (8") on thin slab (6"), and

- Thick overlay (8") on thick slab (12").

As expected, the thin overlay/thin slab combination showed the highest LEF's, while the thick overly/thick slab combination showed the lowest LEF's. Also, the composite pavement LEF's are lower than those of the concrete pavement LEF's. This was expected because the additional overlay thickness significantly increases the pavement structure stiffness. From this analysis, it was found that increased slab thickness and/or overlay thickness from that at the AASHO) Road Test results in lower LEF's than that of the AASHTO LEF's for concrete pavement.

The effect of slab thickness on LEF's is shown in Figure 6.23, while the effect of overlay thickness is shown in Figure 6.24. As expected, as the slab or the overlay thickness increases, the LEF's decrease.

LEF's for two, three and four axle configurations are shown in Figure 6.25. This analysis was made for a 10 inch JRCP overlaid with a 4 inch asphalt concrete overlay. The sample of overload permit applications showed that the average axle spacing is 4 feet. Therefore, a 4 feet axle spacing was assumed for n-axle configurations.

6.4. Advantage of Purdue LEF's

There are no rational LEF's available for composite pavement analysis and the AASHTO LEF's for asphalt and concrete pavements are only valid for number of axles and load ranges used in the AASHO Road Test. The 1993 AASHTO Design Guide [AASHTO 1993] recommends that the concrete pavement LEF's be used for composite pavement. The behavior of composite pavements is different than concrete pavements. If concrete pavement LEF's are used for composite pavement traffic analysis, the significant contribution of the overlay is not

accounted for.

Purdue LEF's can be considered as serviceability based LEF's. They are based on the elastic deflection of all layers and permanent deformation developed in the asphalt overlay and unbound layers underneath the concrete slab. The permanent deformation is related to potential accumulation of roughness which is a large component of serviceability. Elastic deformation of the rigid slabs is related to fatigue capacity. Purdue LEF's have the following advantages:

1. Purdue LEF's are based on dynamic analysis in which moving loads were considered. Also, realistic material properties and models were included in this analysis.
2 The 3D-DFEM dynamic analysis used to develop these LEF's has been verified for static, linear elastic analysis and for dynamic, non-linear analysis of both flexible and rigid pavements and excellent results were obtained.
3. Purdue LEF's consider the effect of load repetitions and does not assume that the pavement response is a linear function in the number of load repetitions.
4. Purdue LEF's are based on an analytical model which means that they can be updated or extended to cover other factors not already included.

CHAPTER 7 THE OVERLOAD PERMITTING PROCEDURE

In this chapter the overload permitting procedure is presented. It should be noted that this procedure is for both bridge and pavement analyses. Details of the bridge analysis are reported by NBR et al. 1993, while details of the pavement analysis are presented in previous chapters.

7.1. Indiana Truck Weight Regulations

Indiana legal limits of truck weights as described in the Oversize-Overweight Vehicular Permit Handbook [IDOH 1988] are as follows:

" *The total gross weight, in pounds, of any vehicle or combination of vehicles with load shall not exceed an overall gross weight on a group of two or more consecutive axles as computed by the following formula:*

$$W=500[(\frac{LN}{N-1})+12N+36]$$

Where,

W = *Overall gross weight on any group of two or more consecutive axles to the nearest 500 pounds.*

L = *Distance in feet between the extreme of any group of two or more consecutive axles.*

N = *Number of axles in the group under consideration.*

However, the weight may not exceed:

- Maximum gross weight - 80,000#

- Maximum Single Axle Weight - 20,000#

- Maximum Tandem Axle Weight - 17,000#

- Maximum Wheel Weight - 800# per linear inch of tire measured between the flanges of the rim.

Exception to the formula is for two consecutive sets of tandem axles which may carry a gross load of 34,000 pounds each, providing the overall distance from center to center between the first and last axles is 36 feet or more. Also, the following weights take precedent when they are grater than the weights allowed by the formula:

- Maximum gross weight - 73,280#

- Maximum Single Axle Weight - 18,000#

- Maximum Tandem Axle Weight - 16,000#

- Maximum Wheel Weight - 800# per linear inch of tire measured between the flanges of the rim."

Trucks exceeding these limits, overloaded trucks, are required to have an overload permit before using the Indiana highway network. The permit is guaranteed for a fee if the overloaded truck does not exceed the following limits [IDOH 1988]:

- Maximum gross weight - 108,000#

- Maximum Single Axle Weight - 28,000#

- Maximum Tandem Axle Weight - 24,000#

- Maximum Axle Group Weight - 51,000#

- Maximum Wheel Weight - 800# per linear inch of tire measured between the flanges of

the rim.

Current INDOT regulations allow a truck exceeding the above limits to apply for an overload permit. In this case, the overload permit is evaluated for bridges and processed in two phases. In Phase 1, a simply supported beam and a two equal-span continuous beam are analyzed for the given permit vehicle for spans from 20 to 120 feet in increments of 10 feet. The equivalent HS loading of the given overloaded truck is calculated by comparing the bending moments induced by the overloaded truck with those induced by the HS20 design truck [AASHTO 1983]. The overloaded truck will be permitted if its equivalent HS loading is less than HS30, i.e., 1.5 times the HS20 design truck. When a truck matches a prior permitted truck, the prior results from Phase 1 are used for a quick evaluation. If the overloaded truck does not satisfy Phase 1 criteria, Phase 2 is implemented which involves a detailed load rating. The detailed load rating of Phase 2 requires specific information about the truck and bridges on the route for which the permit is requested. No evaluation for the damage effect of overloaded trucks on pavements is currently made.

7.2. Typical Pavement Cross Sections for Indiana

Based on the Highway Inventory Annual Report [IDOH 1989], there are approximately 91,500 miles of roads within the state of Indiana. Approximately 11,300 miles are under the control of INDOT and the rest are under the control of different local government units. The 11,300 miles of roads that are the responsibility of INDOT have about 28,203 lane miles. The Road Life data base [Lindly and White 1989 and Pumphrey and White 1989] has detailed information about the cross section and the subgrade for 14,766 lane miles (more than 50% of

the total lane miles). From the data available in the Road Life data base, pavement structure distribution was obtained for different highway classes; Interstate (I), United States (US) and State Roads (SR). Typical pavement cross sections shown in Figure 6.1 (in Chapter 6) were selected to represent the different highway classes. These typical cross sections are used for evaluating the damage effect of overloaded trucks at the network level. Table 7.1 shows typical values of the material properties used in the analysis.

7.3. Stress Models

Regression models were developed to predict maximum stress levels in concrete slabs and the underlying unbound layers and subgrade of the composite pavement typical cross sections shown in Figure 6.1 and unbound layers and subgrade of the asphalt pavement typical cross section shown in Figure 6.1. For each typical cross section, design of experiments (DOE) were set up to consider the effect of load parameters on stress levels. The following DOE's were considered in the analysis:

Highway Class	Composite			Asphalt	
	Slab	Subbase	Subgrade	Base	Subgrade
Interstate	YES	YES	YES	NO	NO
United States	YES	YES	YES	NO	NO
State Roads	YES	YES	YES	YES	YES

For each DOE the following factors were included:

1. Number of axles (1, 2 and 4).
2. Axle load (18, 24 and 36 kip/single axle of the axle group).
3. Axle spacing (2.5, 4.4 and 5.5 feet).

Static loads were assumed and the maximum stress level in each layers were predicted. Analysis of variance (ANOVA) was conducted for each DOE to test the significance of different factors. Significant main effects and two-way interactions were included in the regression models as follow:

1. Single Axle - Composite Pavement Models:

$$SlabStress = -54.6556 + 11.0388 * AxleLoad + 30.483 * HighwayClass$$

$$SubbaseStress = -1.354 + 0.2328 * AxleLoad + 0.79937 * HighwayClass$$

$$SubgradeStress = -0.8589 + 0.1393 * AxleLoad + 0.44696 * HighwayClass$$

2. N_Axle - Composite Pavement Models:

$$SlabStress = 205.064 + 0.1797 * (AxleLoad)^2 + 21.6923 * HighwayClass - 6.401 * N - 14.51 * S$$

$$SubbaseStress = 4.773 + 0.00463 * (AxleLoad)^2 + 0.2992 * N - 0.3637 * S$$

$$SubgradeStress = 2.965 + 0.00371 * (AxleLoad)^2 + 0.3423 * HighwayClass - 0.2406 * S$$

3. Single Axle - Asphalt Pavement Models:

$$BaseCourseStress = 0.3517 * AxleLoad$$

$$SubgradeStress = 0.0941 * AxleLoad$$

4. N_Axle - Asphalt Pavement Models:

$$BaseCourseStress = 6.1229 + 0.000138 * (AxleLoad)^3 + 0.15329 * S$$

$$SubgradeStress = 2.799 + 0.0000434 * (AxleLoad)^3 - 0.14469 * S$$

Where,

axle load = load per single axle in the axle group (kip).

N = number of axles in one group.

S = average spacing between axles in one group (foot).

highway class = 1 for Interstate,
2 for United State, and
3 for State Roads.

slab stress = maximum tensile stress (psi) at a transverse joint edge

7.4. The Overload Permitting Procedure

Figure 7.1 shows the flow chart of the overload permitting procedure. A user friendly

computer software was developed to implement this procedure. The procedure has the following steps:

1. Data entry, which includes:
   - Permit type (overweight, oversize or mobile home)
   - Vehicle information (overall length, width and height, number of axles, gross load, axle loads and spacing, company name, license,..., etc.)
   - Trip information (origin, destination and route, if any).

   The user is permitted to enter, review, and make changes in the data. Details of the data entry step are presented in Appendix A "User Manual".
2. Load parameters for bridge and pavement analyses are extracted from the vehicle information. Bridge analysis load parameters include: wheel base, gross load, number of equivalent axles. An equivalent axle is any group of axles that are placed within a distance of 9 feet center to center for each other. Pavement analysis load parameters include: grouping a truck into axle groups based on the distance between axles.The distance between any two successive axles in a group has to be less than 5-5\., For each axle group, the axle group load, spacing, number of wheels and number of axles are calculated.
3. Selection of the level of analysis:
   - Network level (default). In this analysis typical pavement cross sections are used representing different highway classes. A route independent formula is used for bridge analysis.
   - Project level. In this analysis the user has to enter the pavement cross section

parameters and material properties. Default values are provided as a guide to the user. A route dependent formula is used for bridge analysis.

4. Selection of type of analysis:
   - Bridge analysis only.
   - Pavement analysis only.
   - Bridge and pavement analysis (default).

If the user selects bridge and pavement analyses (the default) the bridge analysis is made first. The pavement analysis will be run regardless of the results of the bridge analysis. If the truck is not permitted, the reason why the truck is not permitted, bridge, pavement or both, will be shown in the permit.

Based on the user selections, the truck damage effects on bridges and pavements are evaluated as described in the next sections.

7.4.1. Network Level Analysis

7.4.1.1. Bridge Analysis

The truck must satisfy the following:

- A minimum of 6 equivalent axles if the wheel base is more than 70 feet or a minimum of 3 equivalent axles if the wheel base is more than 25 feet. The number of equivalent axles for any given truck is obtained by counting closely spaced axles, within 9 feet, as a single equivalent axle.
- The wheel base has to be in the range of 10-120 feet.

If the truck satisfies the above conditions, a route independent model, depending only on truck parameters, is used to evaluate bridge damage. The variance in the allowable load (W) is not found to be homogeneous for the entire range of wheel base. The variance actually increases with the level of allowable load.

$$\sqrt{W}=C_1L+C_2$$

Where, C_1 and C_2 are regression coefficients and their limits are shown in Table 7.2 [NBR and et al. 1993].

W = Maximum allowable load

7.4.1.2. Pavement Analysis

The typical pavement cross sections shown in Figure 6.1 are used in this analysis to represent different highway classes (Interstate, United States and State Roads). Trucks are represented as axle groups. A sample of overload permit applications was reviewed and it was found that the 5.5 feet axle spacing is a break point. Therefore, the spacing between any two successive axles with axle spacing equal to or less than 5.5 feet are considered to be in one group. The pavement analysis has the following steps:

1. Evaluate Stress Levels

When a pavement is subjected to a heavy load, some permanent deformation could develop in one or more of the pavement layers. Figures 4.21 and 5.7 show the effect

of heavy loads on asphalt and concrete pavements, respectively. As can be seen from these figures, when the pavements are subjected to an 18-kip single axle load (SAL), no permanent deformation developed in any of the unbound layers of the asphalt and concrete pavements. When a heavy load is applied, 58-kip SAL on the asphalt pavement and 60-kip SAL on the concrete pavement, some permanent deformation developed in the unbound layers of both the asphalt and concrete pavements. These permanent deformations developed because the unbound layers were subjected to stress levels higher than their yield stresses. Therefore, if the stress levels in the unbound layers are kept below their yield stresses, no permanent deformations are expected and the pavement damage is minimal. For concrete slabs, if the ratio of the stress to modulus of rupture exceeds 0.5, some fatigue damage develops which reduces the slab life.

The purpose of this step is to estimate stress levels developed by the overloaded truck axle groups in the unbound layers and concrete slabs of the typical pavement sections. These stresses are compared with the corresponding yield stress of the unbound layers and the modulus of rupture of the concrete, respectively. The statistical models presented earlier in this chapter were used to estimate stress levels in the unbound layers and the concrete slabs of the typical sections as a function of truck parameters. Previous analysis showed that the effect of static loads are more severe for pavements than moving loads, therefore, static loads were used in the development of the statistical models. For each of the typical cross sections, if the yield stress in any of the unbound layers, including the subgrade, is exceeded or the concrete stress ratio (stress/modulus of rupture of the concrete) exceeds 0.5, the overloaded truck will not be permitted to use this highway

class. Further analysis will be made only for the typical cross sections which passed this check (satisfactory cross sections).

2. Load Equivalency Factors

For each satisfactory cross section, the LEF of each axle group will be determined using the appropriate Purdue LEF set. If the axle group LEF is greater than 32 the truck will not be allowed to use this highway class. The selection of this LEF limit (32) is based on Figure 7.2. In Figure 7.2 the logarithm of composite pavement LEF's are plotted versus maximum surface deformation (MSD) for thin and thick pavements. As can be seen from this figure, the slope of the curve increases sharply for LEF's greater than 32 (logarithm = 1.5).

If the overloaded truck passes the stress and the axle group LEF checks, no severe damage to the pavement is expected. Another check is made to evaluate the reduction in the pavement life due to one pass on the overloaded truck. Accumulated LEF for the truck is calculated by summing the LEF's of all axle groups and comparing it to the design traffic in equivalent single axle load (ESAL) units for different highway classes. If the accumulated LEF exceeds 10% of the daily traffic in EASL's, the truck will not be permitted to use this highway class. Based on the limited information available about design traffic volumes in EASL's for different highway classes, the following numbers are assumed:

Highway Class	AADT	% Truck	ESAL	LEF Limit
I	20,000	20%	6000	600
US	20,000	5%	1500	150
SR	15,000	5%	1125	112.5

Where, one truck = 1.5 ESAL's

The truck is permitted to use highway classes which pass the previous checks. These highway classes will be shown on the permit.

7.4.2. Project Level Analysis

7.4.2.1. Bridge Analysis

In this analysis the allowable load at the operating stress level depends on both bridge and truck parameters. The bridge parameters referred to as HS truck capacity is introduced to develop a route depended model.

$$\sqrt{W}=C_1(HS_{truckcapacity})L+C_2$$

Where, W is the allowable load, and C_1 and C_2 are regression coefficients. Their limits are shown in Table 7.3. The $HS_{truck\ capacity}$ of a bridge is defined as the maximum gross vehicle load that the bridge can carry within the operating stress level for a vehicle having the same configuration in terms of axles and axle load distribution as the standard HS20 truck with variable axle spacing. Also, the truck has to satisfy both the minimum number of axles/wheel

base and length of the wheel base [NBR et al. 1993].

7.4.2.2 Pavement Analysis

In this option, the user has to provide information about the pavement cross section and material properties. This information includes:

1. Pavement type (asphalt, concrete or composite pavement)
2. Layer thickness.
3. Material properties of each layer:
    - Asphalt surface layer: modulus of elasticity, Possion's ratio, G-ratio, damping coefficient and bulk density.
    - Granular layers: modulus of elasticity, Possion's ratio, initial yield stress, yield function, cohesion, angle of internal friction, damping coefficient and bulk density.
    - Cohesive layers: modulus of elasticity, Possion's ratio, initial yield surface, yield function, water content, cohesion, angle of internal friction, damping coefficient and bulk density.

Default typical values for these properties are provided to the user.

Similar to the network level analysis, the overloaded truck has to pass the stress level and LEF checks in order to be permitted.

CHAPTER 8 SUMMARY AND CONCLUSIONS

A truck moving over a pavement creates a load pulse which is transmitted through the pavement layers. The magnitude of the load pulse varies with time. Pavement layers respond differently to this load pulse, depending on each layer's material characteristics. In traditional pavement analysis methods, truck loads are assumed to be static loads and the materials of different layers, including subgrade, are assumed to be linear elastic materials. Some pavement analysis procedures, such as multi-layer analysis and Westergaard analysis, assume that pavements are extended to infinite in the longitudinal and transverse directions, which is not true especially for rigid pavements. The difference in the traditional pavement analysis methods' assumptions and the actual loading conditions and material characteristics leads to inaccurate prediction of pavement response.

A study has been conducted at Purdue University to develop a procedure for permitting overloaded trucks in Indiana. A realistic pavement analysis procedure was required to predict the damage effect of multi-axle, heavy loads on the Indiana highway network. Existing pavement analysis procedures were not found suitable for this study. A sample of overload permit applications was reviewed to determine truck configurations being permitted. The sample revealed that permits were requested for trucks with up to nine axles in one group as well as trucks with a single axle load of 72 kips. Load equivalency Factors (LEF) were required to account for these loads and variation in truck configurations. Two types of LEF's are available: analytical based LEF's and empirical based LEF's. Pavement analysis methods used to develop the analytical based LEF's involve

unrealistic assumptions, such as static loads and linear elastic material properties, while, the empirical LEF's, such as the AASHTO LEF's, are based on single and tandem axle configurations with more then one axle loads of 40 and 48 kips, respectively. Also, for pavements with thick asphalt layers or for composite pavements the validity of these LEF's is questionable.

A three dimension dynamic finite element model (3D-DFEM) was used to analyze flexible, rigid and composite pavements. This analysis was used to develop LEF's for the overload permitting study. Three LEF sets were developed for flexible, rigid and composite pavements.The 3D-DFEM has the capability to simulate actual truck loads moving at different speeds. Also, it can include linear and non-linear material properties. Several material models were used to characterize different paving materials. The Drucker-Prager model was used to model granular and silty materials, while the Cam-Clay model was used for clayey soils. Asphalt mixtures were modeled as visco-elastic materials and concrete was modeled as a elastic-plastic material. The 3D-DFEM has the capability to predict both elastic and plastic pavement response. This capability helps to predict and explain pavement response under different loading conditions and the response of different materials.

The 3D-DFEM was verified for flexible and rigid pavements by comparing its predictions with a multi-layer elastic analysis (for flexible pavement) and Westergaard's equations (for rigid pavement) assuming static loads and linear elastic material properties. High linear correlations were found between the 3D-DFEM predictions and the multi-layer elastic and Westergaard analyses. To verify the dynamic, non-linear analysis capabilities of

the 3D-DFEM, the 3D-DFEM predictions were compared with field measured pavement deflections for both flexible and rigid pavements. The predicted pavement deflections matched the measured deflections for flexible and rigid pavements very well (R^2 = 99.87% and 99.64%, respectively).

Using the 3D-DFEM sensitivity studies were conducted using the 3D-DFEM of the effect of cross section parameters and load parameters on flexible and rigid pavements response. The flexible pavement sensitivity study showed that:

1. The speed of the moving load has a significant effect on elastic and plastic pavement response.
2. The confinement effect of shoulders and degree of continuity at the pavement/shoulder joint were found to reduce pavement deflection.
3. Temperature, loading time and rate of loading were found to have a significant effect on pavement response.
4. Loads that generate stresses higher than yield stresses will increase rutting significantly.

The effect of different load attributes, axle load and spacing, number of axles and number of wheels, as well as cross section attributes, subgrade type, different material properties and deep foundation type, were investigated and found to be significant in flexible pavement response.

The rigid pavement sensitivity study showed that:

1. The speed of the moving load was found to be significant for rigid pavements. The maximum surface deflection was reduced by 60% when the speed increased from 1.75 mph to 10 mph.

2. Subbase courses were found to reduce pavement deflection and improve relative load transfer between slabs. The maximum surface deflection was reduced by 45% when a 4" subbase was used and the joint efficiency was increased by 11%.

3. As compared to an undoweled pavement, 20% reduction in the maximum vertical deflection resulted and the joint efficiency increased by 12% when 1.25"diameter dowels with 12"dowel spacing were used. It was found that the capacity of 1" diameter dowels is adequate for an 18-kip single axle load moving at a speed of 1.75 mph. Also, joint width was found to have a significant effect on joint efficiency.

4. Axle load magnitudes were found to have a significant effect on deflection.

The relation between load magnitude and pavement deflection at low load levels was found to be linear for flexible and rigid pavements. When the load level exceeds a certain limit this relationship became non-linear. Also, at high load levels one or more of the pavement layers were found to behave as an elastic-plastic material and plastic (permanent) deformation developed in these layers. The plastic deformation accumulated with load repetitions. Therefore, heavy loads should be prevented from using pavement sections not designed to carry heavy loads. Also, higher quality pavement layers can prevent severe damage to pavements.

Analytical based LEF's were developed for flexible, rigid and composite pavements (Purdue LEF's). The LEF of any load "j"and cross section "i"was defined as the number of the 18-kip single axle load (SAL) applications required to develop the same pavement response of one pass of load "j"on the same cross section "i".Equal permanent deformation at the pavement surface was used for flexible pavement LEF's, while equal total surface deformation (elastic and plastic) was used for rigid and composite pavement LEF's. Two statistical models were developed for each pavement type. The first model predicts the pavement response to one pass of any load configuration on any cross section, while the second model uses this predicted response (the output of the first model) to estimate the number of the 18-kip SAL applications required to develop the same response on the same cross section.

A comparison was made between the AASHTO LEF's and Purdue LEF's for similar conditions of the AASHO Road Test and no significant difference was found. Purdue LEF's were developed based on an analytical model which can be extended in the future to cover a wider range of pavement and load parameters, while the AASHTO LEF's can and should not be extended.

In the permitting procedure, the damage effects of overloaded trucks are evaluated for pavements and bridges. The bridge analysis includes two steps:

1. The truck must satisfy the following:
   - A minimum of 6 equivalent axles if the wheel base is more than 70 feet or a minimum of 3 equivalent axles if the wheel base is more than 25 feet. The number of equivalent axles for any given truck is obtained by counting closely spaced axles, within 9 feet, as a single equivalent axle.
   - The wheel base has to be in the range of 10-120 feet.

2. The overloaded truck weight is checked versus the allowable weight calculated from statistical models based on analysis using the Bridge Analysis and Rating System (BARS) [BISAR 1972] and selected samples of bridges and overloaded trucks.

The pavement analysis is conducted in two steps:

- Check if the stress level developed by the overloaded truck axle groups in unbound layers of the pavement structure, including the subgrade, exceeds their yield stresses and if the ratio of stress/modulus of rupture of the concrete exceeds 0.5. The stress level in this step is estimated based on static loads.
- Calculate the LEF of each axle group of the overloaded truck using Purdue LEF sets and check if this LEF exceeds a certain limit. Also, check if the accumulated LEF for the truck, which is the sum of the LEF's of the truck axle groups, exceeds a certain limit. This analysis is based on moving loads.

A user friendly computer software was developed to implement this permitting procedure. The software allows the user to run a route independent damage analysis for overloaded trucks at the network level, as well as at the project level, for a specific pavement and/or bridge. At both levels, three options are available: check for pavements only, check for bridges only or check for both, the default. At the project level, the user is permitted to enter all of the cross section and load parameters. Also, typical values for material properties are available as default values.

REFERENCES

1. "ABAQUS, Finite Element Computer Program," Version 4.9, Hibbitt, Karlsson and Sorensen, Inc., 1989.

2. "ABAQUS, Finite Element Computer Program," Theory Manual, Version 4.9, Hibbitt, Karlsson and Sorensen, Inc., 1989.

3. "ABAQUS, Finite Element Computer Program," User Manual, Version 4.9, Hibbitt, Karlsson and Sorensen, Inc., 1989.

4. Acum, W. and L. Fox, " Computation of Load Stresses in a Three-Layer Elastic System," Geotechnique, Vol. 2, 1951.

5. American Association of State Highway Officials (AASHO),"AASHO Road Test Report 5; Pavement Research," Highway Research Board (HRB), HRB Special Report 61E, Washington, D.C., 1962.

6. American Association of State Highway and Transportation Officials (AASHTO), "Interim Guide for Design of Pavement Structures," Washington, D.C., 1972.

7. American Association of State Highway and Transportation Officials (AASHTO), "AASHTO Guide for Design of Pavement Structures," Washington, D.C., 1986.

8. Battelle Resource International, Presentation at Peer Review No. 2, Atlantic City, New Jersey, June, 1991.

9. "Bitumen Structures Analysis in Roads (BISAR), Computer Program," Koninlilijke/Shell - Laboratorium, Amsterdam, July 1972.

10. Boussinesq, J., "Application des potentiels a l'etude de l'equilibre et du mouvement des solides elastique," 1885.

11. Burmister, D., " The Theory of Stresses and Displacements in Layered Systems and Application to The Design of Airport Runways," Proceedings, Highway Research Board, 1943.

12. CanRoad Transportation Research Corporation, "Vehicle Weight and Dimension Study," Ottawa, Canada 1986.

13. Chou, Y., "Structural Analysis Computer Programs for Rigid Multicomponent Pavement Structures with Discontinuities-WESLIQID and WESLAYER," Army Engineer Waterways Experiment Station, 1981.

14. Claessen, A., Edwards, J., Sommer, P. and Uge, P., "Asphalt Pavement Design - Shell Method," Proceedings, Fourth International Conference on Structural Design of Asphalt Pavements, University of Michigan, Ann Arbor, Michigan, 1977.

15. Cobb, C. and Kenis, W., "Pavement Response Load Equivalent Factors," Presented at the 69th Annual Meeting of the Transportation Research Board, Washington D. C., 1990.

16. Coree, Brian and White, Thomas, "Layer Coefficients in Terms of Performance and Mixture Characteristics," Joint Highway Research Project, FHWA/IN/JHRP-88/13, Purdue University, 1988.

17. Derucher, K. and Korfiatis, G., "Materials for Civil and Highway Engineers,: Second Edition, Prentice Hall, New Jersey, 1988.

18. Drucker, D. C., and W. Prager, "Soil Mechanics and Plastic Analysis or Limit Design," Quarterly of Applied Mathematics, Vol. 10,pp. 157-165, 1952.

19. Elliott, R. and David, L., "Improved Characterization Model for Granular Base," Transportation Research Board, Transportation Research Record (TRR) 1227, Washington, D.C., 1989.

20. Federal Highway Administration, "Load Equivalency Workshop Synthesis," Publication No. FHWA-RD-89-117, April 1989.

21. Federal Highway Administration, "Rigid Pavement Analysis and Design," FHWA-RD-88-068, Virginia, June 1989.

22. Friberg, B., "Design of Dowels in Transverse Joints of Concrete Pavements," Proceeding, Highway Research Board, 1938.

23. Finn, F., Saraf, C., Kulkarni, K., Smith, W. and Abdullah, A., "The Use of Distress Prediction Subsystems for the Design of Pavement Structures," Proceedings, Fourth International Conference on Structural Design of Asphalt Pavements, University of Michigan, Ann Arbor, Michigan, 1977.

24. George, K. P., "Resilient Testing of Soils Using Gyratory Testing Machine," Transportation Research Board, 71 st Annual Meeting, Washington, D.C., January 12-16, 1992.

25. Hallin, J., Sharma, J. and Mahoney J., "Development of Rigid and Flexible Pavement Load Equivalency Factors for Various Widths of Single Tires," Transportation Research Board, Transportation Research Record (TRR) 949, Washington, D.C.,

1983.

26. Hilber, H., Hughes, T. and Taylor, R., "Collocation Dissipation and 'Overshoot' for Time Integration Schemes in Structural Dynamics," Earthquake Engineering and Structural Dynamics, Vol. 6, pp. 99-117, 1978.

27. Idelin, M., Bhatti, M. and Stoner, J., "Nonlinear Response of Rigid Concrete Pavements to Simulated Vehicle Loads, Midwest Transportation Center, Iowa, May 1991.

28. Ioannides, A., "Analysis of Slabs-on-Grade for a Variety of Loading and Support Conditions," Ph. D. Thesis, University of Illinois Urbana, 1984.

29. Jones, A., "Tables of Stresses in Three-Layer Elastic Systems," Highway Research Board Bulletin 342, 1962.

30. Kenis, W., "Predictive Design Procedure, VESYS User Manual -An Interim Design Method for Flexible Pavements Using the VESYS Structural Subsystem," Report No. FHWA-RD-87-154, Federal Highway Administration, Washington D. C., January 1987.

31. Kim, D. and Stokoe, K. H., "Characterization of Resilient Modulus of Compacted Subgrade Soils Using Resonant Column and Torsional Shear Test," Transportation Research Board, 71 st Annual Meeting, Washington, D.C., January 12-16, 1992.

32. Logan, D., "A First Course in the Finite Element Method," PWS-KENT Co., 1986.

33. Mahoney, J., "The Relationship Between Axle Configuration, Wheel Loads and Pavement Structures," Society of Automotive Engineers (SAE), 1988.

34. Majidzadeh, K., Ilvies, G. and Sklyut, H., "Mechanistic Design of Rigid Pavements," Resource International Inc., 1984.

35. McCullough, B., Abou-Ayyash, A., Hudson, W. and Randall, J., "Design of Continuously Reinforced Concrete Pavements for Highways," NCHRP Report 1-15, The University of Texas at Austin, 1975.

36. NBR, Prasad, White, D., Ramirez, J. and Kuczek, T., "Statistical Analysis of Overload Vehicle Effects on Indiana Highway Bridges," Joint Highway Research Project, FHWA/IN/JHRP/93-1, Purdue University, Indiana, 1993.

37. Odemark, N., "undersokning av elasticitetegenskaperna hos olika," moddeland 77, 1949.

38. Okamoto, P. and Packard, R., Effect of High Tire Pressures on Concrete Pavement Performance," Proceedings, 4th International Conference on Concrete Pavement Design and Rehabilitation, Purdue University, April 1989.

39. O'Reilly, M. and Brown, S., "Cyclic Loading of Soils: from theory to design," Van Nostrand Reinhold, New York, 1991.

40. Papagiannakis, A, Hass, R., Woodrooffe, J, and Leblanc, P., "Impact of Roughness-Induced Dynamic Load on Flexible Pavement Performance," ASTM STP 1031, American Society for Testing and Materials, Philadelphia, 1990, pp. 383-397.

41. Parry, R. H., Editor, Stress-Strain Behavior of Soils, G. T. Foulis and Co., Henley, England, 1972.

42. Peattie K., "Stress and Strain Factors for Three-Layer Elastic Systems," Highway Research Board Bulletin 342, 1962.

43. Pickett, G. and Ray, G., "Influence Charts for Rigid Pavements," Transactions, American Society yof Civil Engineers (ASCE), 1951.

44. Rilett, L. R. and Hutchinson, B. G., "LEF Estimation from Canroad Pavement Load-Deflection Data," Transportation Research Record 1196 ,Transportation Research Board, Washington, D.C., 1988, pp. 171-178.

45. Roque, R., Tia, M. and Ruth, B. E., "Asphalt Rheology to Define the Properties of Asphalt Concrete Mixtures and the Performance of Pavements," Asphalt Rheology: Relationship to Mixture, ASTM STP 941, O. E. Briscoe, Ed., American Society for Testing Materials, Philadelphia, 1987, pp. 3-27.

46. Santucci, L. E., "Thickness Design Procedure of Asphalt and Emulsified Asphalt Mixtures," Proceedings, Fourth International Conference on Structural Design of Asphalt Pavements, University of Michigan, Ann Arbor, Michigan, 1977.

47. Schofield, A., and C. P. Worth, "Critical State Soil Mechanics," McGraw-Hill, New York, 1968.

48. Sebaaly, B., Mamlouk, M. and Davies, T., "Dynamic Analysis of Falling Weight Deflectometer Data," Transportation Research Board (TRB), TRR 1070, 1986.

49. Sawan, J., Darter, M. and Dempsey, B., "Structural Analysis and Design of Portland Cement Concrete Highway Shoulders," Technical Report FHWA/RD-81/122, Federal Highway Administration (FHWA), 1982.

50. Tabatabaie-Raissi, A., "Structural Analysis of Concrete Pavement Joints," Ph. D. thesis, University of Illinois Urbana, 1977.

51. Trapani, R. and Scheffey, C., "Load Equivalency: Issues for Further Research," Public Roads, Volume 53 n2, September, 1989, pp 39-45.

52. "Vehicle Weight and Dimension Study," Canroad Transportation Research Corporation, Ottawa, Canada 1986.

53. Westergaard, H. M., "Stresses in Concrete Pavements Computed by Theoretical Analysis," Public Roads, April 1926.

54. Wood, D., "Soil Behaviour and Critical State Soil Mechanics," Cambridge University Press, 1990.

55. Yoder, E. J. and Witczak, M. W., Principles of Pavement Design, Second Edition, Hohn Wiley and Sons, Inc., 1975

56. Zaman, M., Taheri, M. and Alvappillai, A., "Dynamic Response of a Thick Plate on Viscoelastic Foundation to Moving Loads," International Journal for Numerical and Analytical Methods in Geomechanics, Vol. 15, 627-647, 1991.

57. Zienkiewicz, O., "The Finite Element Method," Third Edition, McGraw-Hill, 1977.

Table 2.1 Boussinesq's Equations for a Point Load [Ullidtz, 1987]

Normal Stresses $\sigma_z = 3P/(2\pi R^2) * \cos^3\theta$ $\sigma_r = P/(2\pi R^2) * [3\cos\theta \sin^2\theta - (1-2\mu)/(1+\cos\theta)]$ $\sigma_t = P/(2\pi R^2) * (1-2\mu)[-\cos\theta + 1/(1+\cos\theta)]$ $\sigma_1 = 3P/(2\pi R^2) * \cos\theta$ $\sigma_v = 1/3(\sigma_1 + \sigma_2 + \sigma_3) = P/(3\pi R^2) * (1+\mu)\cos\theta$
Shear Stresses $\tau_{rz} = 3P/(2\pi R^2) * \cos^2\theta \sin\theta$ $\tau_{rt} = \tau_{tz} = 0$
Normal Strains $\varepsilon_z = (1+\mu)P/(2\pi R^2 E) * (3\cos^3\theta - 2\mu\cos\theta)$ $\varepsilon_r = (1+\mu)P/(2\pi R^2 E) * [-3\cos^3\theta + (3-2\mu)\cos\theta - (1-2\mu)/(1+\cos\theta)]$ $\varepsilon_t = (1+\mu)P/(2\pi R^2 E) * [-\cos\theta + (1-2\mu)/(1+\cos\theta)]$ $\varepsilon_v = \varepsilon_z + \varepsilon_r + \varepsilon_t = (1+\mu)P/(\pi R^2 E) * (1-2\mu)\cos\theta$
Displacements $d_z = (1+\mu)P/(2\pi RE) * [2(1-\mu) + \cos^2\theta]$ $d_r = (1+\mu)P/(2\pi RE) * [\cos\theta \sin\theta - (1-2\mu)\sin\theta/(1+\cos\theta)]$ $d_t = 0$

Table 2.2 Available FEM's for Rigid Pavements [FHWA, 1989]

FEM	Slab Model	Subgrade	Load	Concrete
ILLI-SLAB	Thick Plate	Winkler	Static	Linear Elastic
JSLAB	Thick Plate	Spring	Static	Linear Elastic
Wesliqud	Thick Plate	Winkler	Static	Linear Elastic
Weslayer	Thick Plate	Elastic	Static	Linear Elastic
JCS-1	Thick Plate	Elastic	Static	Linear Elastic
RISC	Thick Plate	Winkler	Static	Linear Elastic
CMS	Thick Plate	Elastic	Static	Linear Elastic

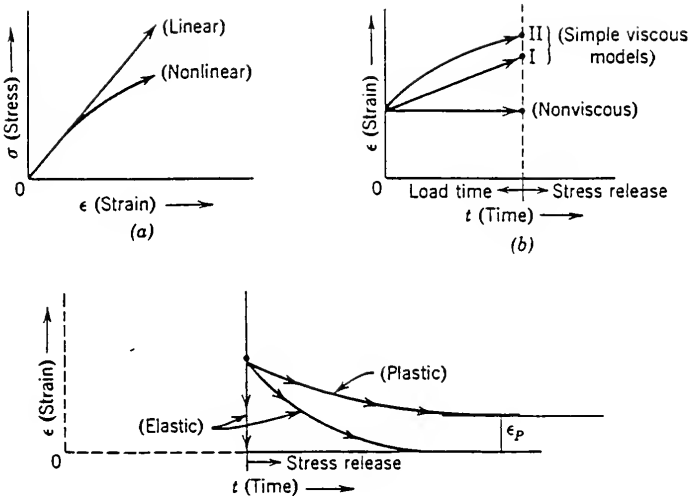

Figure 2.1 Material Characteristics [Yoder and Witczak, 1975]

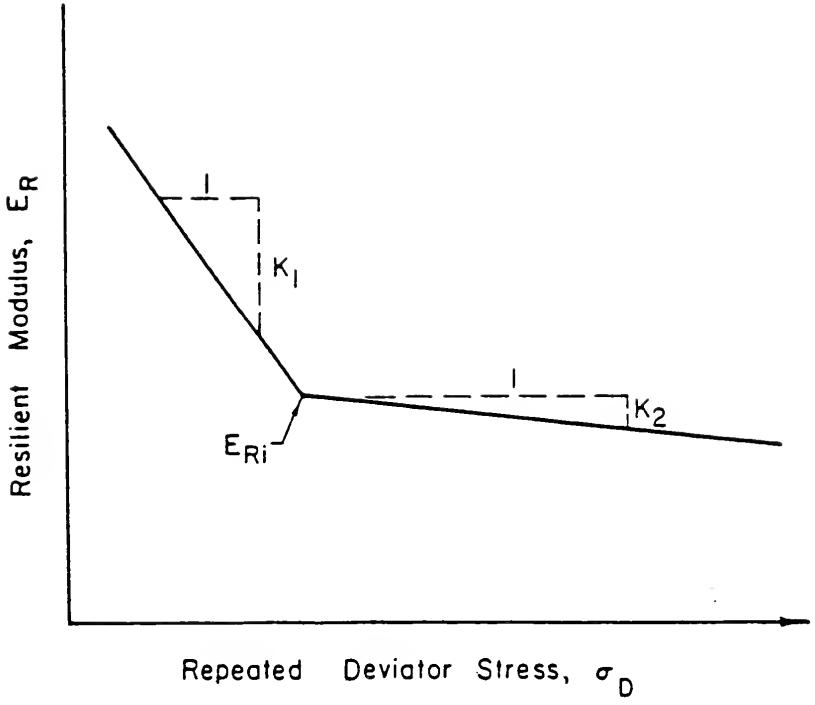

Figure 2.2 Stress Dependent Material Behavior [Elliott and David, 1989]

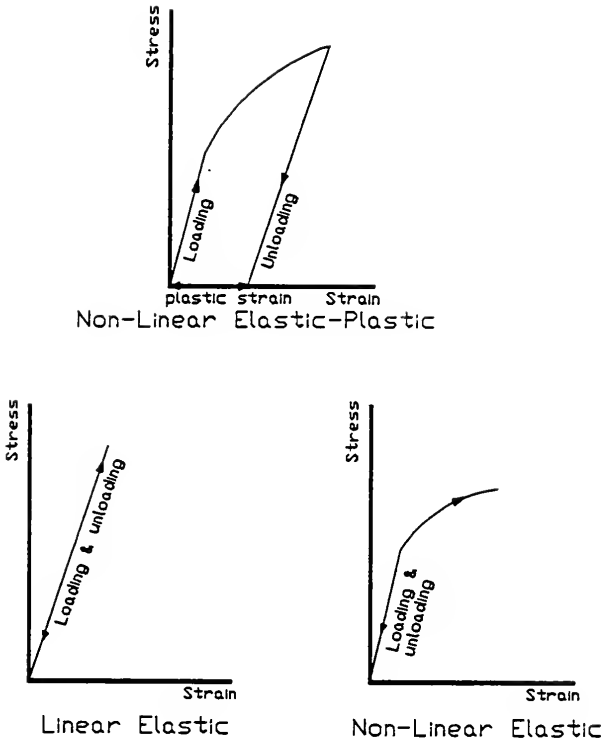

Figure 2.3 Linear and Non-Linear Materials

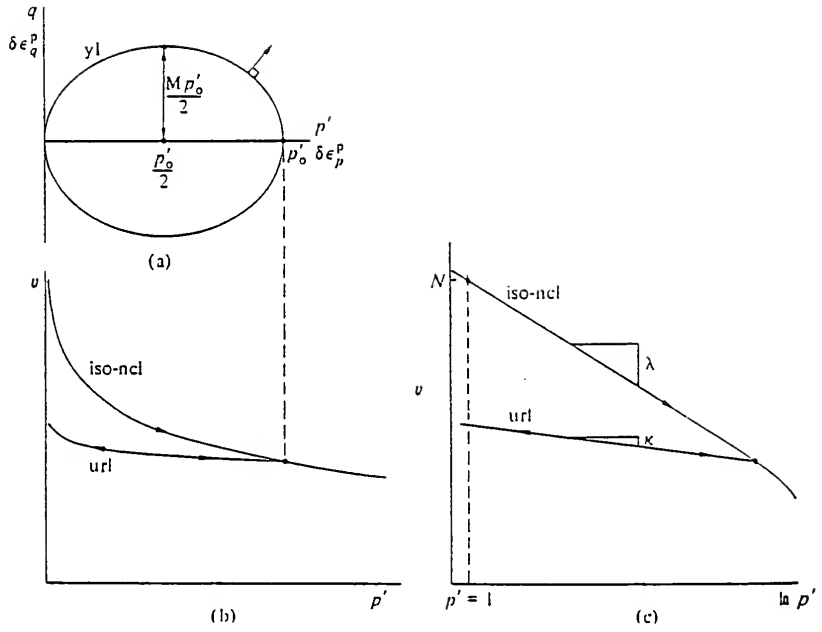

Figure 2.4 Elliptical Yield Locus for Cam-Clay Model [Wood, 1990]

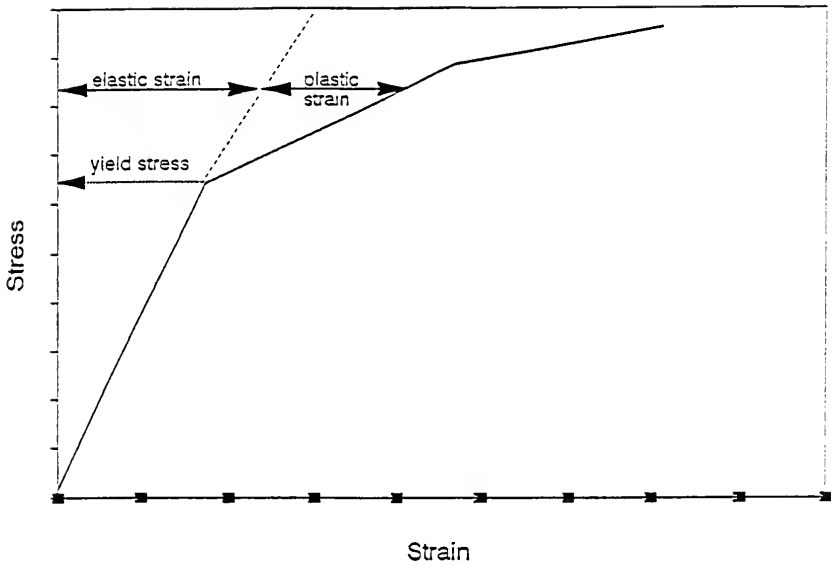

Figure 2.5 Drucker-Prager Model [ABAQUS, 1989]

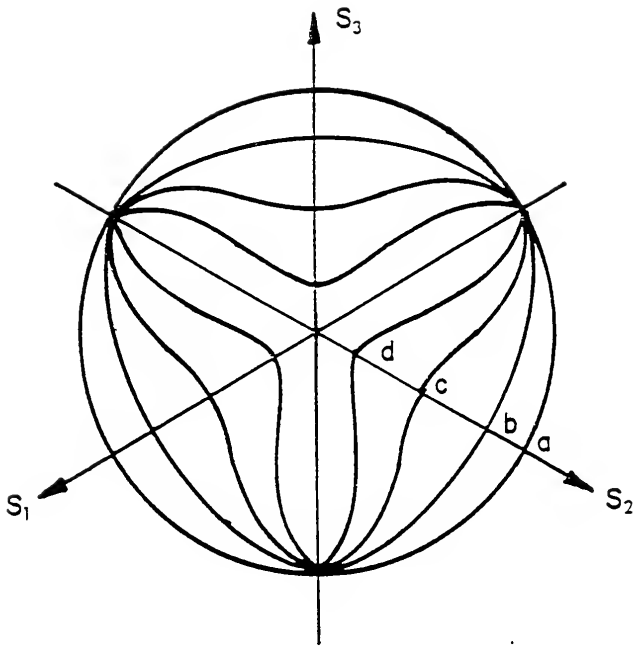

k = Shape Factor

S_i = Deviatoric Stress

Curve	K
a	1.0
b	0.8
c	0.5
d	0.2

Figure 2.6 Typical Yield/flow Surfaces in the Deviatoric Plane for Drucker-Prager Model [ABAQUS, 1989]

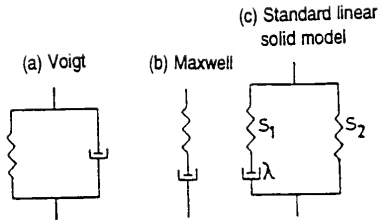

Figure 2.7 Viscoelastic Models [O'Reilly and Brown, 1991]

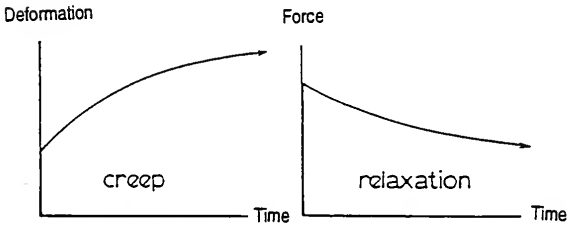

Figure 2.8 Viscoelastic Response [O'Reilly and Brown, 1991]

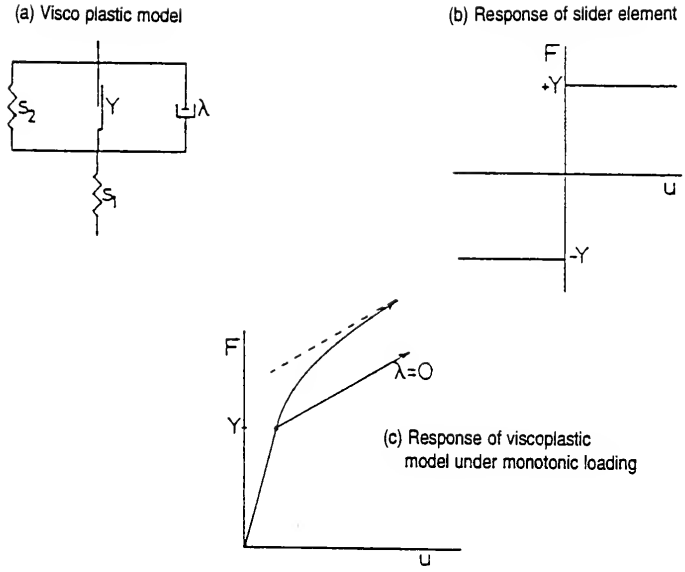

Figure 2.9 Viscoplastic Model [O'Reilly and Brown, 1991]

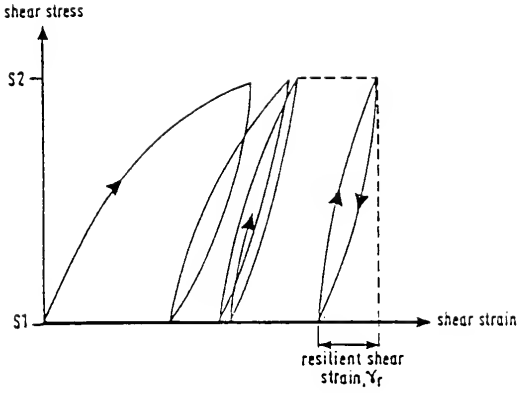

Figure 2.10 Development of Shear Strain During Repeated Load Test [O'Reilly and Brown, 1991]

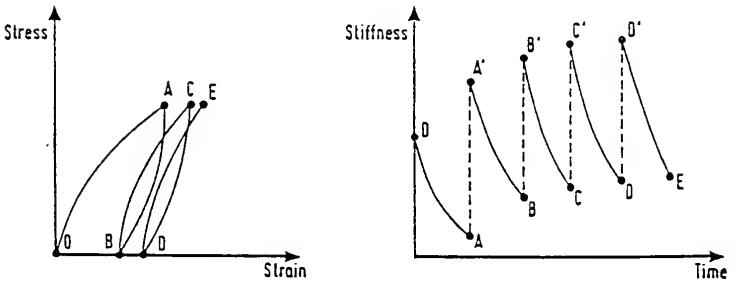

Figure 2.11 The Effect of Stress Reversals on Stiffness [O'Reilly and Brown, 1991]

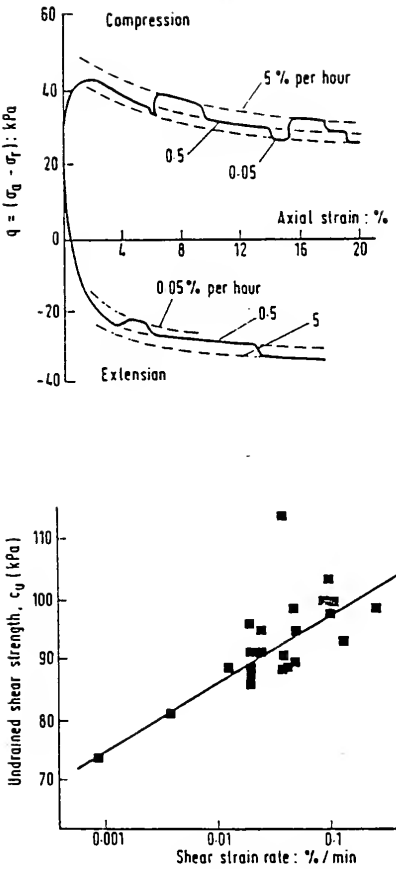

Figure 2.12 Rate-Dependent Response of Clays [Wood, 1990]

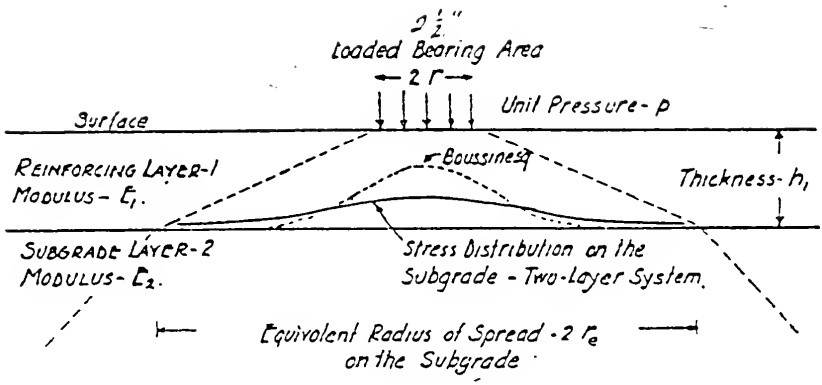

Figure 2.13 The Two-Layer Theory [Burmister, 1943]

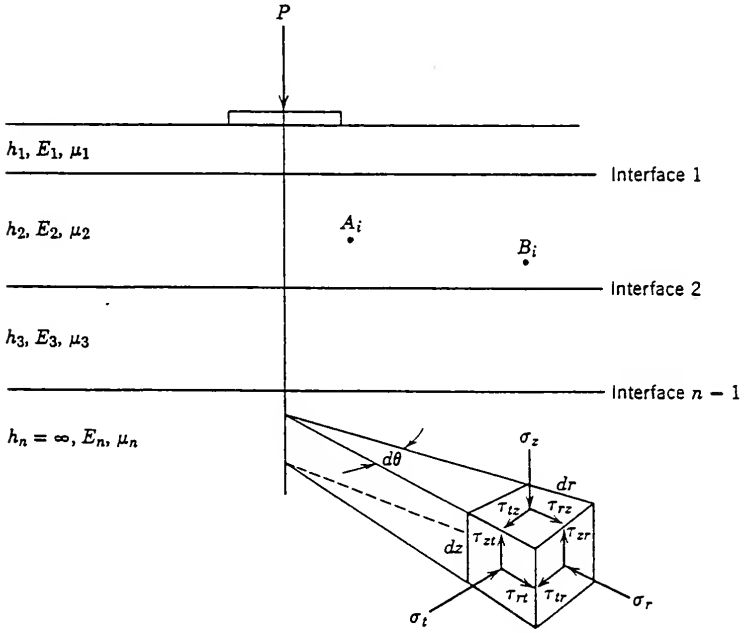

Figure 2.14 Generalized N-Layer Elastic System [Yoder and Witczak, 1975]

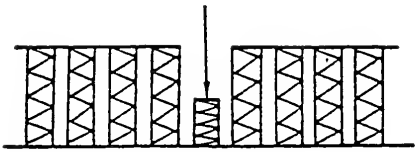

(a) Winkler foundation

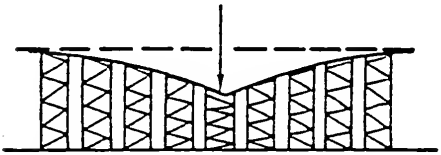

(b) Elastic solid foundation

Figure 2.15 Difference Between a Winkler Subgrade and an Elastic Subgrade [Westergaard, 1925]

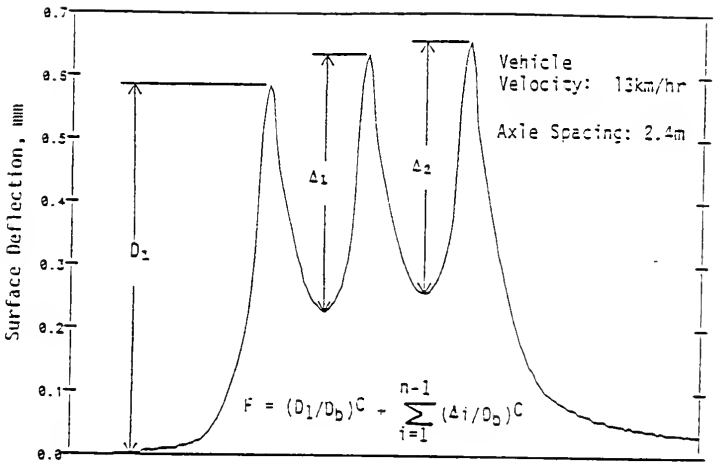

Figure 2.16 CanRoad LEF's for Tridem Axle Configuration [CanRoad, 1986]

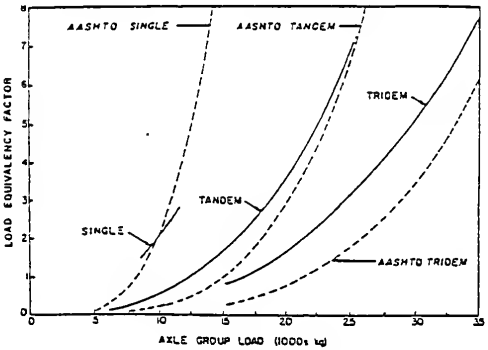

Figure 2.17 Comparison Between the AASHTO LEF's and CanRoad LEF's [Rilett and Hutchinson, 1988]

Table 3.1 Features of SSD Elements [ABAQUS, 1989]

Load Type	Description
Hydrostatic pressure	Hydrostatic pressure on faces 1 to 6 in global Z direction.
Uniform pressure	Uniform Pressure on faces 1 to 6, perpendicular on the face.
Non-uniform pressure	Non-uniform pressure on faces 1 to 6. The magnitude is define via user subroutine.
Elastic Foundation	Elastic foundation on faces 1 to 6.

Table 3.2 Material Options Available in ABAQUS [ABAQUS,1989]

Material Option	Description	Required Options
Clay Plasticity	Defines the plastic part of elastic-plastic materials that use Cam-Clay plasticity model	Porous Elastic
Concrete	Defines concrete properties beyond the elastic range	Elastic
Conductivity	Defines materials thermal conductivity	
Creep	Defines materials creep behavior	Elastic
Damping	Defines material damping	
Density	Defines materials bulk density	
Deformation Plasticity	Defines the mechanical behavior of a material as a deformation theory Ramberg-Osgood model	
Drucker- Prager	Defines yield surface parameters for elastic-plastic materials that use the Drucker-Prager model	Yield & Elastic Porous
Elastic	Defines linear elastic moduli	
Expansion	Defines thermal expansion	

Table 3.2 (continued)

Material Option	Description	Required Options
Hyperelastic	Defines material constants for general hyperelastic materials based on the strain potential energy	
Hypoelastic	Defines a nonlinear elastic material	
No Compression	Introduces a compression failure theory (tension only material)	Elastic
No Tension	Introduce a tension failure theory (compression only material)	Elastic
Permeability	Defines permeability tensor for pore fluid flow	
Plastic	Defines the plastic part of elastic-plastic materials using Mises or Hills surface	Elastic
Porous Bulk Moduli	Defines bulk moduli for soils whenever compressibility and permeability must be considered	

Table 3.2 (continued)

Material Option	Description	Required Options
Swelling	Specify time dependent volumetric swelling	Elastic
Rate Dependent	Introduces strain rate dependence in a material (visco-plastic model definition)	Drucker-Prager or Plastic
visco-elastic	Dissipative behavior specification for use with elasticity to define visco-elastic behavior	Elastic or Hyperel-astic
Water Penetration	Water penetration into failed (racked or crushed) material	
Yield	Defines the hardening part for elastic-plastic materials that use Drucker-Prager yield surface	Drucker-Prager

Table 3.3 Response Parameters Used in the Analysis [ABAQUS, 1989]

Parameter	Description
Stress	Stress components in all directions (XX, YY, ZZ, XY, XZ and YZ).
Principal stress	Three principal stress components (largest, intermediate and smallest).
Strain	Total strain components in all directions.
Elastic strain	Elastic strain components in all directions.
Plastic strain	Plastic strain components in all directions.
Displacement	Displacement in XX, YY and ZZ directions.

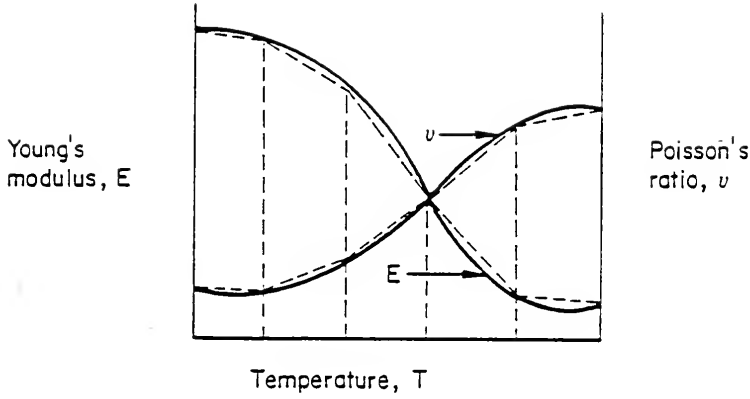

Figure 3.1 Linear Elastic Material Model [ABAQUS, 1989]

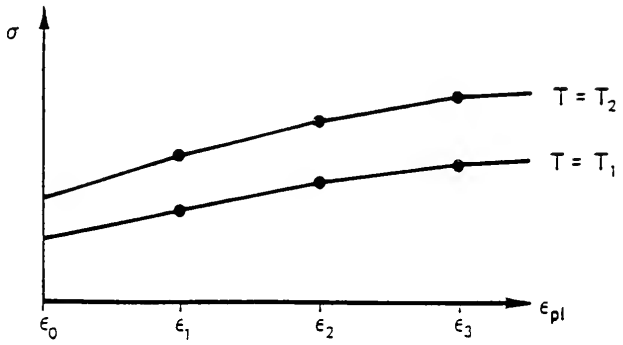

Figure 3.2 Yield Stress of an Elastic-Plastic Material [ABAQUS, 1989]

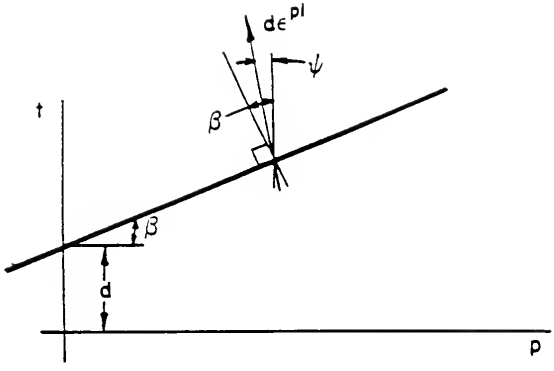

Figure 3.3 Yield Surface in the p-t Plane for Drucker-Prager Model [ABAQUS, 1989]

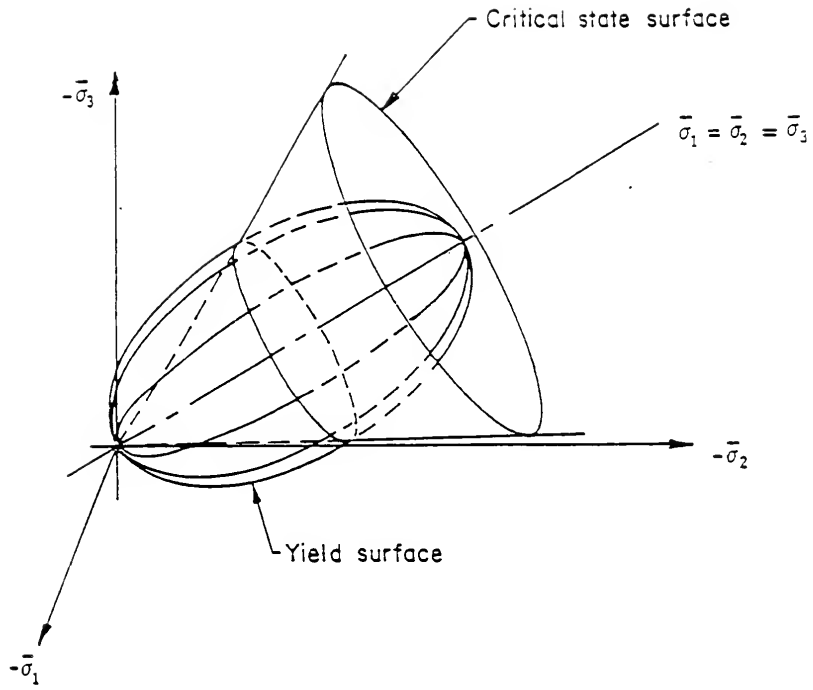

Figure 3.4 Critical State Surface in the Principal effective Stresses Plane [ABAQUS, 1989]

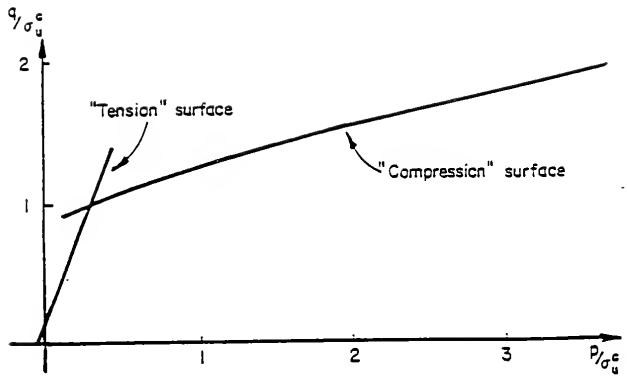

Figure 3.5 Yield and Failure Surfaces for Concrete [ABAQUS, 1989]

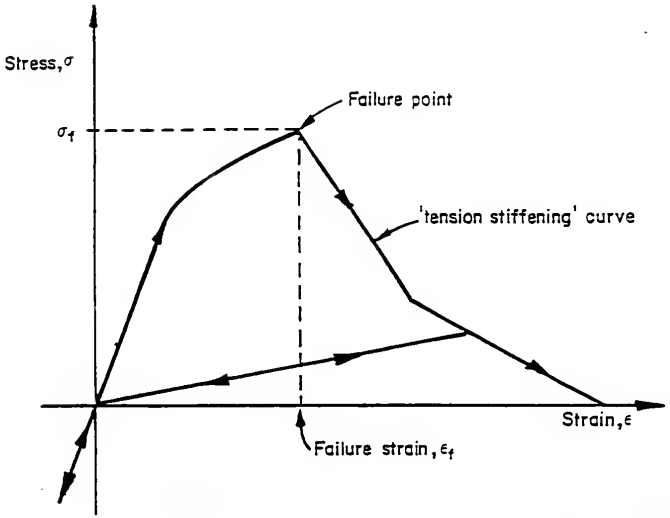

Figure 3.6 Stress-Strain Curve for Concrete [ABAQUS, 1989]

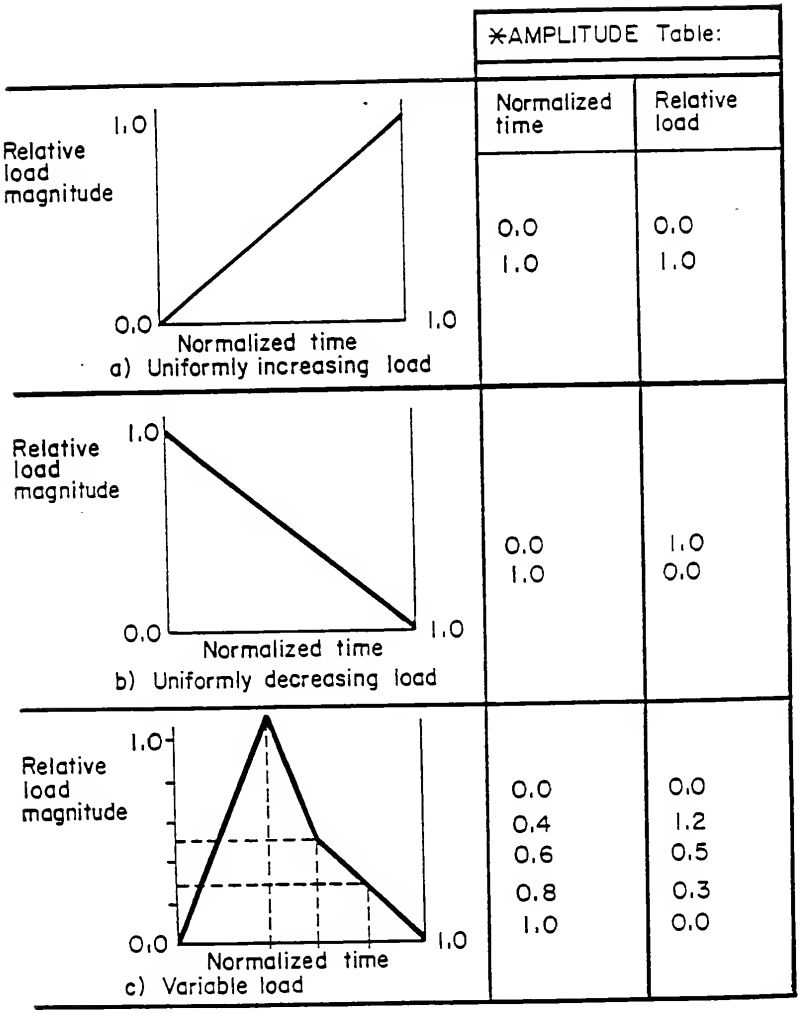

Figure 3.7 Examples of Load Amplitude [ABAQUS, 1989]

Table 4.1 Design of Experiment of the Static Analysis Verification

Surface Thickness (in)	Base Thickness (in)	Subgrade Modulus of Elasticity (psi)	
		5,000	30,000
4	10	1^	2
4	20	3	4
8	10	5	6
8	20	7	8

^Section Number

Table 4.2 Comparison Between the Multi-layer Analysis and the 3D-DFEM Predictions

Ptype^	X (in)	Z (in)	3D-DFEM	BISAR	Ptype^	X (in)	Z (in)	3D-DFEM	BISAR
1	0	34	0.001	0.001	5	0	34	0.002	0.003
1	0	24	0.001	0.001	5	0	24	0.002	0.003
1	0	14	0.001	0.001	5	0	14	0.002	0.004
1	0	4	0.001	0.001	5	0	4	0.003	0.004
1	0	0	0.002	0.002	5	0	0	0.004	0.004
1	5.56	0	0.001	0.001	5	5.56	0	0.003	0.004
1	11.11	0	0.001	0.001	5	11.11	0	0.003	0.004
1	16.68	0	0.001	0.001	5	16.68	0	0.002	0.003
1	22.22	0	0.001	0.001	5	22.22	0	0.002	0.003
1	44.44	0	0.000	0.000	5	44.44	0	0.002	0.002
2	0	44	0.000	0.000	6	0	44	0.001	0.002
2	0	34	0.001	0.001	6	0	34	0.002	0.002
2	0	24	0.000	0.001	6	0	24	0.001	0.002
2	0	4	0.001	0.001	6	0	4	0.002	0.003
2	0	0	0.002	0.001	6	0	0	0.003	0.003
2	5.56	0	0.001	0.001	6	5.56	0	0.002	0.002
2	11.11	0	0.001	0.001	6	11.11	0	0.002	0.002
2	16.68	0	0.001	0.001	6	16.68	0	0.001	0.002
2	22.22	0	0.001	0.001	6	22.22	0	0.001	0.002
2	44.44	0	0.000	0.000	6	44.44	0	0.001	0.002
3	0	38	0.001	0.001	7	0	38	0.001	0.002
3	0	28	0.001	0.001	7	0	28	0.002	0.002
3	0	18	0.001	0.001	7	0	18	0.002	0.003
3	0	8	0.001	0.001	7	0	8	0.002	0.003
3	0	0	0.002	0.001	7	0	0	0.004	0.003
3	5.56	0	0.001	0.001	7	5.56	0	0.002	0.003
3	11.11	0	0.001	0.001	7	11.11	0	0.002	0.003
3	16.68	0	0.001	0.001	7	16.68	0	0.002	0.003
3	22.22	0	0.001	0.001	7	22.22	0	0.002	0.003
3	44.44	0	0.000	0.000	7	44.44	0	0.001	0.002
4	0	48	0.000	0.000	8	0	48	0.000	0.002
4	0	38	0.000	0.000	8	0	38	0.001	0.002
4	0	28	0.001	0.001	8	0	28	0.001	0.002
4	0	8	0.000	0.001	8	0	8	0.001	0.002
4	0	0	0.002	0.001	8	0	0	0.003	0.002
4	5.56	0	0.000	0.001	8	5.56	0	0.001	0.002
4	11.11	0	0.001	0.001	8	11.11	0	0.001	0.002
4	16.68	0	0.001	0.001	8	16.68	0	0.001	0.002
4	22.22	0	0.000	0.000	8	22.22	0	0.001	0.002
4	44.44	0	0.000	0.000	8	44.44	0	0.001	0.002

^See Table 1

Table 4.3 Material Properties Used in The Dynamic Analysis Verification

Material	Layer	Site # 3a	Site # 4	Site # 10
Modulus Of Elasticity (ksi)	Surface	200	150	200
Bulk Density (pcf)		150	150	150
Possion's Ratio		0.3	0.3	0.3
Modulus Of Elasticity (ksi)^	Base	50	30	20
Bulk Density (pcf)		140	140	140
Angle of Internal Friction		38	38	38
Cohesion (pcf)		0	0	0
Possion's Ratio		0.35	0.35	0.35
Modulus Of Elasticity (ksi)^	Subbase	15	7.5	no subbase
Bulk Density (pcf)		130	130	
Angle of Internal Friction		35	33	
Cohesion (pcf)		0	0	
Possion's Ratio		0.35	0.35	
Modulus Of Elasticity (ksi)^	Subgrade	10	3	3
Bulk Density (pcf)		130	125	125
Angle of Internal Friction		35	0	0
Cohesion (pcf)		0	750	750
Possion's Ratio		0.35	0.4	0.4

^ Based on E = 1500*CBR

- General References [George, 92, kim and Stokoe, 92, Roque and Ruth, 87, Derucher and Korfiatis, 84, Yoder and Witczak, 75

Table 4.4 Comparison Between Measured and Predicted Flexible Pavement Deflections

CanRoad Section Number^	Load (kg)	Speed (km/h)	Measured Deflection (mils)	Predicted Deflection (mils)
3A	9,182	6.0	20.91	20.97
3A	9,182	50.0	19.29	20.3
3A	11,127	6.0	19.49	18.1
3A	11,127	50.0	17.91	17.31
10	9,182	6.0	29.88	30.16
10	9,182	50.0	24.8	23.56
10	11,127	6.0	25.2	24.9
10	11,127	50.0	22.0	23.4
4	9,182	6.0	52.0	51.61
4	9,182	50.0	46.81	45.99
4	11,127	6.0	44.8	42.59
4	11,127	50.0	40.5	37.95

^After Reference [Canroad, 1986]

Table 4.5 Subgrade Properties

Material	Sand	Silt	Clay
Possion's Ratio	0.4	0.4	0.45
Bulk Density (pcf)	120	120	120 -
Angle of Internal Friction	33	27	0
Cohesion (pcf)	0	100	750
Modulus Of Elasticity (ksi)^	25	15	10

^ Based on E = 1500*CBR

- General References [George, 92, kim and Stokoe, 92, Roque and Ruth, 87, Derucher and Korfiatis, 84, Yoder and Witczak, 75 and ABAQUS 89b]

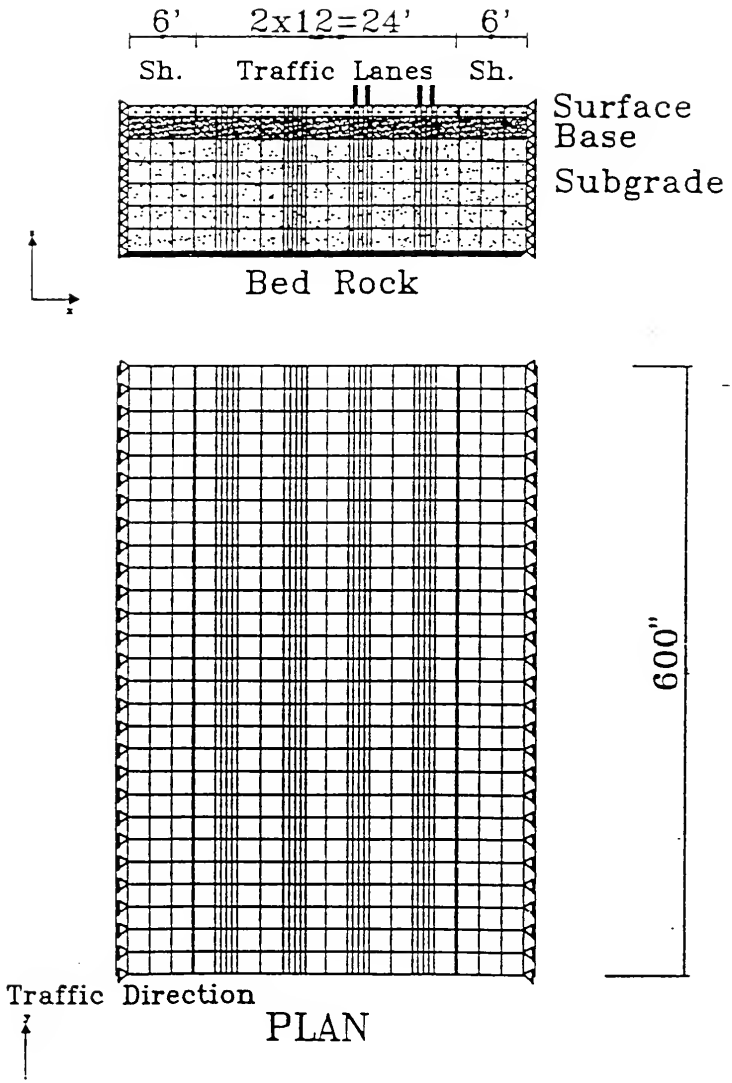

Figure 4.1 Finite Element Mesh for Flexible Pavement Analysis

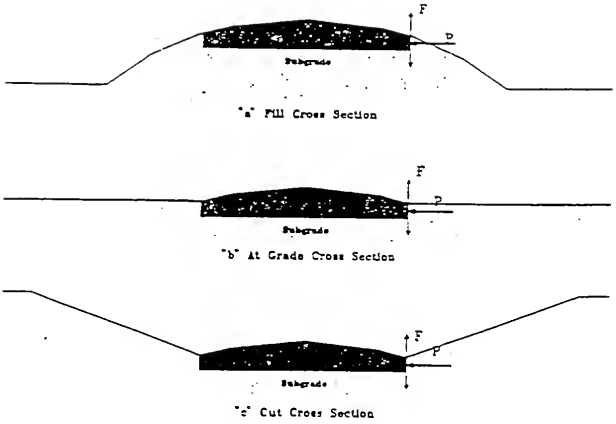

Figure 4.2 Flexible Pavement Cross Sections

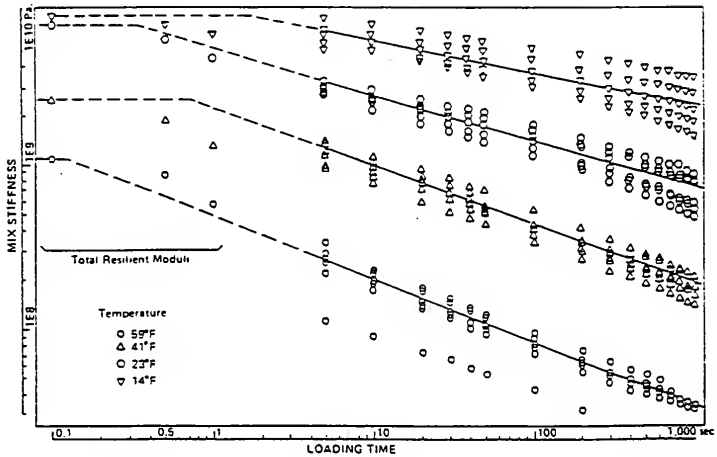

Figure 4.3 Effect of Loading Time and Temperature on Asphalt mixtures Stiffness [Koyue et al., 1987]

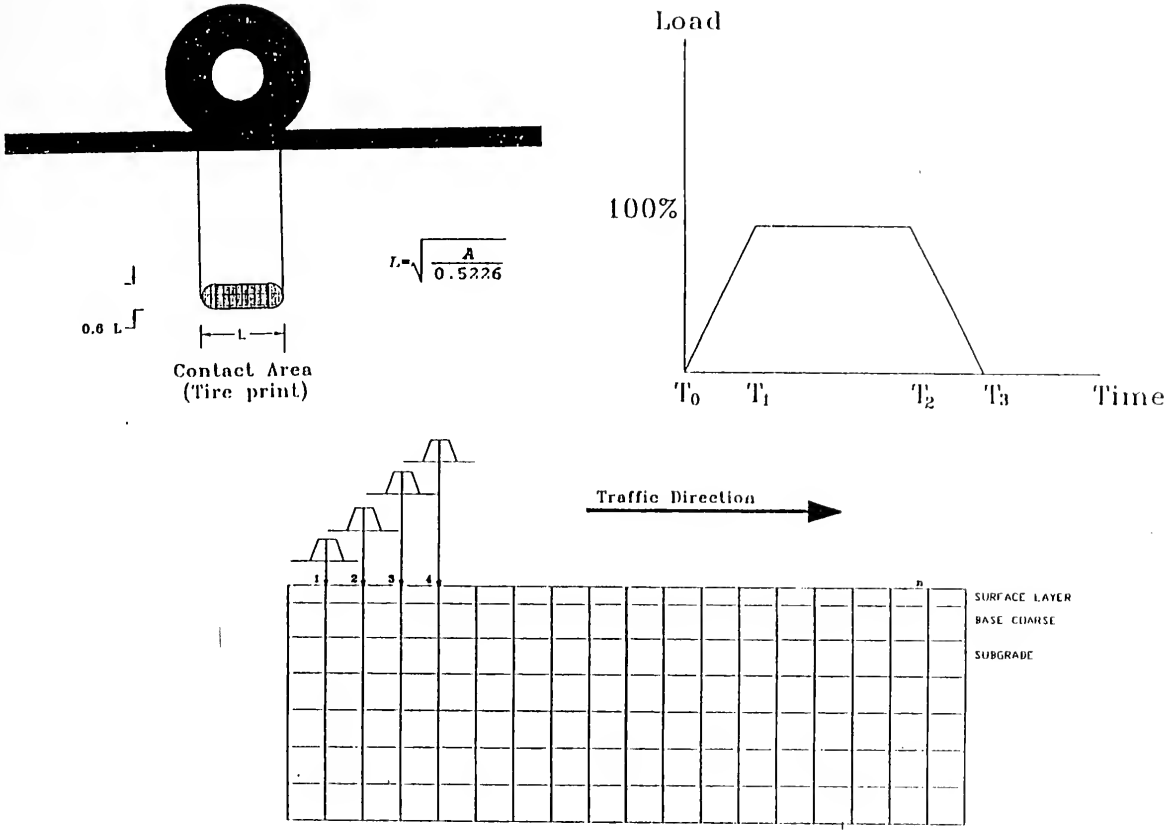

Figure 4.4 Load Cycle Used in the Analysis

The SAS System

General Linear Models Procedure

Dependent Variable: DB

Source	DF	Sum of Squares	Mean Square	F Value	Pr > F
Model	15	0.00008157	0.00000544	114.68	0.0001
Error	64	0.00000304	0.00000005		
Corrected Total	79	0.00008461			

R-Square	C.V.	Root MSE	DB Mean
0.964128	13.14506	0.0002178	0.0016566

Source	DF	Type I SS	Mean Square	F Value	Pr > F
DF	1	0.00006051	0.00006051	1275.92	0.0001
PTYPE	7	0.00002077	0.00000297	62.56	0.0001
DF*PTYPE	7	0.00000030	0.00000004	0.90	0.5146

Figure 4.5 Static Analysis Verification (Flexible Pavement)

Dependent Variable: MEASURED DEFLECTION

R-Square	C.V.	Root MSE	DM Mean
0.998691	4.054384	1.2284444	30.299167

Source	DF	Type I SS	Mean Square	F Value	Pr > F
DF	1	12662.721067	12662.721067	8391.04	0.0001

Source	DF	Type III SS	Mean Square	F Value	Pr > F
DF	1	12662.721067	12662.721067	8391.04	0.0001

Parameter	Estimate	T for H0: Parameter=0	Pr > |T|	Std Error of Estimate
DF	1.020945219	91.60	0.0001	0.01114537

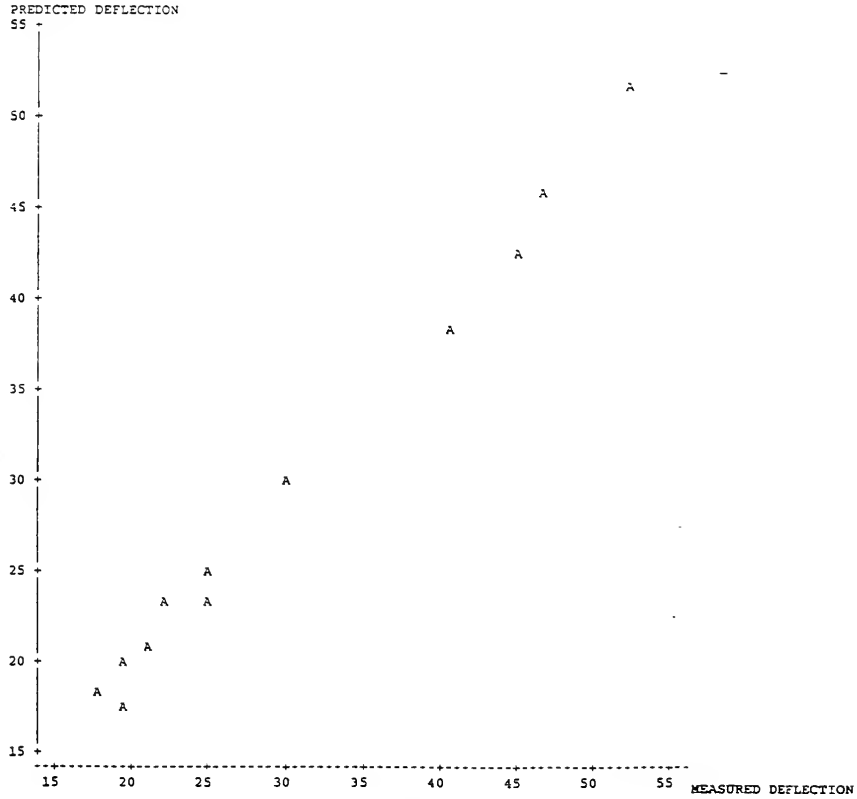

Figure 4.6 Dynamic Analysis Verification (Flexible Pavement)

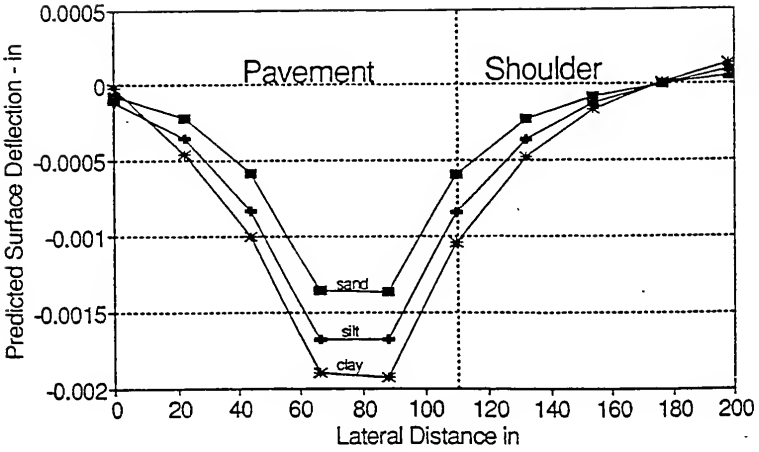

Figure 4.7 Effect of Subgrade Type on Pavement Deflection

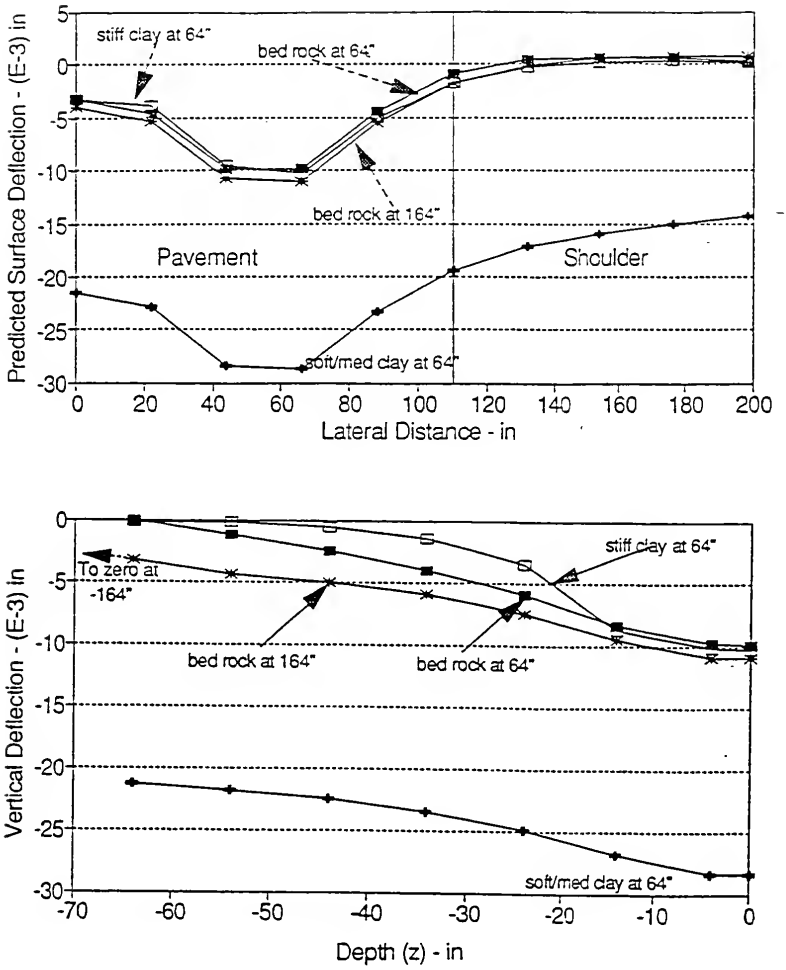

Figure 4.8 Effect of Deep Foundation Type on Pavement Deflection

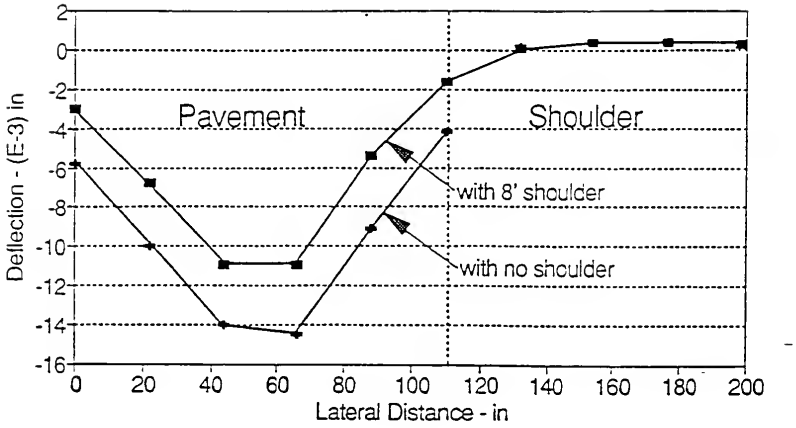

Figure 4.9 Effect of Shoulder Width on Pavement Deflection

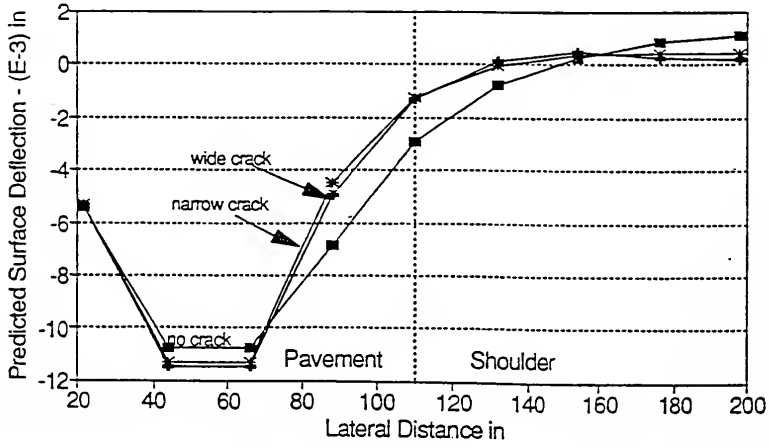

Figure 4.10 Effect of Pavement/Shoulder Joint on Pavement Deflection

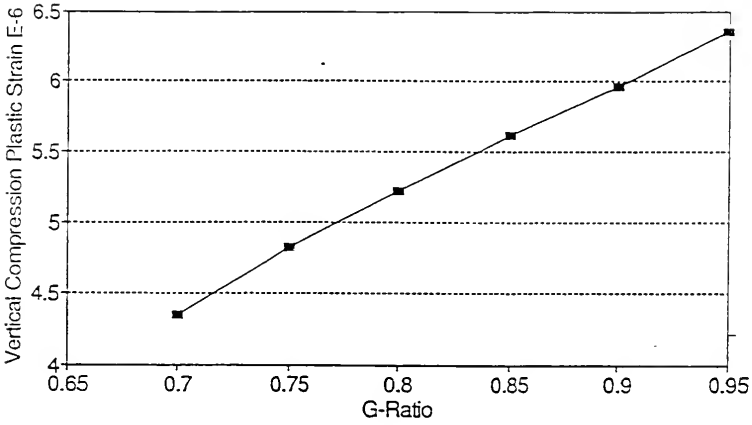

Figure 4.11 Effect of G-Ratio on Vertical Compressive Strain

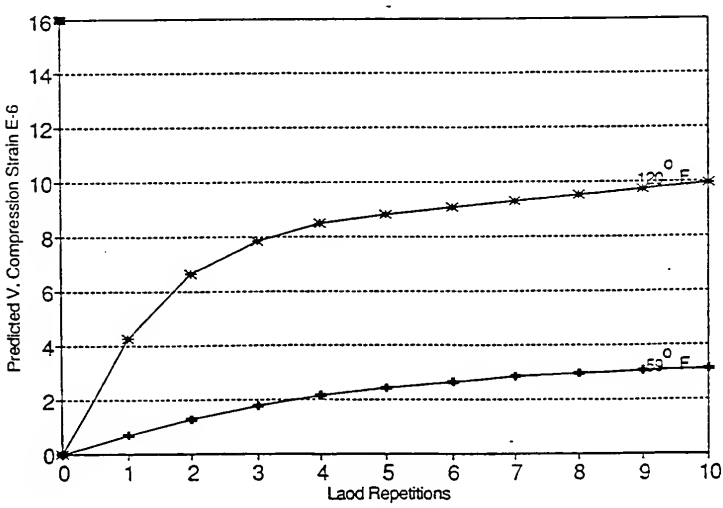

Figure 4.12 Effect of Temperature on Vertical Compressive Strain

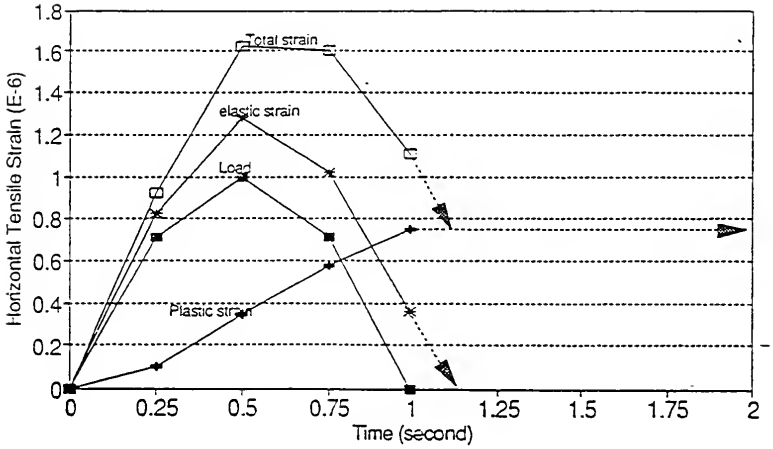

Figure 4.13 Components of Horizontal Tensile Strains

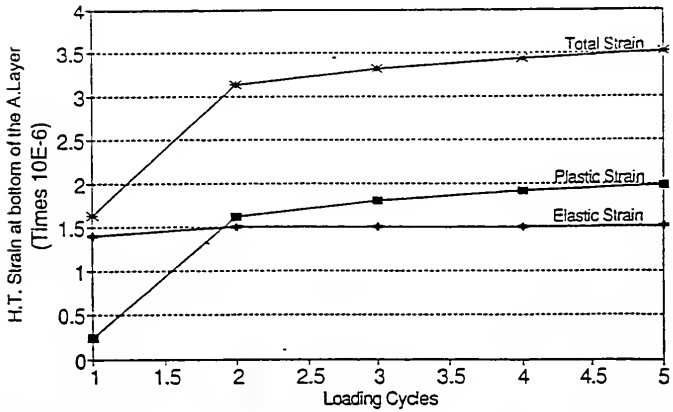

Figure 4.14 Effect of Load Repetitions on Horizontal Tensile Strain

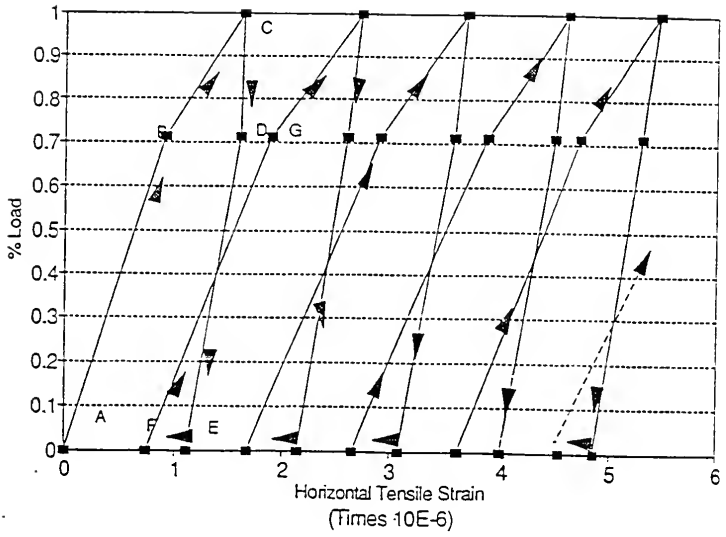

Figure 4.15 History of Horizontal Tensile Strain at the Bottom of the Asphalt Layer

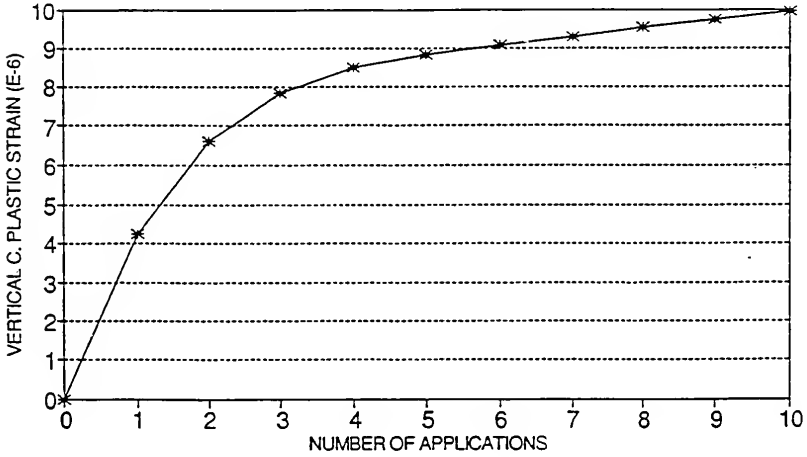

Figure 4.16 Effect of Load Repetitions on Vertical Compressive Strain

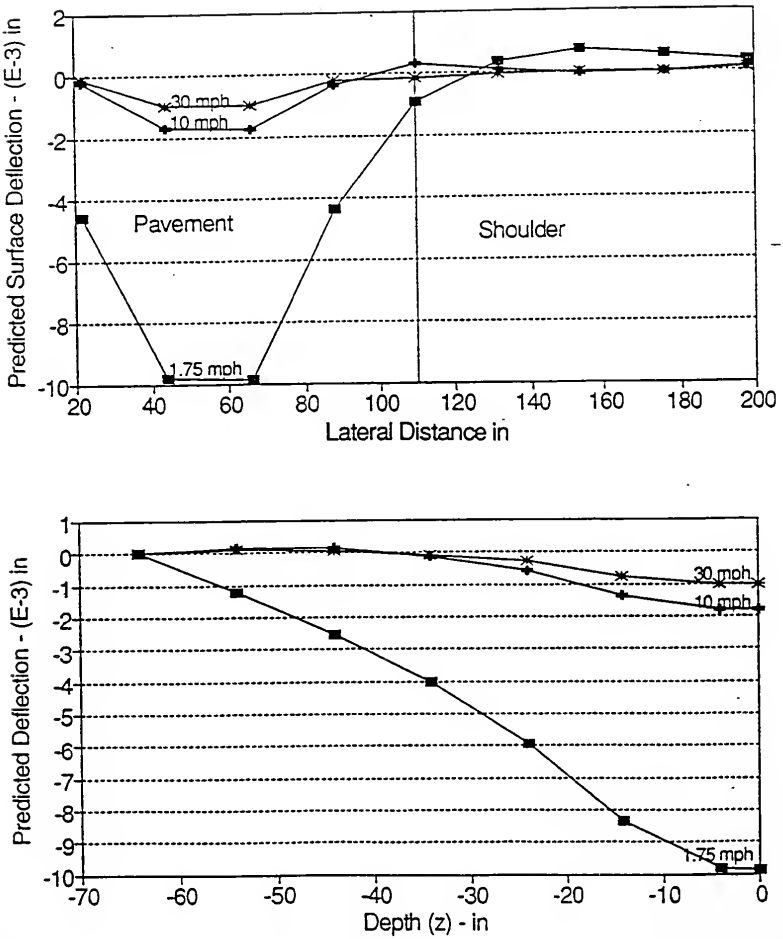

Figure 4.17 Effect of Speed on Pavement Deflection

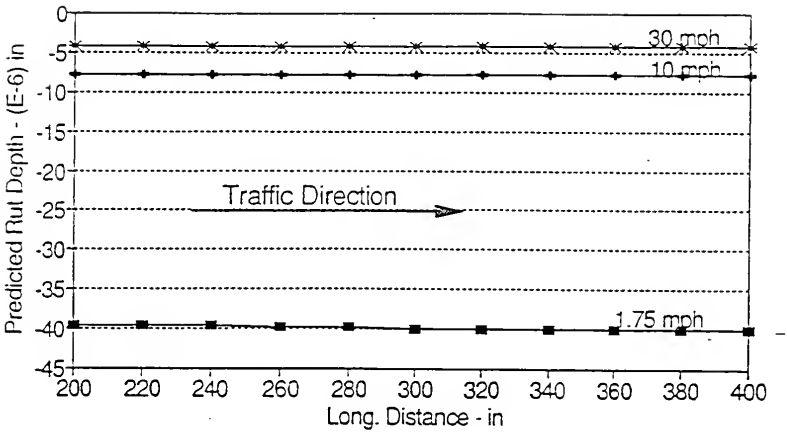

Figure 4.18 Effect of Speed on Pavement Rutting

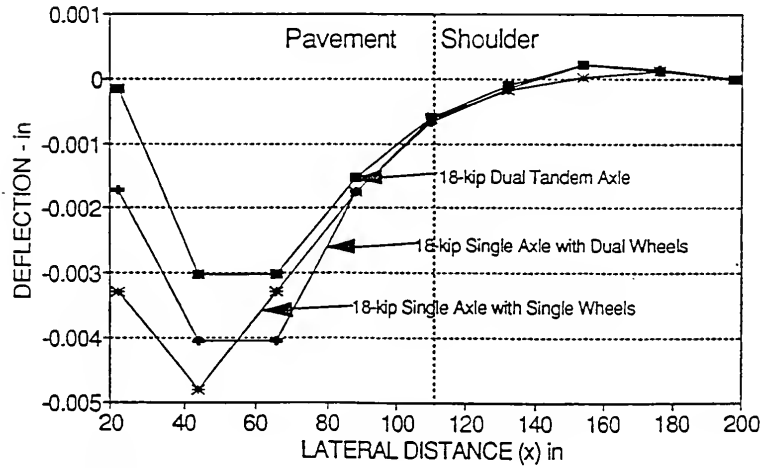

Figure 4.19 Effect of Axle Configuration on Pavement Deflection

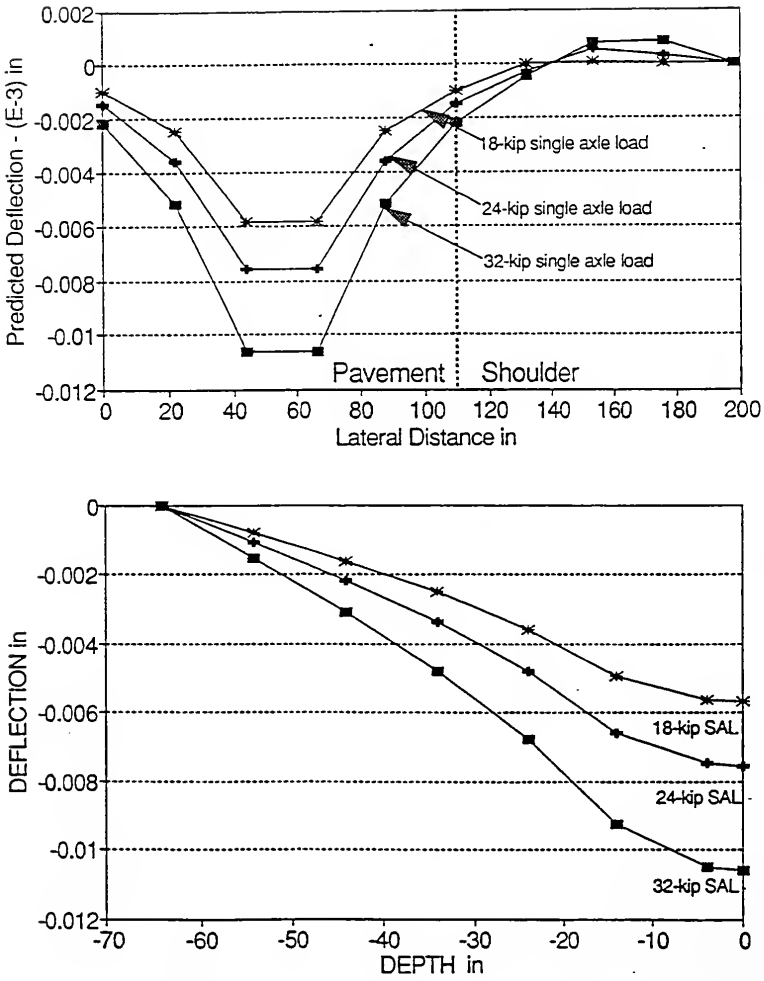

Figure 4.20 Effect of Axle Load on Pavement Deflection

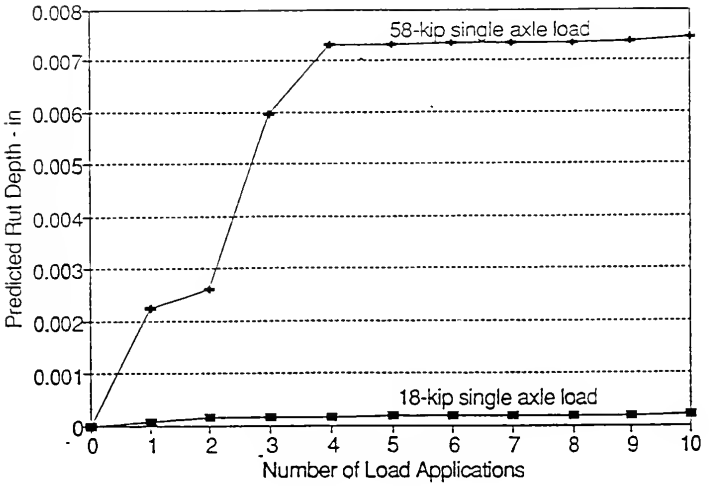

Figure 4.21 Effect of Axle Load on Pavement Rutting

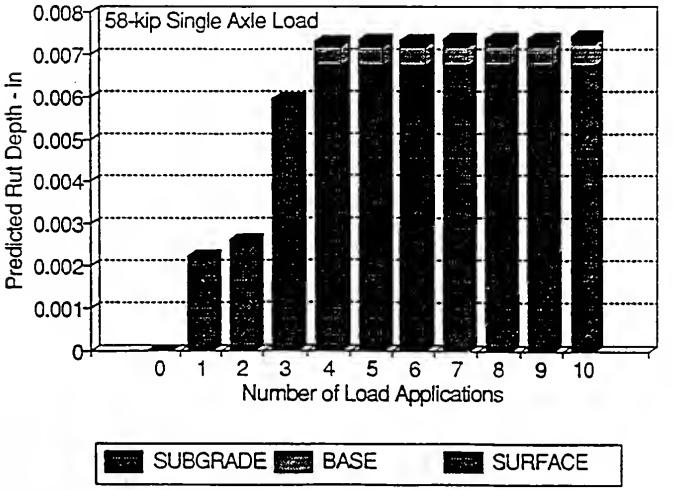

Figure 4.22 Predicted Pavement Rutting (58-kip SAL)

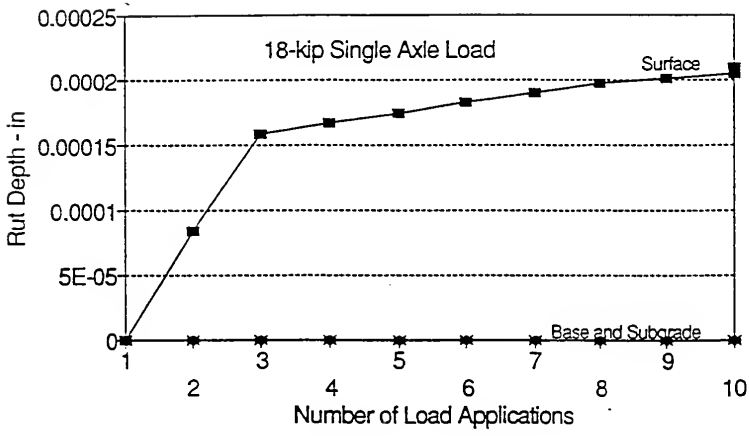

Figure 4.23 Predicted Pavement Rutting (18-kip SAL)

Table 5.1 Factor Levels Included in the Static Analysis Verification

SLAB THICKNESS	SUBGRA TYPE	LOAD POSITION		
		CORNER	EDGE	INTERIOR
6	SAND			
	CLAY			
10	SAND			
	CLAY			
14	SAND			
	CLAY			

Table 5.2 Comparison Between Measured and Predicted Rigid Pavement Deflections

Axle Configuration	Axle Load	Slab Thickness	Base Thickness	Measured Deflection	Predicted Deflection
Single	18-kip	9"	6"	0.007	0.0076
Single	18-kip	8"	6"	0.009	0.0086
Single	18-kip	9"	6"	0.0085	0.0081
Single	18-kip	9"	6"	0.00817	0.00793
Tandem	34-kip	9"	6"	0.016	0.0173
Tandem	34-kip	8"	6"	0.018	0.019
Tandem	34-kip	9"	6"	0.0165	0.0162
Tandem	34-kip	9"	6"	0.01683	0.01773

* All deflections in inches

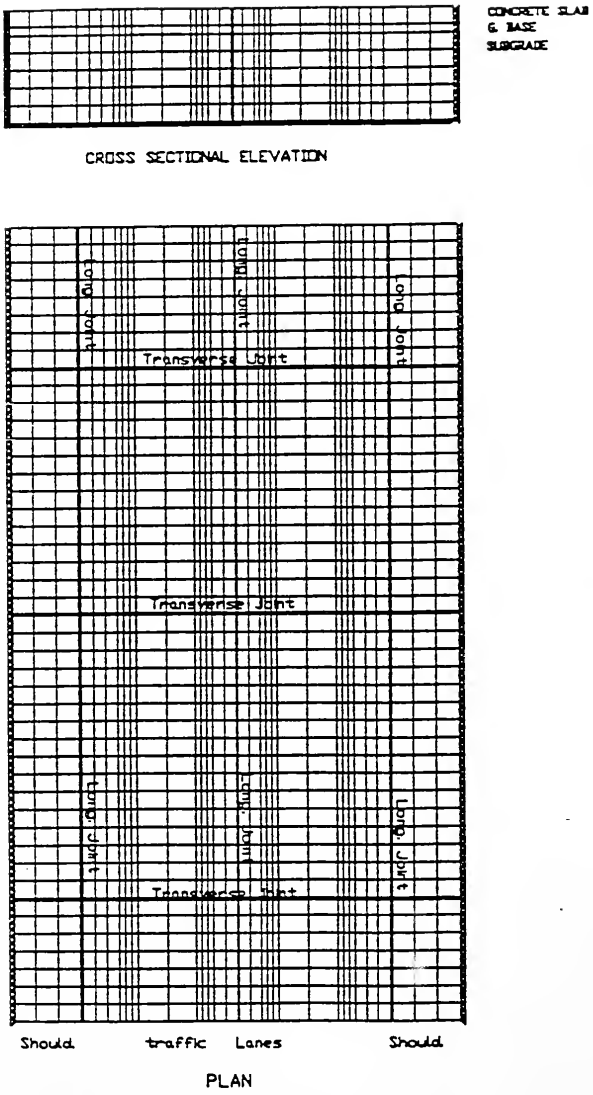

Figure 5.1 Finite Element Mesh for Rigid Pavement Analysis

The SAS System

General Linear Models Procedure

Dependent Variable: STH

Source	DF	Sum of Squares	Mean Square	F Value	Pr > F
Model	10	1064944.4601	106494.4460	30.57	0.0001
Error	7	24382.8016	3483.2574		
Corrected Total	17	1089327.2616			

R-Square	C.V.	Root MSE	STH Mean
0.977617	25.72966	59.019127	229.38167

Source	DF	Type I SS	Mean Square	F Value	Pr > F
SF	1	924904.93363	924904.93363	265.53	0.0001
PTYPE	4	138903.75286	34725.93822	9.97	0.0051
SF*PTYPE	5	1135.77357	227.15471	0.07	0.9958

Source	DF	Type III SS	Mean Square	F Value	Pr > F
SF	1	0.000000	0.000000	0.00	1.0000
PTYPE	4	60852.740753	15213.185188	4.37	0.0438
SF*PTYPE	5	1136.942371	227.388474	0.07	0.9958

Figure 5.2 Static Analysis Verification (Rigid Pavement)

The SAS System

General Linear Models Procedure

Number of observations in data set = 8

The SAS System

General Linear Models Procedure

Dependent Variable: MEASURED

Source	DF	Sum of Squares	Mean Square	F Value	Pr > F
Model	1	0.00139947	0.00139947	1947.78	0.0001
Error	7	0.00000503	0.00000072		
Uncorrected Total	8	0.00140450			

R-Square	C.V.	Root MSE	MEAS Mean
0.996419	6.781121	0.0008476	0.0125000

NOTE: No intercept term is used: R-square is not corrected for the mean.

Source	DF	Type I SS	Mean Square	F Value	Pr > F
PREDICTED	1	0.00139947	0.00139947	1947.78	0.0001

Source	DF	Type III SS	Mean Square	F Value	Pr > F
PREDICTED	1	0.00139947	0.00139947	1947.78	0.0001

Parameter	Estimate	T for H0: Parameter=0	Pr > |T|	Std Error of Estimate
PREDICTED	0.9613819643	44.13	0.0001	0.02178341

Figure 5.3 Dynamic Analysis Verification (Rigid Pavement)

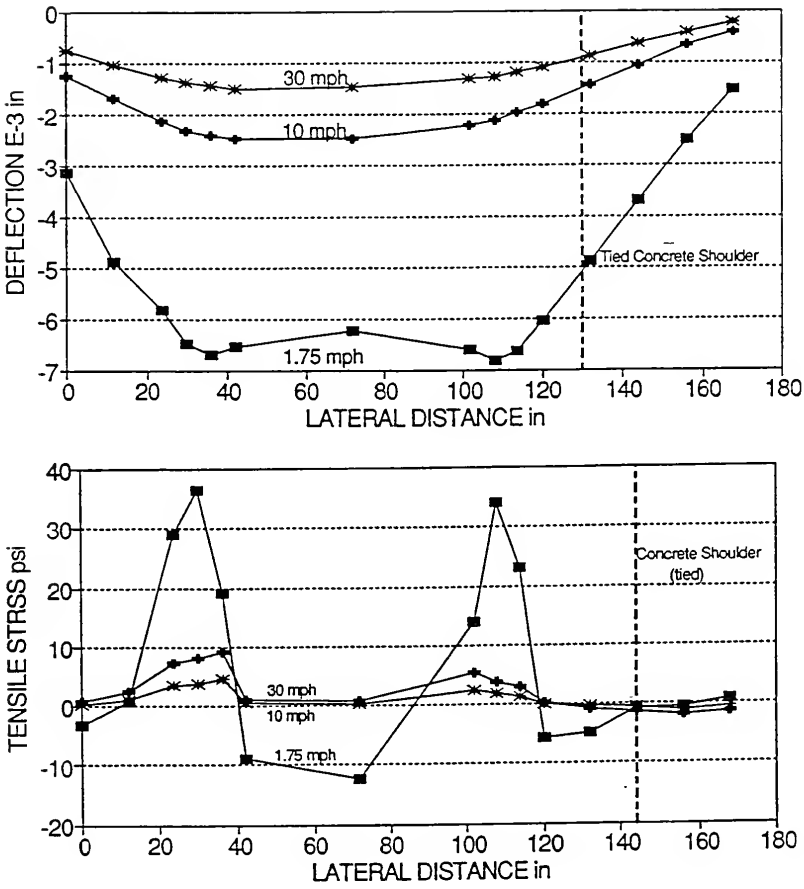

Figure 5.4 Effect of Truck Speed on Pavement Response

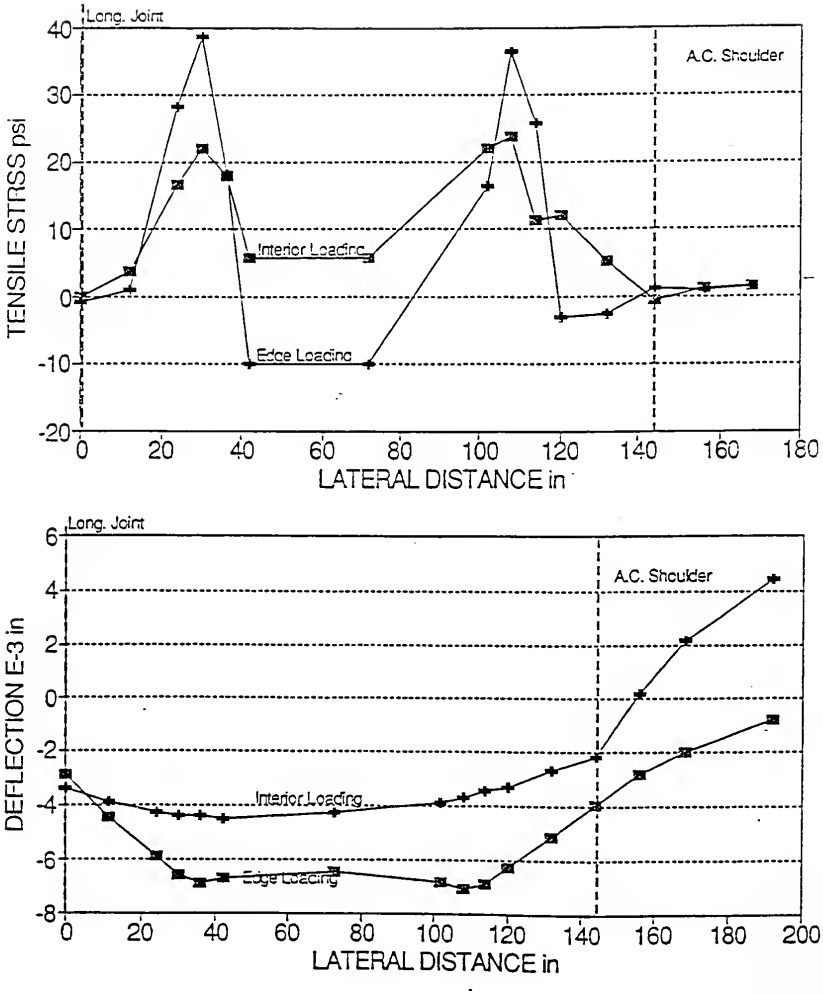

Figure 5.5 Effect of Load Position on Pavement Response

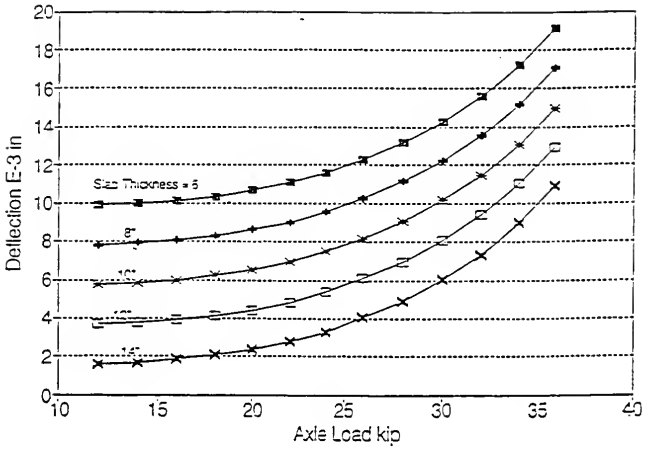

Figure 5.6 Effect of Axle Load and Slab Thickness on Pavement Deflection

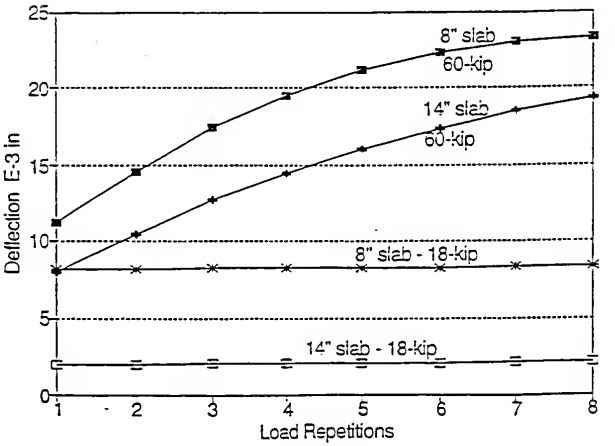

Figure 5.7 Effect of Load Repetitions on Pavement Deflection

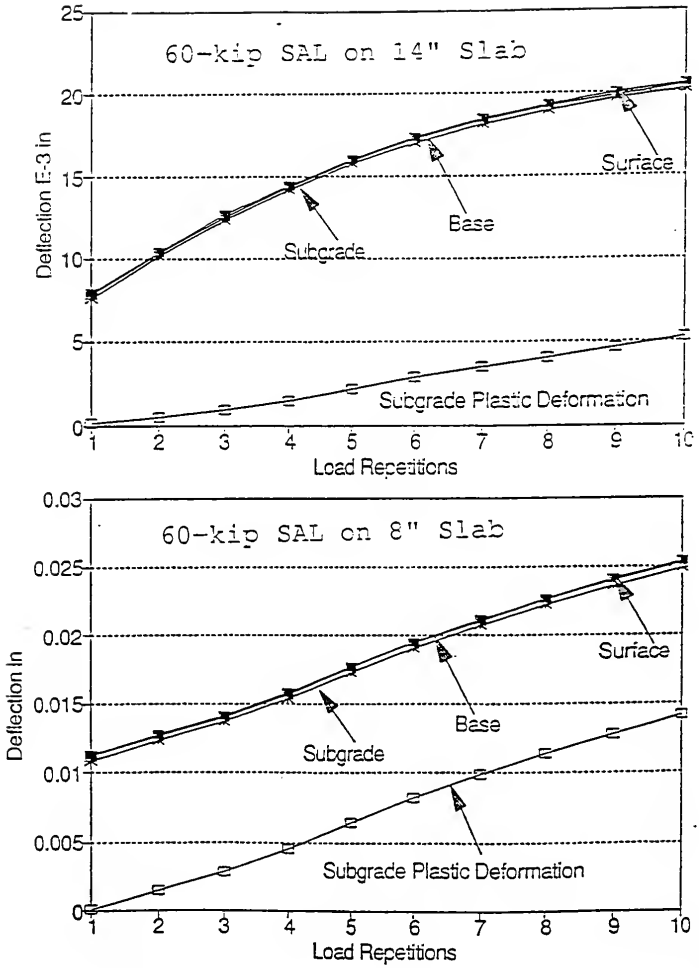

Figure 5.8 Effect of Load Repetitions on Permanent Deformation

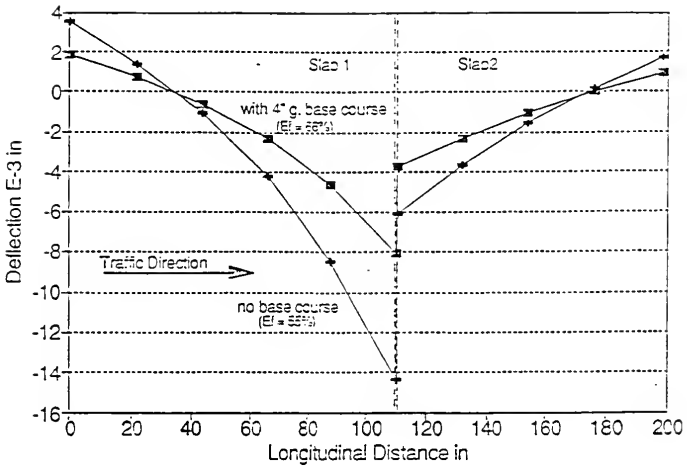

Figure 5.9 Effect of Subbase on Pavement Deflection

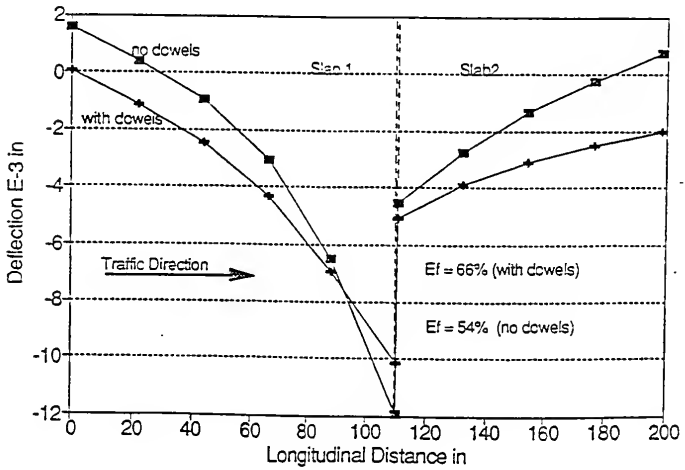

Figure 5.10 Effect of Dowel Bars on Surface Deflection (No Subbase)

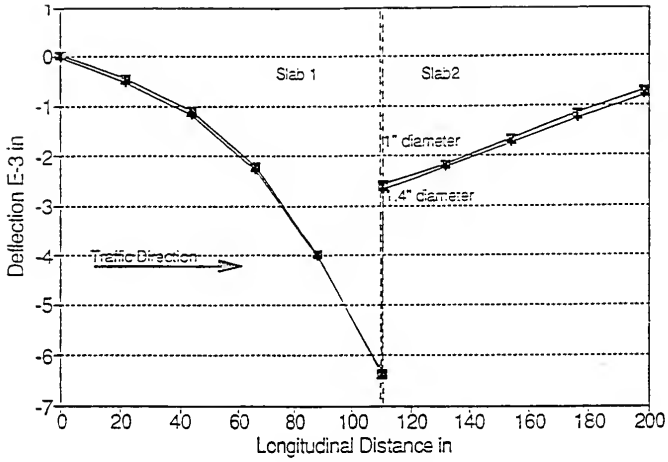

Figure 5.11 Effect of Dowel Bars Diameter on Surface Deflection

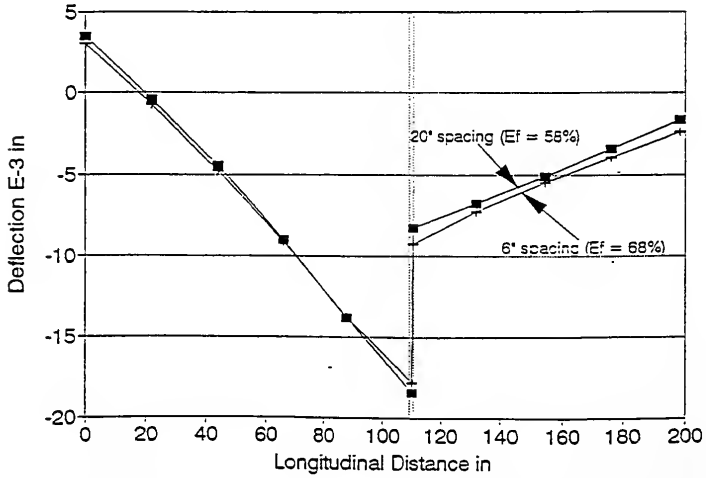

Figure 5.12 Effect of Dowel Bars Spacing on Surface Deflection

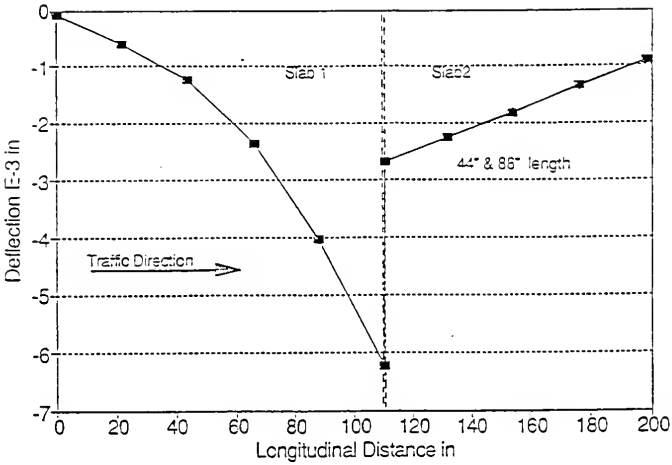

Figure 5.13 Effect of Dowel Bars length on Surface Deflection

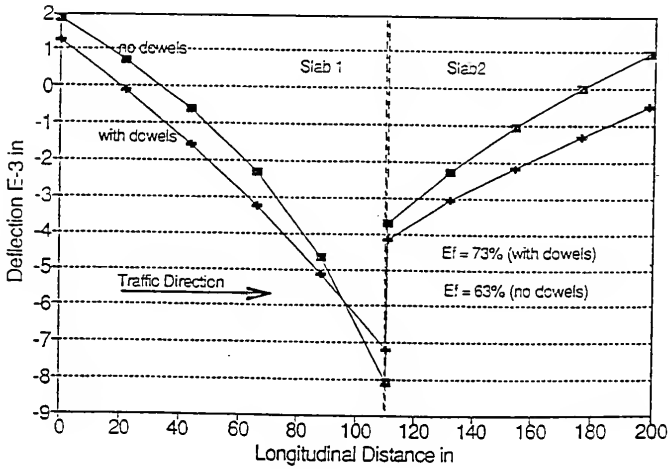

Figure 5.14 Effect of Dowel Bars on Surface Deflection (with 4" Granular Subbase)

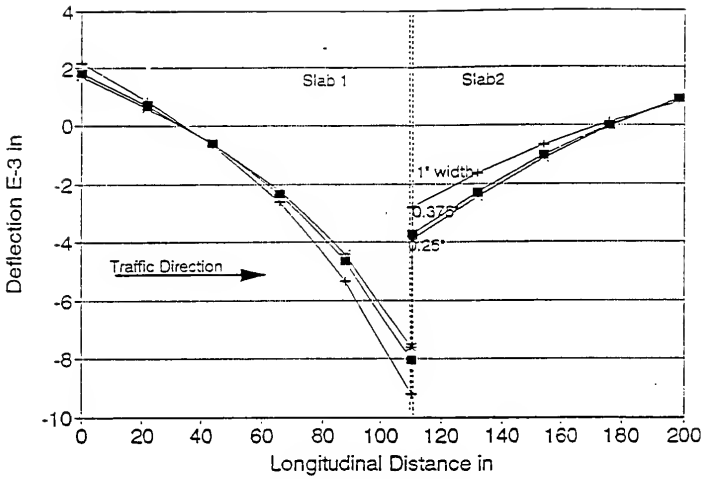

Figure 5.15 Effect of Joint Width on Surface Deflection

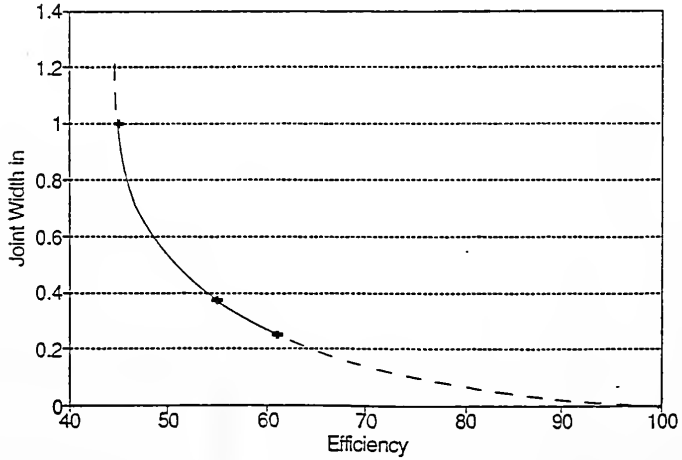

Figure 5.16 Effect of Joint Width on Load Transfer Efficiency

Table 6.1 Factor Levels Included in the FDOE1

Factors	Levels		
	1	2	3
Axle Load (kip)	18	24	36
No. of Axles	1	2	4
Surface Layer Modulus of Elasticity (ksi)	400	900	
G-ratio	0.7	0.9	
Total Pavement Thickness	10"	16"	
Asphalt Layer Thickness	4"	6"	
Subgrade Type	Sand	Clay	

Table 6.2 Regression Coefficients of Different DOE's

DOE	MODEL	Factor								
		a	b	c	d	e	f	g	h	i
FDOE1		9.8E-06	-3.414	-0.02829	17.882	0.00217	-2.6E-07	0.4423	0.1683	-0.0121
FDOE2	MEM	19.78	-0.0123	-0.145	0.774	-0.000133				
FDOE2	FIM	1.084	0.0698	0.938	-0.00161	-0.0177	-15.44E-6			
RDOE1	LSM	5.6E-06	18.402	-1.036	-2.416					
RDOE1	HSM	3E-06	0.3051	-0.0088	-0.0057	-3.3E-09	5.5E.05			
RDOE2		0.17	0.00959							
CDOE1		6.6E-06	1.0254	-2.3E-07						
CDOE2		4.653	1.2438	-0.0502	-0.0421					

Table 6.3 Factor Levels Included in the FDOE2

Factors	Levels	
	1	2
No. of 18-kip SAL Applications	Up to 30 applications	
Surface Layer Modulus of Elasticity (ksi)	400	900
G-ratio	0.7	0.9
Total Pavement Thickness	10"	16"
Asphalt Layer Thickness	4"	6"
Subgrade Type	Sand	Clay

Table 6.4 Factor Levels Included in the RDOE1

Factors	Levels		
	1	2	3
Axle Load (kip)	18	24	36
No. of Axles	1	2	4
Slab Thickness (in)	6.0	12.0	18.0
Speed (mph)	1.75	20	40

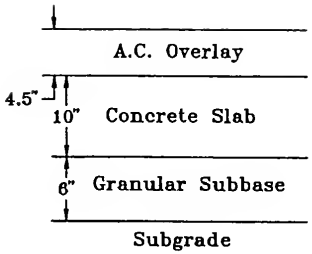

Typical JRCP Cross Section
for Interstate Highways

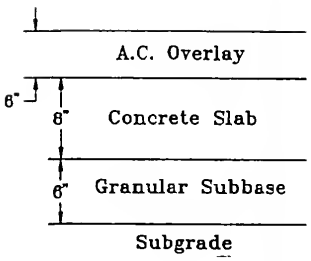

Typical JRCP Cross Sectic
for U.S. Highways

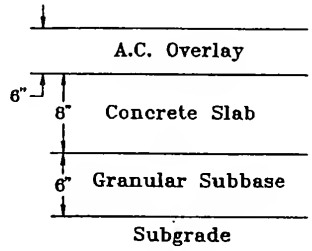

Typical JRCP Cross Section
for State Roads

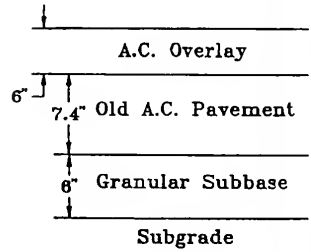

Typical JRCP Cross Sectic
for State Roads

Figure 6.1 Typical Pavement Cross Sections for Indiana

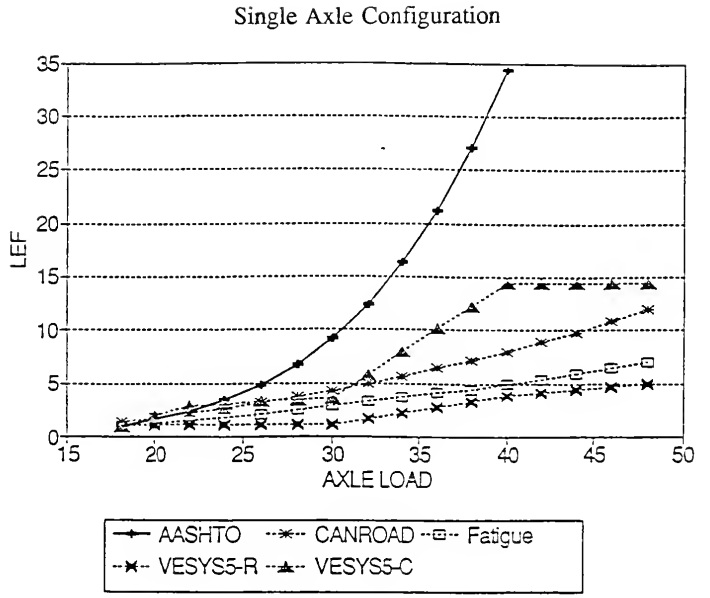

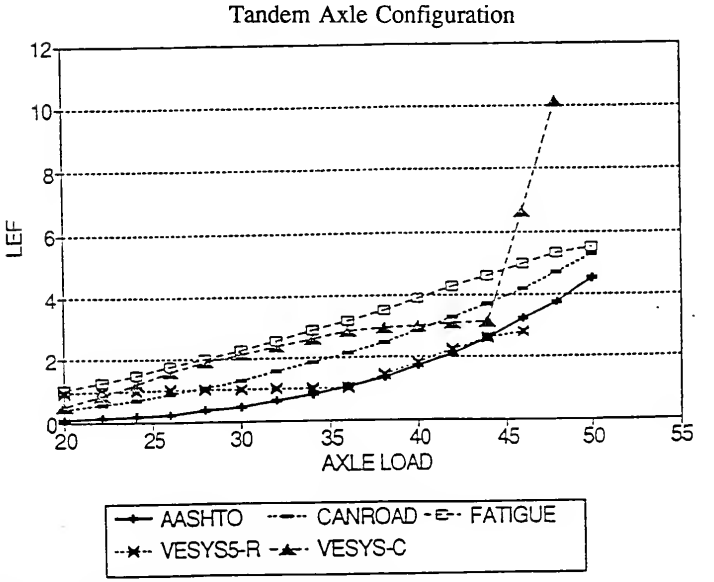

Figure 6.2 Flexible Pavement LEF's for Single and Tandem Axle Configurations

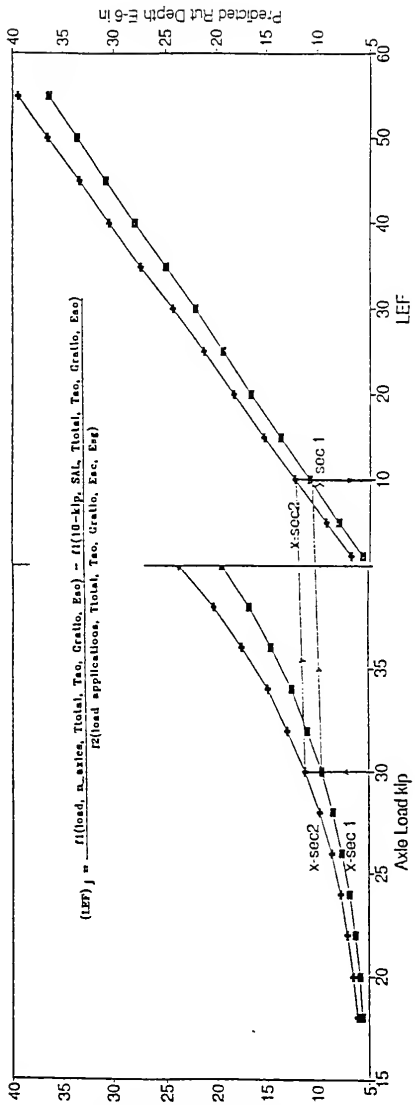

Figure 6.3 Purdue LEF's for Flexible Pavements

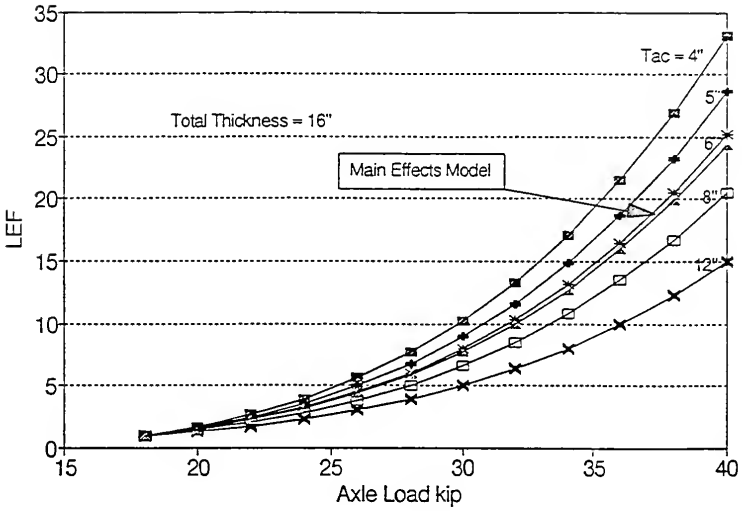

Figure 6.4 Comparison Between Main Effects and Full Interaction Models

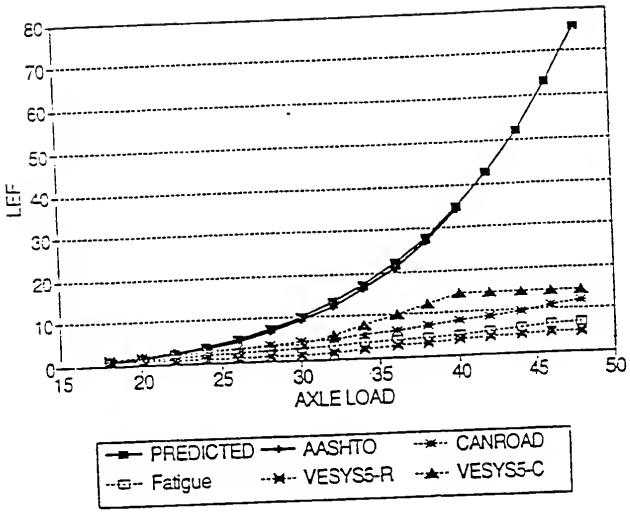

Figure 6.5 Comparison Between Purdue LEF's and Other Flexible Pavement LEF's (Single Axle Configuration)

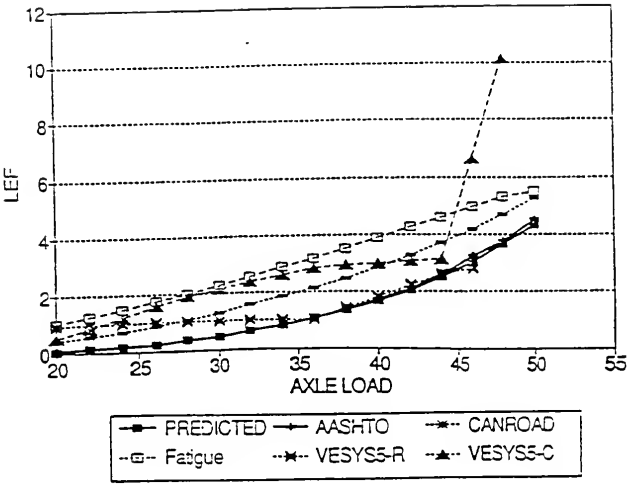

Figure 6.6 Comparison Between Purdue LEF's and Other Flexible Pavement LEF's (Tandem Axle Configuration)

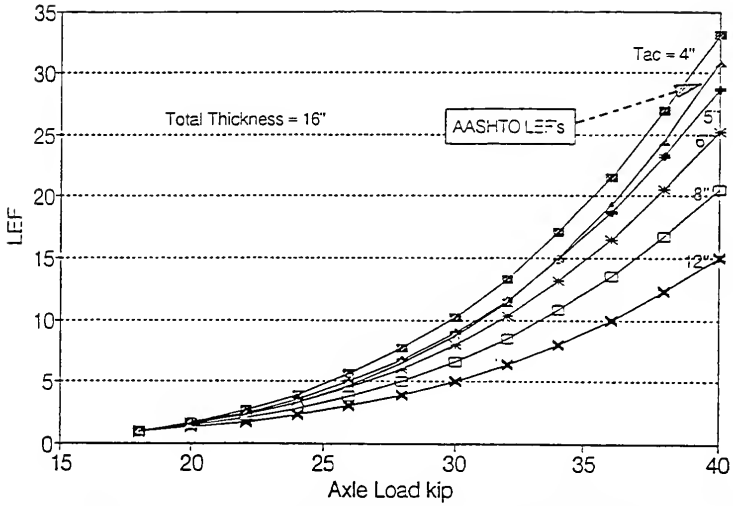

Figure 6.7 Effect of Asphalt Layer Thickness on LEF's (Single Axle Configuration)

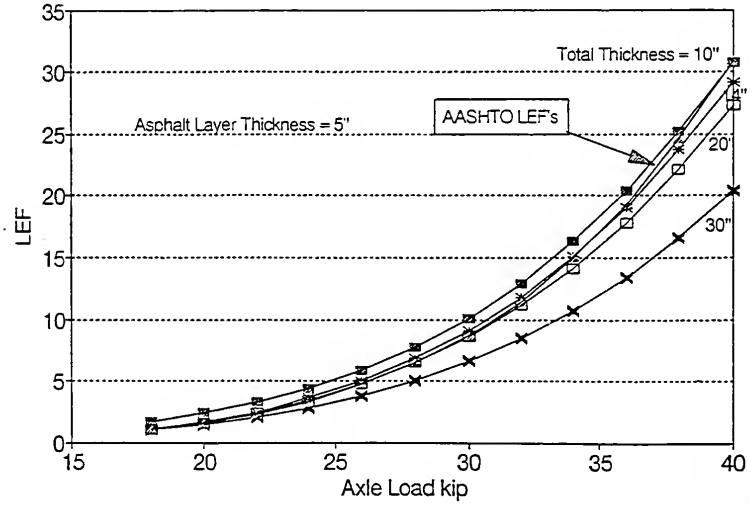

Figure 6.8 Effect of Total Pavement Thickness on LEF's (Single Axle Configuration)

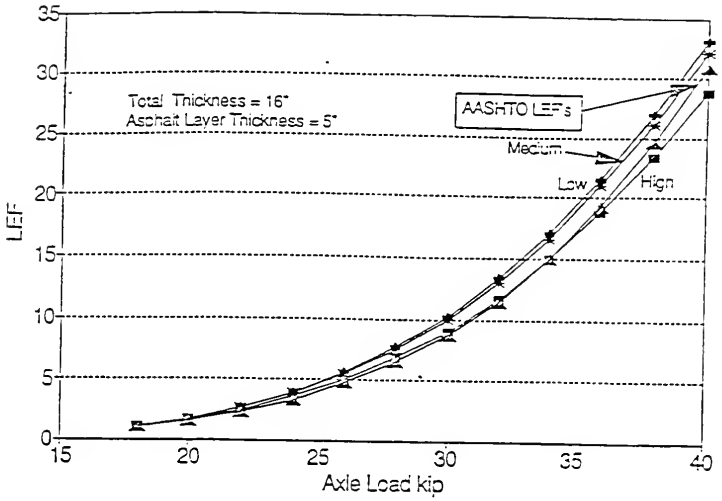

Figure 6.9 Effect of Asphalt Mixture Quality on LEF's (Single Axle Configuration)

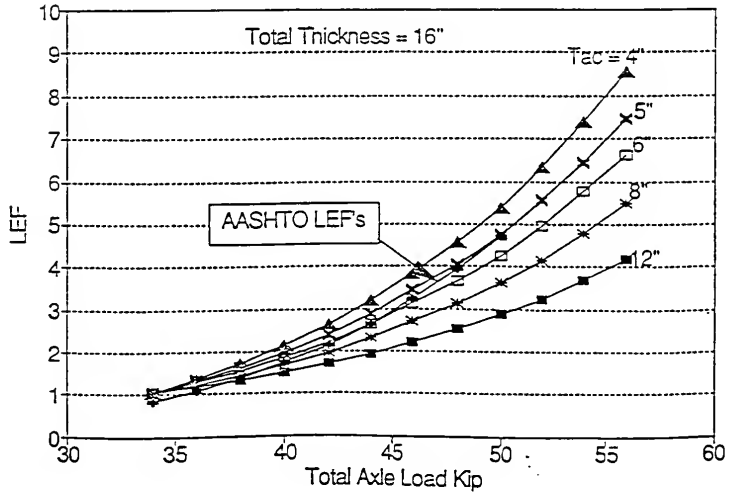

Figure 6.10 Effect of Asphalt Layer Thickness on LEF's (Tandem Axle Configuration)

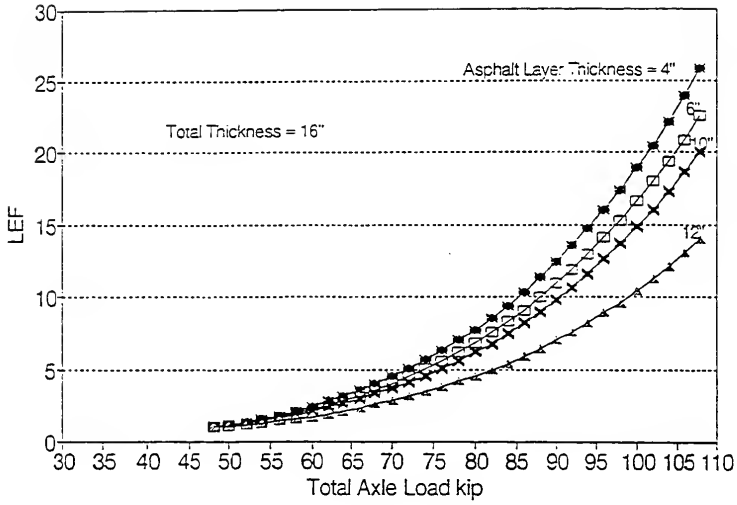

Figure 6.11 Effect of Asphalt Layer Thickness on LEF's (Tridem Axle Configuration)

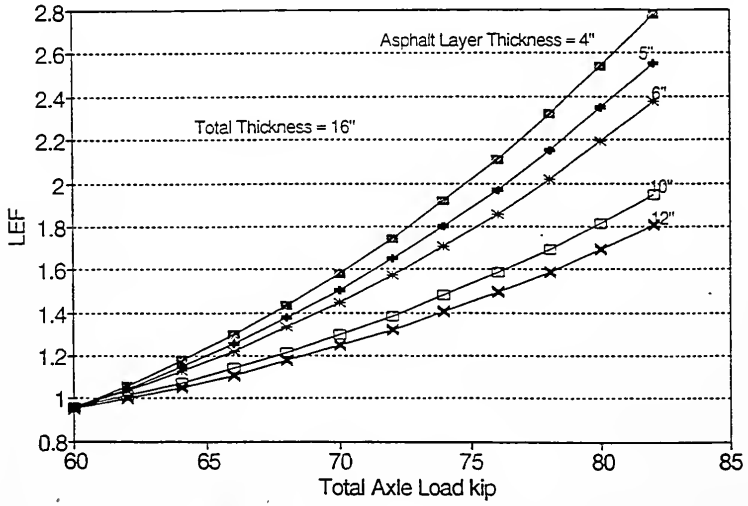

Figure 6.12 Effect of Asphalt Layer Thickness on LEF's (Four Axle Configuration)

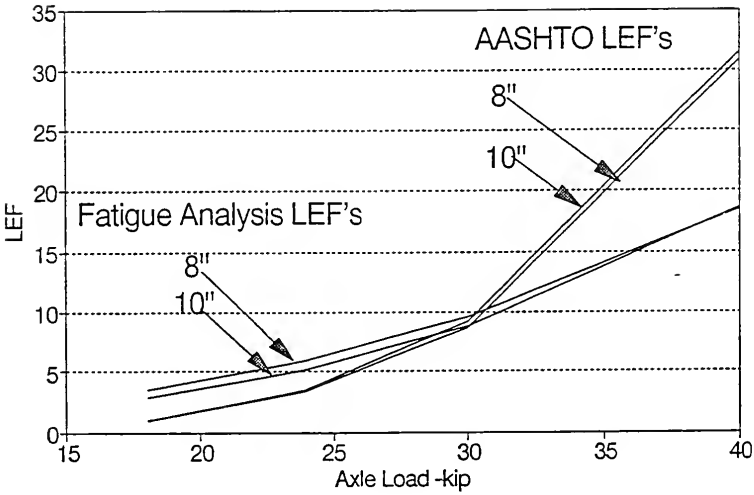

Figure 6.13 Comparison Between The AASHTO LEF's and Fatigue Analysis LEF's (Single Axle Configuration)

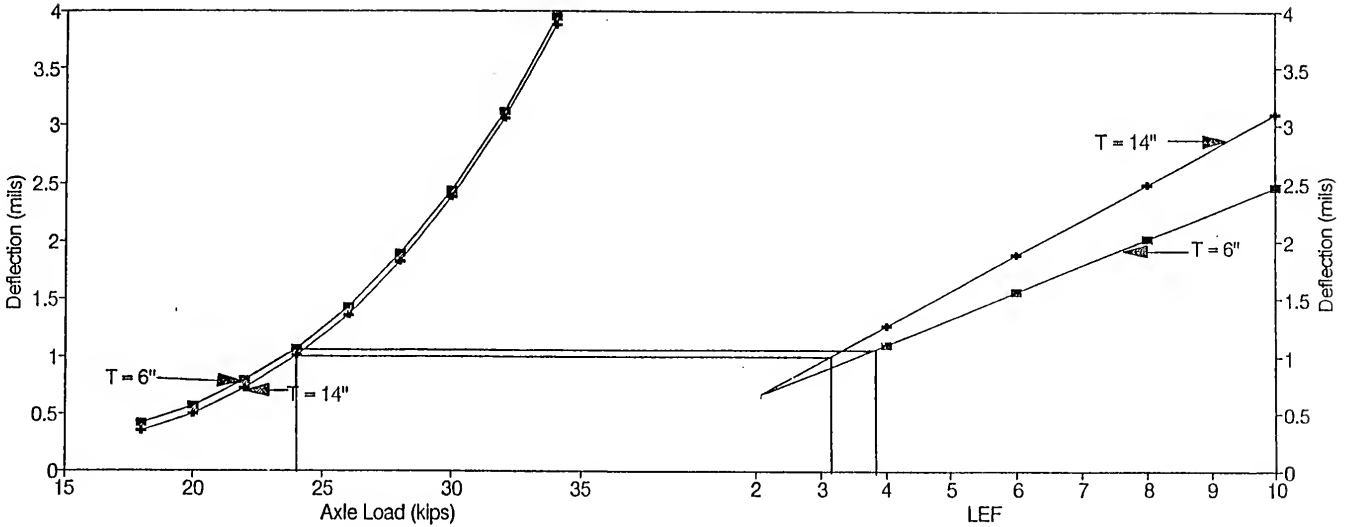

Figure 6.14 Purdue LEF's

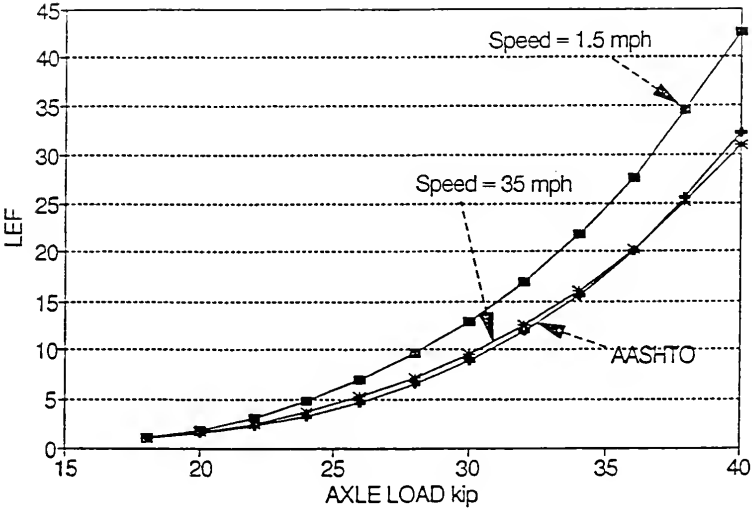

Figure 6.15 Effect of Speed on LEF's

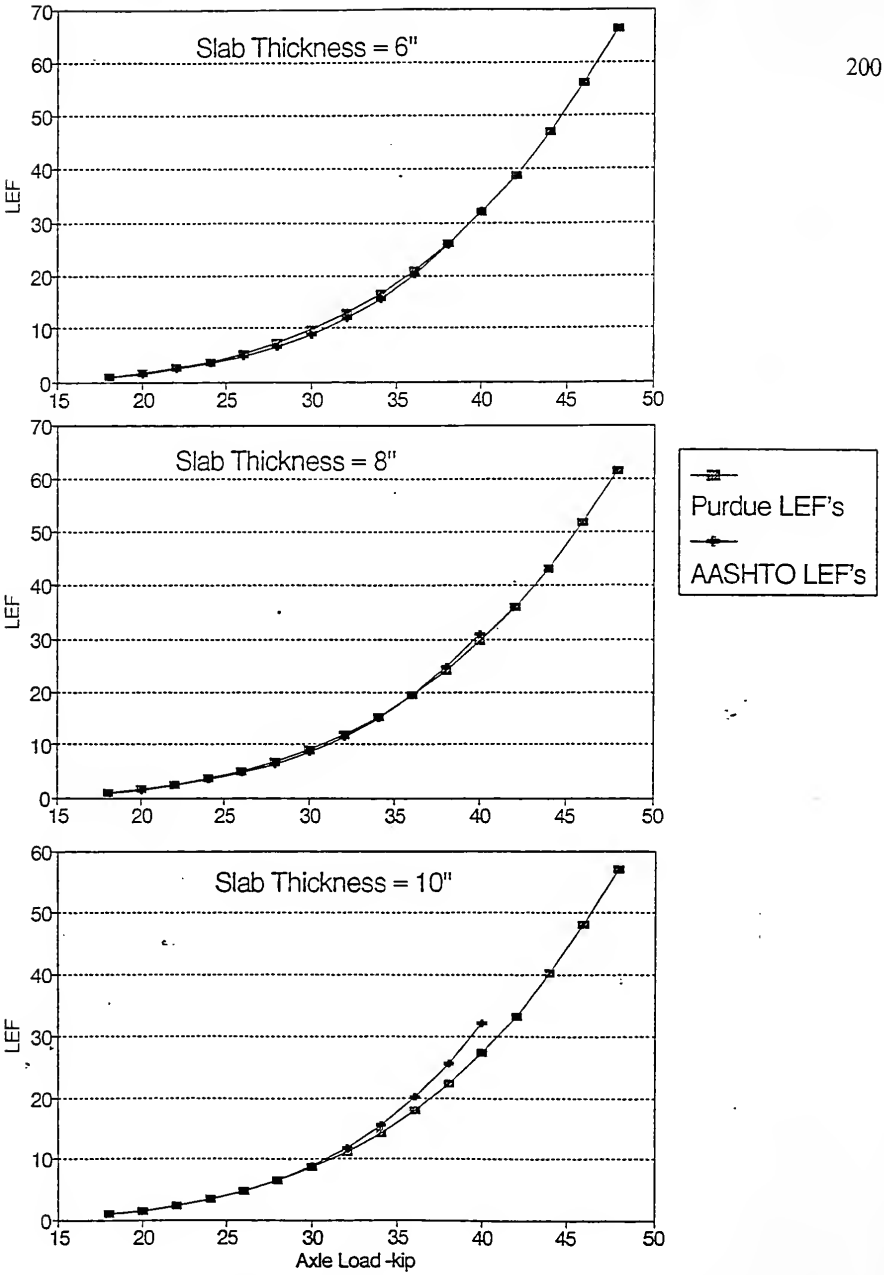

Figure 6.16 Comparison Between the AASHTO LEF's and Purdue LEF's (Single Axle Configuration)

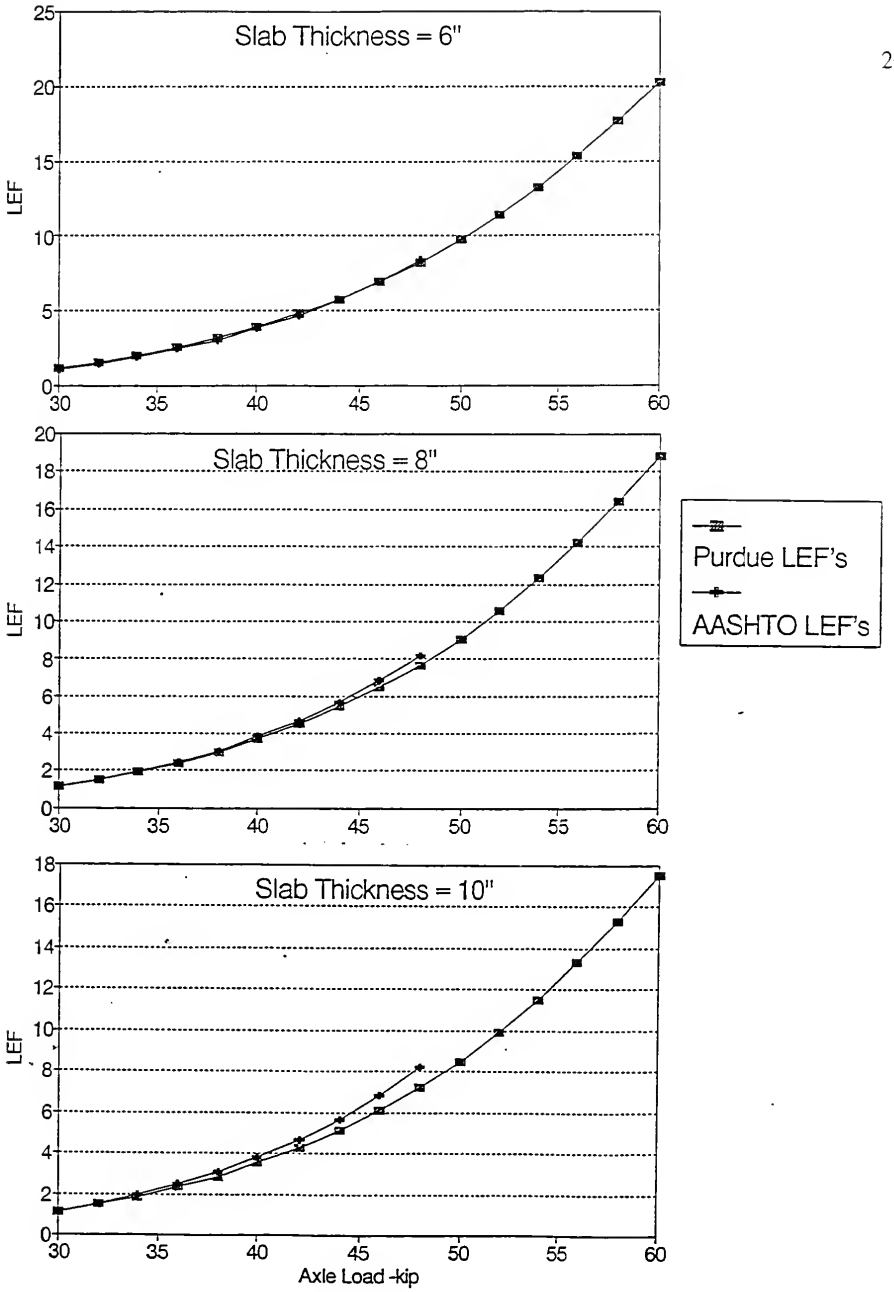

Figure 6.17 Comparison Between the AASHTO LEF's and Purdue LEF's (Tandem Axle Configuration)

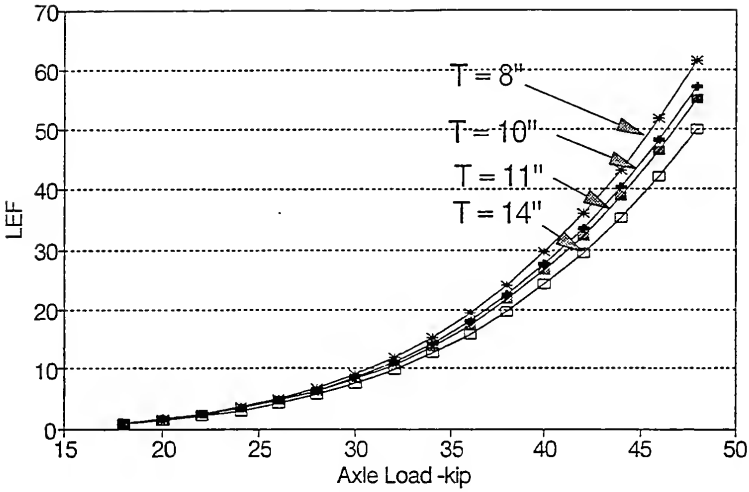

Figure 6.18 Effect of Slab Thickness on LEF's (Single Axle Configuration)

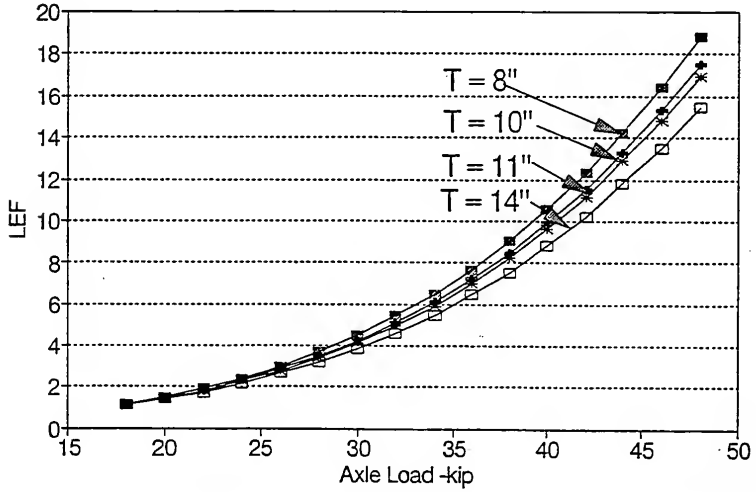

Figure 6.19 Effect of Slab Thickness on LEF's (Tandem Axle Configuration)

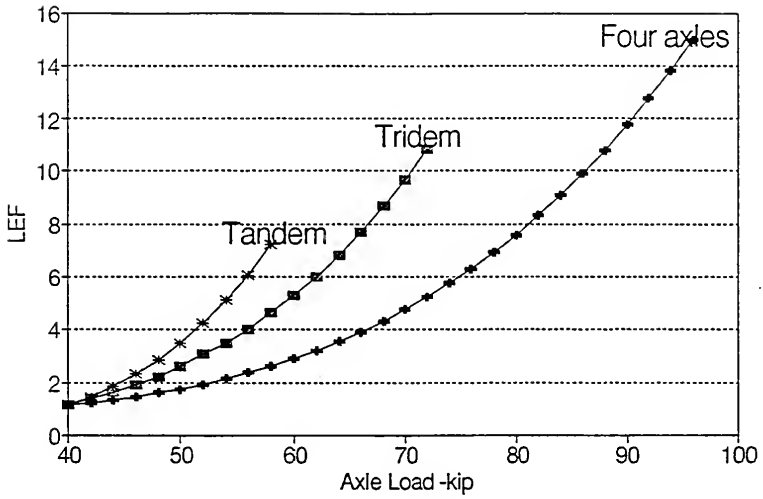

Figure 6.20 Effect of Number of Axles on LEF's

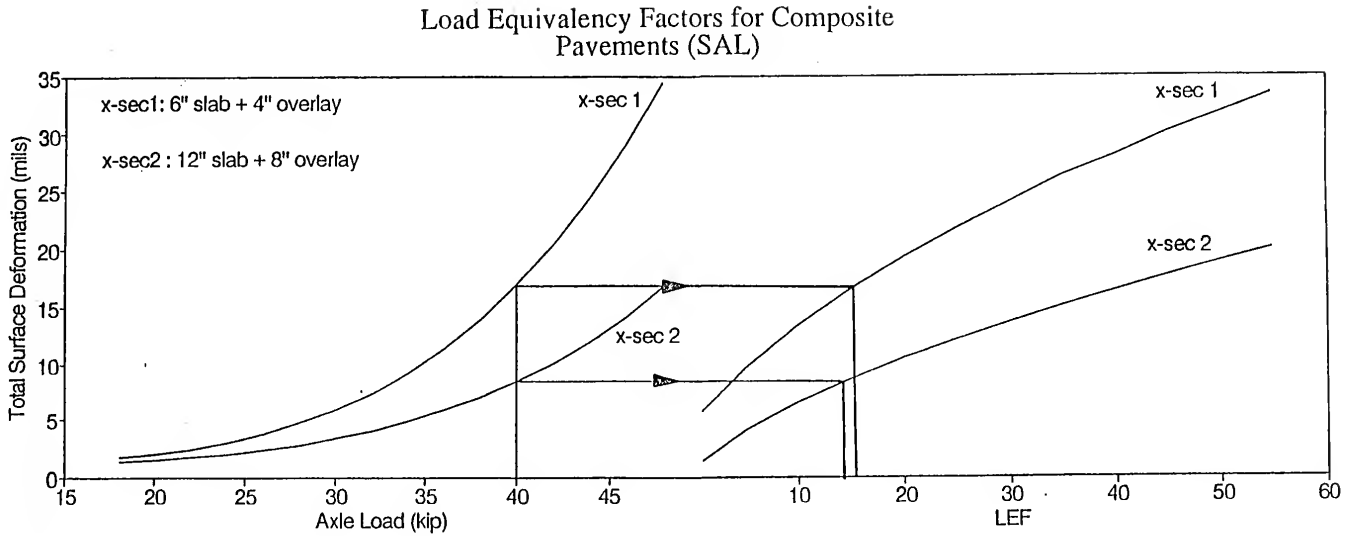

Figure 6.21 Purdue LEF's

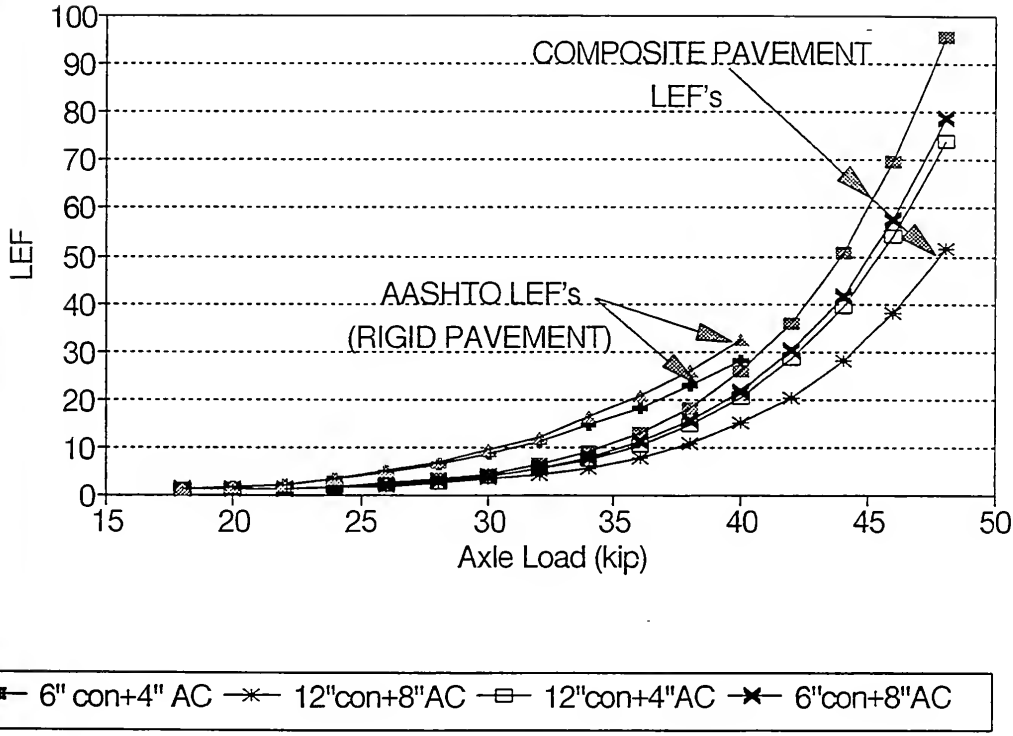

Figure 6.22 Comparison Between the AASHTO LEF's for Concrete Pavements and Purdue LEF's for Composite Pavements

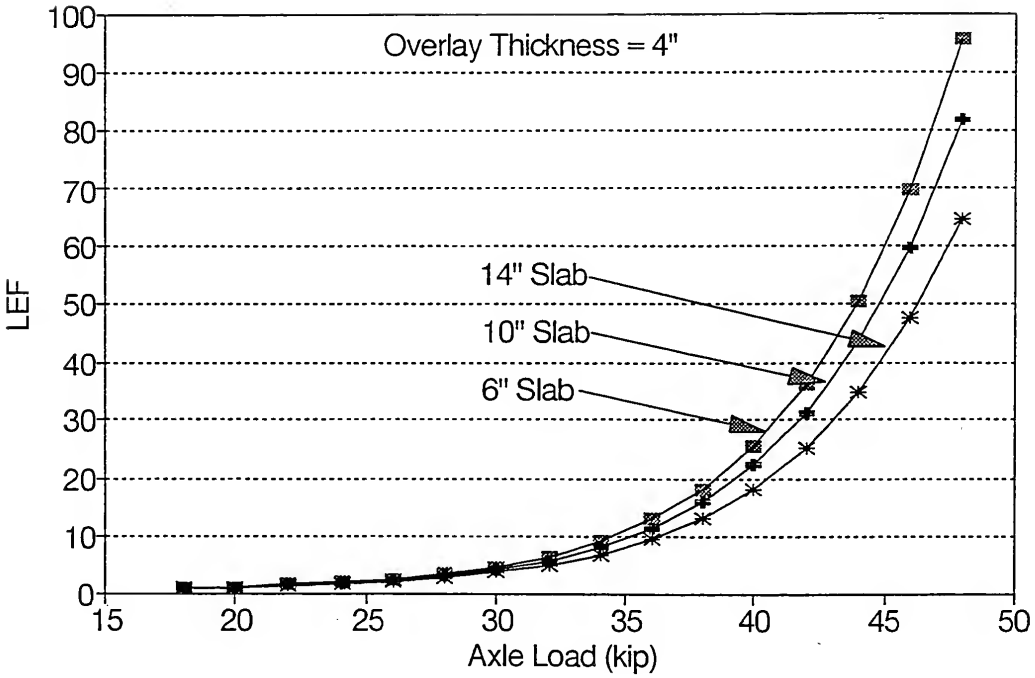

Figure 6.23 Effect of the Slab Thickness on LEF's

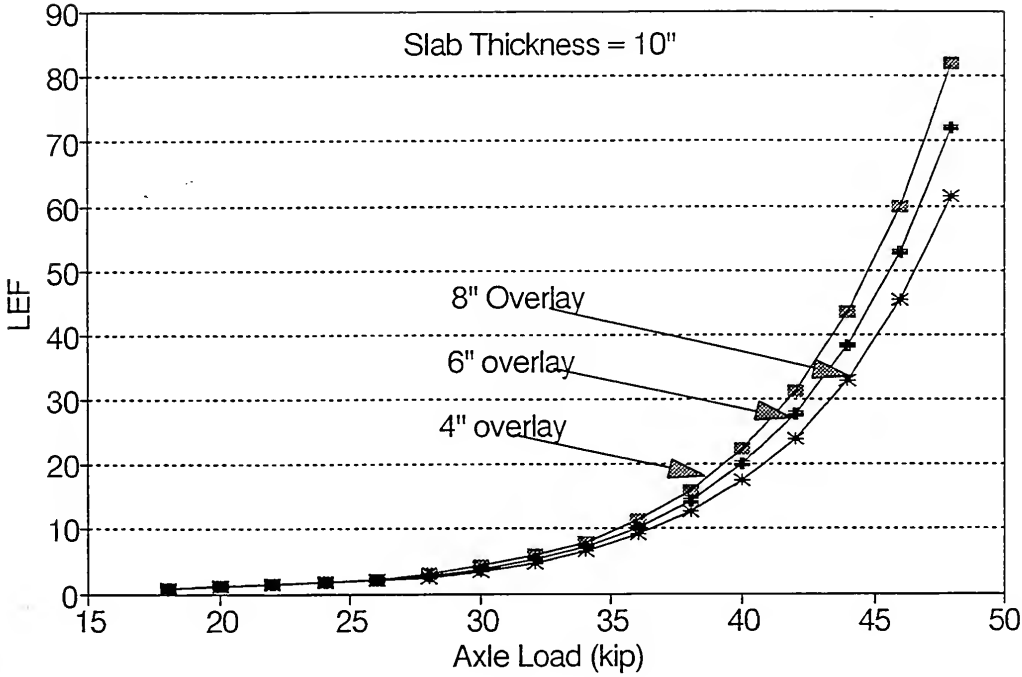

Figure 6.24 Effect of the Overlay Thickness on LEF's

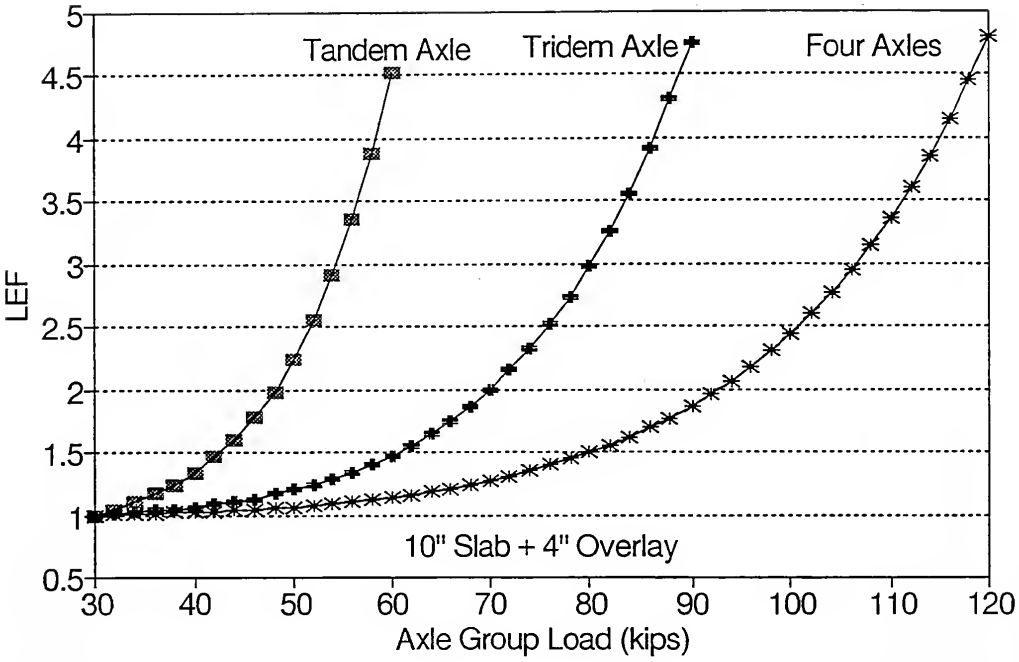

Figure 6.25 Effect of Number of Axles on LEF's

Table 7.1 Typical Material Properties Used in the Analysis

Material Name	Material Property	Typical Value
Asphalt Surface	Modulus of Elasticity (psi)	400,00
	Poisson's Ratio	0.3
	G-Ratio	0.8
	Density (pcf)	150
	Damping Coefficient (%)	5
Granular Base	Modulus of Elasticity (psi)	80,000
	Poisson's Ratio	0.3
	Initial Yield Stress (psi)	28.79
	Initial Plastic Strain (in/in)	0.0
	Angle of Friction (degree)	38
	Density (pcf)	140
	Damping Coefficient (%)	5
Granular Subbase	Modulus of Elasticity (psi)	40,000
	Poisson's Ratio	0.3
	Initial Yield Stress (psi)	19.29
	Initial Plastic Strain (in/in)	0.0
	Angle of Friction (Degree)	33
	Density (pcf)	135
	Damping Coefficient (%)	5
Lean Clay (CL) Subgrade	Shear Modulus (psi)	2750

Table 7.1 (continued)

Material Name	Material Property	Typical Value
Lean Clay (CL) Subgrade (cont.)	Poisson's Ratio	0.3
	Logarithmic Hardening Modulus (log psi)	0.174
	Initial Overconsolidation Parameter (psi)	8.455
	Permeability (ft/s)	0.000021
	Initial Void Ratio (%)	8
	Initial Stress (psi)	weight of the pavement layers
	Density (pcf)	130
	Damping Coefficient (%)	5

Table 7.2 Summary of the Route Independent Model [NBR et al., 1993]

$\sqrt{W} = c_1 L + c_2$ for trucks with $10 \le L \le 120$ft.

c_1 (coeff.)	0.0484 ($ton^{1/2}$/ft.)
c_2 (intercept)	6.891 ($ton^{1/2}$)
σ_{in} for individual prediction	1.031 ($ton^{1/2}$)
r, coefficient of Correlation	0.830
$W^{1/2}$ ($ton^{1/2}$) at 50%	0.0484L + 6.891
$W^{1/2}$ ($ton^{1/2}$) at 85%	0.0484 L + 5.822
$W^{1/2}$ ($ton^{1/2}$) at 90%	0.0484L + 5.570
$W^{1/2}$ ($ton^{1/2}$) at 95%	0.0484 L + 5.195
$W^{1/2}$ ($ton^{1/2}$) at 99%	0.0484L + 4.493
W (ton) at 50%	$2.34x10^{-3}L^2 + 0.667L + 47.48$
W (ton) at 85%	$2.34x10^{-3}L^2 + 0.564L + 33.90$
W (ton) at 90%	$2.34x10^{-3}L^2 + 0.539L + 31.02$
W (ton) at 95%	$2.34x10^{-3}L^2 + 0.503L + 26.99$
W (ton) at 99%	$2.34x10^{-3}L^2 + 0.435L + 20.19$

Table 7.3 Summary of the Route Dependent Model

$\sqrt{W} = c_1$ *HS truck cap.* $x\ L + c_2$ *for truck with* $10 \le L \le 120$

c_1 (coeff.)	$7.495x10^{-4} \frac{ton^{-\frac{1}{2}}}{ft.}$
c_2 (intercept)	6.795 ($ton^{1/2}$)
σ_{in} for individual prediction	0.686 ($ton^{1/2}$)
r, coefficient of Correlation	0.93
$W^{1/2}$($ton^{1/2}$) at 50%	$7.495x10^{-4}$ HS truck cap. x L + 6.795
$W^{1/2}$($ton^{1/2}$) at 85%	$7.495x10^{-4}$ HS truck cap. x L + 6.084
$W^{1/2}$($ton^{1/2}$) at 90%	$7.495x10^{-4}$ HS truck cap. x L + 5.916
$W^{1/2}$($ton^{1/2}$) at 95%	$7.495x10^{-4}$ HS truck cap. x L + 5.667
$W^{1/2}$($ton^{1/2}$) at 99%	$7.495x10^{-4}$ HS truck cap. x L + 5.200

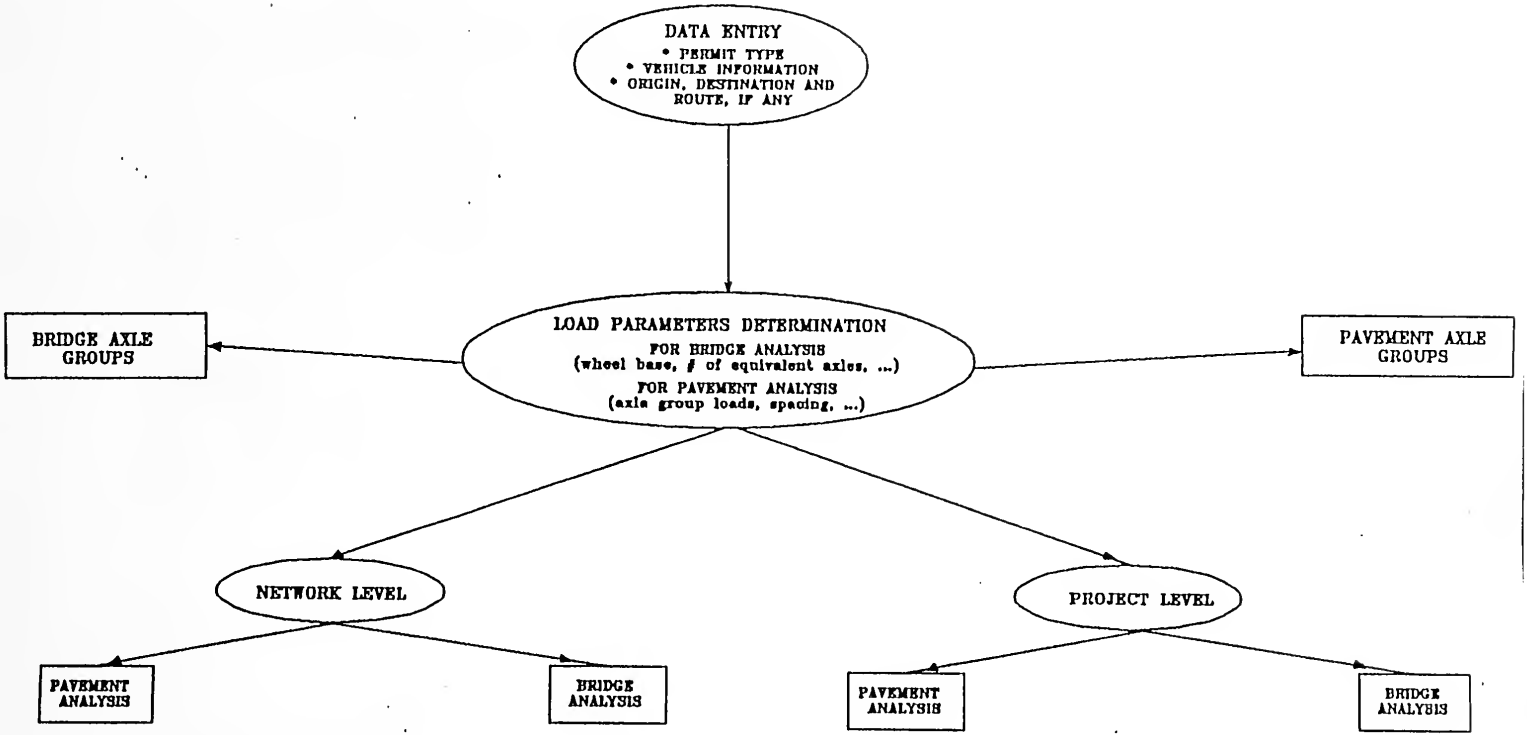

Figure 7.1 Flow Chart of the Overload Permit Procedure

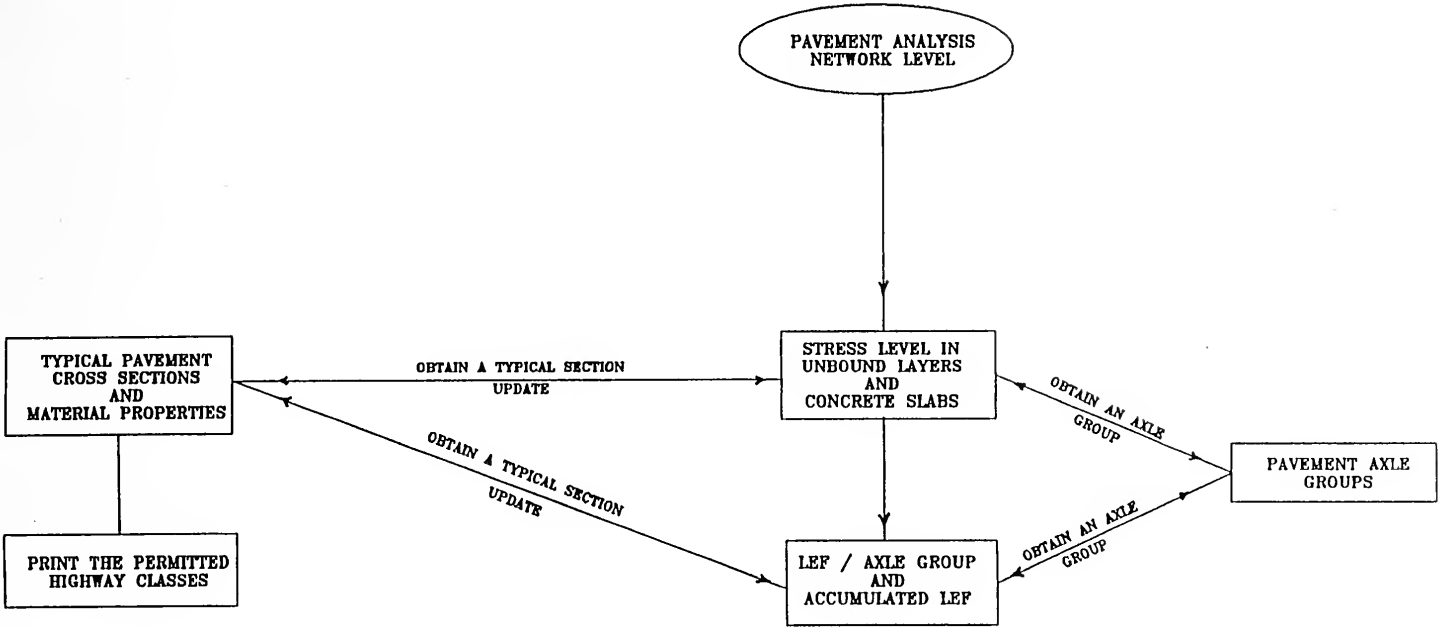

Figure 7.1 (continued)

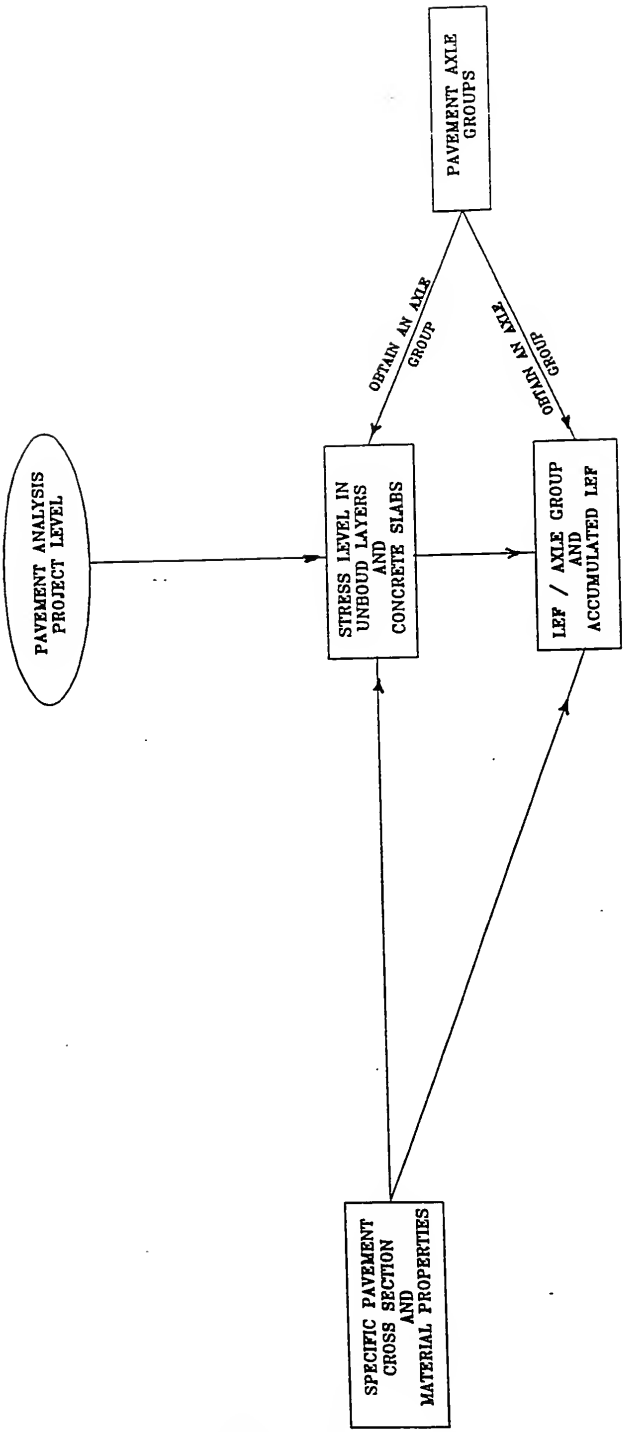

Figure 7.1 (continued)

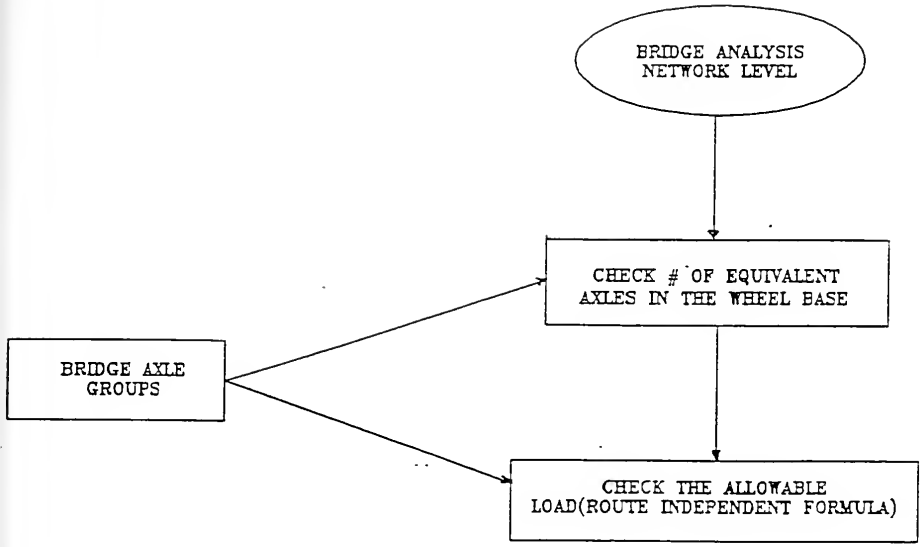

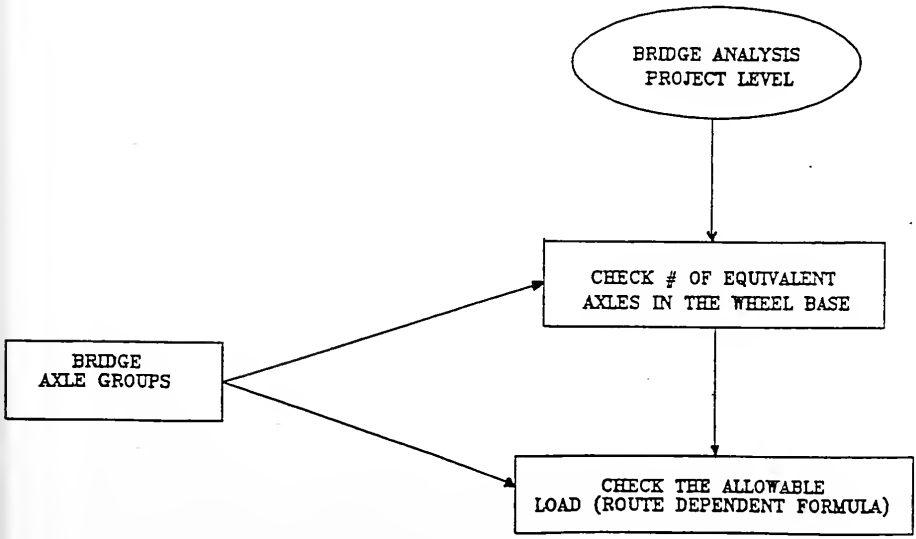

Figure 7.1 (continued)

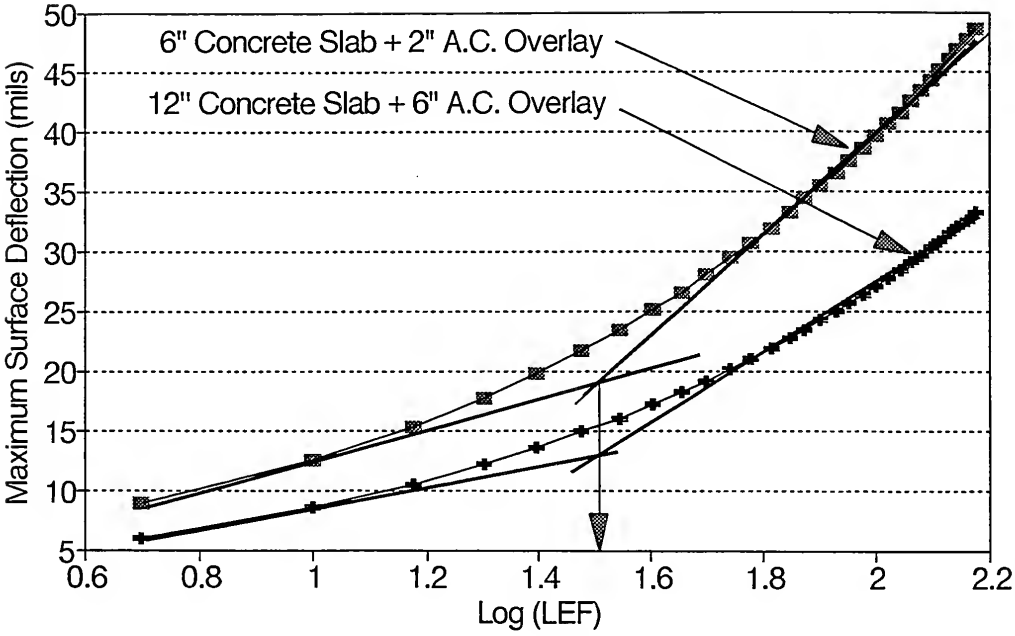

Figure 7.2 Effect of LEF's on Maximum Surface Deflection

APPENDIX A: RECOMMENDATIONS ON TRUCK CONFIGURATIONS

The purpose of these recommendations is to minimize pavement damage due to overloaded trucks. The regression models presented in Chapter 7, Section 7.3 are used to predict stress levels in different pavement layers. These models were extended to cover wider ranges of load parameters as follows:

1. Axle load: 18, 70 and 114 kip/axle.
2. Number of axles: 1, 2, 4 and 8.
3. Axle spacing: 3, 4.5 and 6 feet.
4. Number of wheels: 2, 4 and 8 /axle.

The extended models were used to determine values of load parameter for which the stress/modulus of rapture ratio for concrete is less than 0.5 and the stress level in the unbound layers is less than their yield stress. LEF's were calculated for load configurations which satisfy the stress analysis. Recommended load configurations for different load levels are presented in Table A1. It should be noted that number of wheels are assumed to be 4/axle (dual tires) for all configurations. For single axle configuration, an axle load of 28 kips is recommended as a limit.

Table A.1 Minimum Axle Spacing for Different Load Levels

Axle Group Load (kip)	Number of Axles				
	2	3	4	5	6
30-40	—	—	—	—	—
40-50	—	—	—	—	—
50-60	4.8	—	—	—	—
60-70	N/A	—	—	—	—
70-80	N/A	—	—	—	—
80-90	N/A	4.35	—	—	—
90-100	N/A	N/A	—	—	—
100-110	N/A	N/A	—	—	—
110-120	N/A	N/A	3.9	—	—
120-130	N/A	N/A	5.85	—	—
130-140	N/A	N/A	N/A	—	—
140-150	N/A	N/A	N/A	3.55	—
150-160	N/A	N/A	N/A	5.0	—
160-170	N/A	N/A	N/A	N/A	—
170-180	N/A	N/A	N/A	N/A	—
180-190	N/A	N/A	N/A	N/A	4.3
190-200	N/A	N/A	N/A	N/A	5.65

N/A = not applicable

- Axle spacing is in feet
- Maximum load for single axle configuration = 28 kip

APPENDIX B USER MANUAL

A user friendly computer software was developed to implement the overload permitting procedure for bridges and pavements. In the following sections, the software menus and options will be explained. The software menus will be shown in bold italic letters. The program uses the default values when the input is blank.

LEVEL OF ANALYSIS

1. Network Level

2. Project Level

This menu allows the user to select the analysis level. ***Network level*** is the default.

ANALYSIS TYPE

1. Check for Pavements only

2. Check for Bridges only

3. Check for Both

This menu allows the user to select the analysis type. Check for ***Both*** pavements and bridges is the default.

PERMIT TYPE

1. Oversize

2. Overweight

3. Oversize/Overweight

4. Mobile Home I

5. Mobile Home II

This menu allows the user to select the permit type. The program will not allow the user to leave this item blank. ***Mobile Home I*** option includes mobile home widths in the range of 8' to 12.33', while ***Mobile Home II*** option includes mobile home widths in the range of 12.33' to 14.33'. If ***Mobile Home I or II*** are selected the mobile home menu will be displayed and the user is permitted to enter the following information:

MOBILE HOME INFORMATION

- ***Mobile Home Annual Number***

- ***Mobile Home Serial Number***

Both annual and serial numbers are in free format form.

VEHICLE DESCRIPTION

1. Tractor Trailer

2. Truck Trailer

3. Self Prop. Equipment

4. Truck

5. Auto Trailer

6. Other

This menu allows the user to select the appropriate vehicle type. The program will not allow the

user to leave this item blank.

TRUCK INFORMATION

- *Starting Date (mm/dd/yy)*
- *Expiration Date (mm/dd/yy)*
- *Make of the Tractor (20 character maximum)*
- *Serial Number (10 character maximum)*
- *License and State (10 character maximum)*
- *Company Name (20 character maximum)*
- *Address (street - 20 character maximum)*
- *City, State and Zip Code (20 character maximum and no ",'s" are allowed)*
- *Phone Number (area code) ddd-dddd*

In this menu the user is permitted to enter the truck information. Formats of the starting and expiration dates are month/day/year, two digits each, while the other items are in free format form.

In the following menus the user are permitted to enter the truck dimensions and weights as follows:

TRUCK DIMENSION

- *Overall Length (feet xx.xx)*
- *Overall Width (feet xx.xx)*
- *Overall Height (feet xx.xx)*

LOAD INFORMATION

- *Gross Load (kip xxx.xx)*

_ *Number of Axles*

For each axle the axle number is displayed and the user has to enter the following:

Axle Number

- *Axle Load (kip xx.xx)*

- *Axle Spacing (feet xx.xx)*

- *Number of Wheels*

It should be noted that the sum of axle loads has to be equal to the gross load and if not the program will display an error message and let the user to reenter the load information again. Also, the axle spacing is the distance between an axle and the following axle and for the last axle the program skip the axle spacing.

TRIP INFORMATION

- ***From (location - 20 character maximum and no ",'s" are allowed)***

- ***To (location - 20 character maximum and no ",'s" are allowed)***

- ***Route, if any (location - 20 character maximum and no ",'s" are allowed)***

This menu allows the user to enter the trip information in free format form. The user is allowed to leave these items blank.

After the user enters all of the necessary information a summary screen will be displayed and the user is permitted to revise the entered data by selecting the item number and reentering the revised values. The program will ask if the user wants to forward this information to the

printer and if the answer is "y" the summary screen will be printed. Also, the day and time will be included in the printout.

Based on the user selected analysis level and type the program will continue.

1. Network Level

No more information is required for the network level analysis and the result of the evaluation will be displayed on the screen as well as printed with the summary data for pavements and/or bridges.

2. Project Level

If project level analysis is selected, pavement cross section and/or bridge information are required. The user will be permitted to enter this data as follows:

2.1. Bridge Data

If the truck overall length and number of axle groups satisfy the evaluation criteria, the user will be asked to enter the following:

- ***Enter the 'HS' Truck Capacity***
- ***Enter the desired confidence level (50/85/90/95/99)***

No more information is required for this step and the results will be displayed as well as printed automatically.

2.2. Pavement Data

PAVEMENT TYPE

- *Asphalt Pavement (F)*
- *Concrete Pavement (R)*
- *Composite Pavement (C)*

- Enter the Pavement Type

The user has to enter the pavement type ("F" for asphalt pavements, "R" for concrete pavements and "C" for composite pavements. Depending on the pavement type, the user will be permitted to enter the cross section information as follows:

2.1.1. Asphalt Pavement

- Thickness of the Asphalt Surface, Including any Asphalt Stabilized Layers (in)

- Thickness of Granular Layers, Base and Subbase if any (in)

- Total Thickness (in)

The program will check if the total thickness equals to the sum of the asphalt surface and granular layers and if it not equal, an error message will be printed and the user will be permitted to reenter the layer thicknesses.

Subgrade Type

- *Gravel (G)*
- *Sand (S)*
- *Silt (M)*
- *Lean Clay (CL)*
- *High Plasticity Clay (CH)*

- Subgrade Type

Do you want to change Material Properties (y/n)

If the user wants to use the default material values the answer should be "y". If the answer is "n" the user will be permitted to enter material parameters.

Information on the Asphalt Surface, Including any Asphalt Stabilized Layers

- *Modulus of Elasticity (ksi xxx.xx)*
- *Ratio of the Instantaneous Shear Modulus to Long Term Shear Modulus (0.xxx)*

Information on the Base Course

- *Modulus of Elasticity (ksi xxx.xx)*
- *Angle of Internal Friction (degree)*
- *Cohesion (psi)*
- *Yield Stress (psi)*

Information on the Subbase Course (if any)

- *Modulus of Elasticity (ksi xx.xx)*
- *Angle of Internal Friction (degree)*
- *Cohesion (psi)*
- *Yield Stress (psi)*

Information on the Subbase Course (if any)

- *Modulus of Elasticity (ksi xx.xx)*
- *Angle of Friction (degree)*

- *Cohesion (psi)*

- *Yield Stress (psi)*

2.1.2. Concrete Pavement

- *Thickness of the Concrete Slab, Including any Cement Stabilized Layers (in)*

- *Thickness of Granular Layers, Base and Subbase if any (in)*

- *Total Thickness (in)*

The program will check if the total thickness equals to the sum of the asphalt surface and granular layers and if it not equal, an error message will be printed and the user will be permitted to reenter the layer thicknesses.

Subgrade Type

- *Gravel (G)*
- *Sand (S)*
- *Silt (M)*
- *Lean Clay (CL)*
- *High Plasticity Clay (CH)*

- *Subgrade Type*

Do you want to change Material Properties (y/n)

If the user wants to use the default material values the answer should be "y". If the answer is "n" the user will be permitted to enter material parameters.

Information on the Concrete Slabs, Including any Cement Stabilized Layers

- *Modulus of Elasticity (ksi xxx.xx)*

- *Modulus of Rupture (psi)*

Information on the Subbase Course

- *Modulus of Elasticity (ksi xx.xx)*
- *Angle of Friction (degree)*
- *Cohesion (psi)*
- *Yield Stress (psi)*

Information of the Subbase Course (if any)

- *Modulus on Elasticity (ksi xx.xx)*
- *Angle of Internal Friction (degree)*
- *Cohesion (psi)*
- *Yield Stress (psi)*

2.1.3. Composite Pavement

- *Thickness of the Asphalt Overlay (in)*
- *Thickness of the Concrete Slab (in)*
- *Thickness of Granular Layers, Subbase if any (in)*
- *Total Thickness (in)*

The program will check if the total thickness equals to the sum of the layer thicknesses and if it not equal, an error message will be printed and the user will be permitted to reenter the layer thicknesses.

Subgrade Type

- *Gravel (G)*
- *Sand (S)*
- *Silt (M)*
- *Lean Clay (CL)*
- *High Plasticity Clay (CH)*

- Subgrade Type

Do you want to change Material Properties (y/n)

If the user wants to use the default material values the answer should be "y". If the answer is "n" the user will be permitted to enter material parameters.

Information on the Asphalt Surface

- Modulus of Elasticity (ksi xxx.xx)

- Ratio of the Instantaneous Shear Modulus to Long Term Shear Modulus (0.xxx)

Information on the Concrete Slabs, Including any Cement Stabilized Layers

- Modulus of Elasticity (ksi xxx.xx)

- Modulus of Rupture (psi)

Information on the Subbase Course (if any)

- Modulus of Elasticity (ksi xx.xx)

- Angle of Internal Friction (degree)

- Cohesion (psi)

- *Yield Stress (psi)*

COVER DESIGN BY ALDO GIORGINI